ULTRASOUND-ASSISTED EXTRACTION OF COLLAGEN

FROM BROILER CHICKEN TRACHEA AND ITS

BIOCHEMICAL CHARACTERIZATION

Kitsanapong Kaewbangkerd

A Thesis Submitted in Partial Fulfillment of the Requirements for the

Degree of Master of Science in Food Technology

Suranaree University of Technology

Academic Year 2019

การสกัดคอลลาเจนจากหลอดลมไก่ด้วยอัลตราซาวด์และคุณลักษณะทางชีวเคมี

นายกฤษณพงศ์ แก้วบังเกิด

ULTRASOUND-ASSISTED EXTRACTION OF COLLAGEN FROM BROILER CHICKEN TRACHEA AND ITS BIOCHEMICAL CHARACTERIZATION
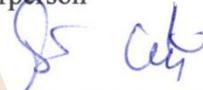
Suranaree University of Technology has approved this thesis submitted in partial fulfillment of the requirements for a Master's Degree.
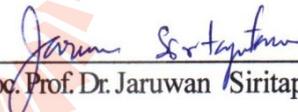
Thesis Examining Committee

_____

(Dr. Thanawit Kulrattanarak)

Chairperson

_____

(Assoc. Prof. Dr. Jirawat Yongsawatdigul)

Member (Thesis Advisor)

_____

(Assoc. Prof. Dr. Jaruwan Siritapetawee)
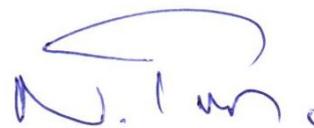
Member

_____

(Asst. Prof. Dr. Piyada Ngernsoungnern)

Member

_____

(Assoc. Prof. Flt. Lt. Dr. Kontorn Chamniprasart)

Vice Rector for Academic Affairs and

Internationalization

_____

(Prof. Dr. Neung Teaumroong)

Dean of Institute of Agricultural

Technology

กฤษณพงศ์ แก้วบังเกิด : การสกัดคอลลาเจนจากหลอดลมไก่ด้วยอัลตราซาวด์และ
คุณลักษณะทางชีวเคมี (ULTRASOUND-ASSISTED EXTRACTION OF COLLAGEN
FROM BROILER CHICKEN TRACHEA AND ITS BIOCHEMICAL
CHARACTERIZATION) อาจารย์ที่ปรึกษา : รองศาสตราจารย์ ดร.จิรวัฒน์ ยงสวัสดิกุล,
142 หน้า.

หลอดลมไก่เนื้อเป็นผลิตผลพลอยได้จากโรงชำแหละไก่ โดยปกติจะนำไปผลิตเป็นอาหาร
สัตว์ซึ่งมีมูลค่าต่ำแม้จะมีปริมาณคอลลาเจนสูงก็ตาม โดยทั่วไปการสกัดคอลลาเจนด้วยกรด
และ/หรือเอนไซม์เพปซินมักจะให้ผลผลิต (Yield) ต่ำ การใช้คลื่นอัลตราซาวด์เข้าช่วยในการสกัด
สามารถช่วยเพิ่มผลผลิตของคอลลาเจนได้ วัตถุประสงค์ในการศึกษาครั้งนี้คือเพื่อศึกษาปัจจัยของ
ของกระบวนการคลื่นความถี่สูงต่อปริมาณผลผลิตและคุณลักษณะทางชีวเคมีของคอลลาเจนจาก
หลอดลมไก่ การสกัดคอลลาเจนแบบดั้งเดิมกรด (Acid-soluble collagen: AS) และเอนไซม์เพปซิน
(Pepsin-soluble collagen: PS) ที่เวลา 48 ชั่วโมง ทำให้ได้ผลผลิตคอลลาเจนที่ 0.65 และ 3.10%
ตามลำดับ เมื่อประยุกต์คลื่นอัลตราซาวด์ที่ระดับความเข้ม 17.87 วัตต์ต่อตารางเซนติเมตร เป็นเวลา
20 นาที ตามด้วยการสกัดด้วยกรดเป็นเวลา 42 ชั่วโมง (U-AS) ปริมาณผลผลิตของคอลลาเจน
เพิ่มขึ้นเป็น 1.58% และผลผลิตของคอลลาเจนเพิ่มขึ้นเป็น 6.28% เมื่อใช้คลื่นอัลตราซาวด์สกัดต่อ
ด้วยเพปซินเป็นเวลา 36 ชั่วโมง (U-PS) โดยคอลลาเจน PS และ U-PS ที่สกัดได้มีความบริสุทธิ์
82.84 และ 85.70% ตามลำดับ คอลลาเจนสกัดทุกตัวอย่างประกอบด้วยกรดอะมิโนหลักที่สำคัญคือ
ไกลซีน อะลานีน โพรลีน และไฮดรอกซีโพรลีน ภาพถ่ายจากกล้องจุลทรรศน์อิเล็กตรอนแบบส่อง
กราด (Scanning electron microscopy: SEM) เผยให้เห็นว่า คลื่นความถี่สูงไม่ส่งผลต่อการ
เปลี่ยนแปลงโครงสร้างระดับจุลภาคของคอลลาเจน ทุกคอลลาเจนแสดงโครงสร้างเกลียวสามสาย
(Triple helix) ที่ชัดเจนเมื่อวิเคราะห์ด้วยเทคนิคเซอร์คูลาร์ไดโครอิสซึมสเปกโทรสโกปี (Circular
dichroism: CD spectroscopy) ผลจากการวิเคราะห์ฟูเรียร์ทรานสฟอร์มอินฟาเรดสเปกโทรสโกปี
(Fourier Transform Infrared: FT-IR spectroscopy) บ่งชี้ว่า คลื่นความถี่สูงไม่มีผลต่อโครงสร้าง
ระดับทุติยภูมิ โดยทุกตัวอย่างมีโครงสร้างหลักที่สำคัญคือแอลฟาฮีลิกซ์ที่ประมาณ 30% การ
วิเคราะห์การเสียสภาพธรรมชาติของคอลลาเจนด้วยเทคนิคไมโครดิฟเฟอเรนเชียลสแกนนิงแคลอริ
มิเตอร์ (μDSC) พบว่า อุณหภูมิการเสียสภาพ (Denaturation temperature: T_d) ของคอลลาเจนเมื่อ
ละลายในน้ำปราศจากไอออนนั้นสูงกว่าคอลลาเจนที่ละลายในสารละลายกรดอะซิติกเข้มข้น 0.5
โมลาร์ ไม่ว่าจะสกัดด้วยวิธีใดๆ อุณหภูมิการเสียสภาพของคอลลาเจน AS และ U-AS อยู่ที่ 34.3 ถึง
35.1 องศาเซลเซียส ในขณะที่อุณหภูมิการเสียสภาพของคอลลาเจน PS และ U-PS อยู่ที่ 45.0 ถึง

45.6 องศาเซลเซียส จากการวิเคราะห์น้ำหนักโมเลกุลของโปรตีน คอลลาเจนทุกตัวอย่าง ประกอบด้วยเกลียวแอลฟา 1 และ 2 ที่มีมวลโมเลกุล 135 และ 116 กิโลดาลตัน ตามลำดับ ซึ่ง สอดคล้องกับคุณลักษณะของคอลลาเจนชนิดที่ 1 (Type I) นอกจากนี้ผลจากการวิเคราะห์รูปแบบ เพปไทด์โดยเทคนิคการแยกสารด้วยโครมาโตกราฟีแบบของเหลวพร้อมแมสสเปคโตรมิเตอร์ (Liquid chromatography with mass spectrometry: LC-MS/MS) บ่งชี้ถึงความคล้ายคลึงของคอลลาเจน PS และ U-PS กับคอลลาเจนชนิดที่ 1 ผลของการศึกษาเหล่านี้ชี้ให้เห็นว่า หลอดลมไก่เป็นวัตถุ ทางเลือกหนึ่งที่ใช้สำหรับผลิตคอลลาเจนชนิดที่ 1 และการใช้คลื่นอัลตราซาวด์ช่วยในการสกัดเป็น เทคนิคที่สามารถเพิ่มผลผลิตโดยที่ไม่มีการทำลายโครงสร้างของคอลลาเจน
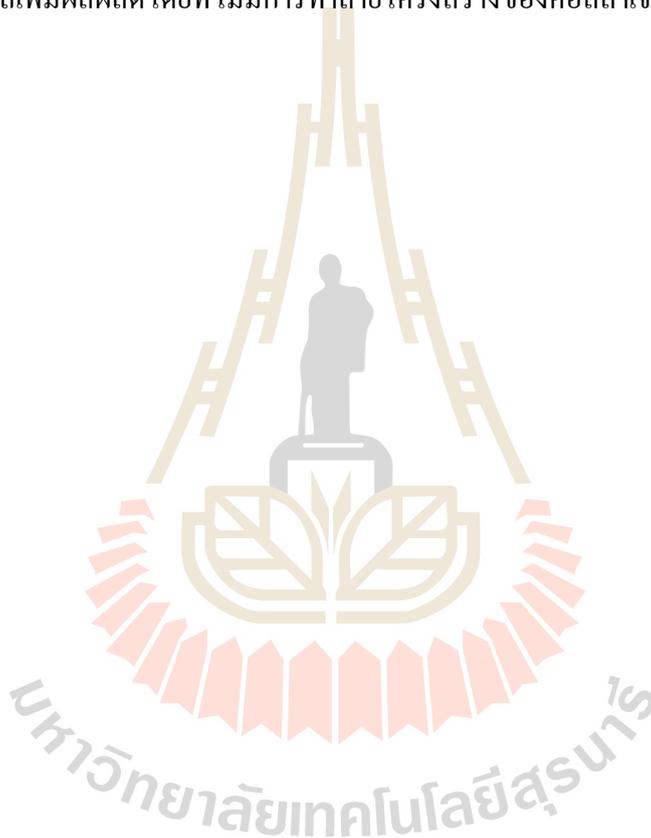
สาขาวิชาเทคโนโลยีอาหาร   ลายมือชื่อนักศึกษา_____

ปีการศึกษา 2562   ลายมือชื่ออาจารย์ที่ปรึกษา_____

KITSANAPONG KAEWBANGKERD : ULTRASOUND-ASSISTED

EXTRACTION OF COLLAGEN FROM BROILER CHICKEN TRACHEA

AND ITS BIOCHEMICAL CHARACTERIZATION. THESIS ADVISOR :

ASSOC. PROF. JIRAWAT YONGSAWATDIGUL, Ph.D., 142 PP.

TRACHEA/COLLAGEN/ULTRASOUND-ASSISTED EXTRACTION/FT-IR/CD

Broiler chicken trachea (T) is a coproduct from chicken slaughterhouse and normally turned into low value animal feed despite their high collagen. Typical collagen extraction by acid and/or pepsin usually results in lower yield. Ultrasound-assisted extraction (UAE) could be a means to improve collagen yield. The objectives of this study were to investigate the effects of ultrasonic parameters on yield and biochemical properties of T collagen. Conventional extraction using acetic acid and pepsin for 48 h resulted in acid-soluble (AS) and pepsin-soluble (PS) collagen with the yield of 0.65 and 3.10%, respectively. When ultrasound intensity of 17.87 $W \cdot cm^{-2}$ was applied for 20 min exposure time, followed by acid extraction for 42 h (U-AS), collagen yield was increased to 1.58%. A yield of 6.28% was obtained when ultrasound treatment was followed by pepsin for 36 h (U-PS). Collagen content of PS and U-PS was 82.84 and 85.70%, respectively. Glycine was a major amino acid along with alanine, proline and hydroxyproline. Scanning electron microscopy (SEM) images revealed that ultrasound did not affect the collagen microstructure. All collagens showed an obvious triple helix structure as measured by circular dichroism (CD) spectroscopy. Fourier transform infrared (FT-IR) spectroscopy indicated that ultrasound did not disturb protein secondary structure where approximately 30% of α-helix content is a major structure in all collagen samples. Micro-differential scanning
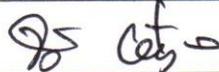
calorimetry (μDSC) demonstrated that the denaturation temperature (T_d) of collagen in the presence of deionized water was higher than collagen solubilized in 0.5 M acetic acid, regardless of the extraction method. Furthermore, T_d values of AS and U-AS collagen were 34.3 to 35.1^{o}C, whereas those of PS and U-PS collagen were 45.0 to 45.6^{o}C. All collagens comprised of α1 and α2 units with molecular weight of approximately 135 and 116 kDa, respectively, corresponding to the type I characteristic. Based on LC-MS/MS peptide mapping, PS and U-PS collagens indicated high similarity to type I collagen. These results suggested that T is an alternative source of type I collagen and UAE is a promising technique that could increase yield without damaging the collagen structure.
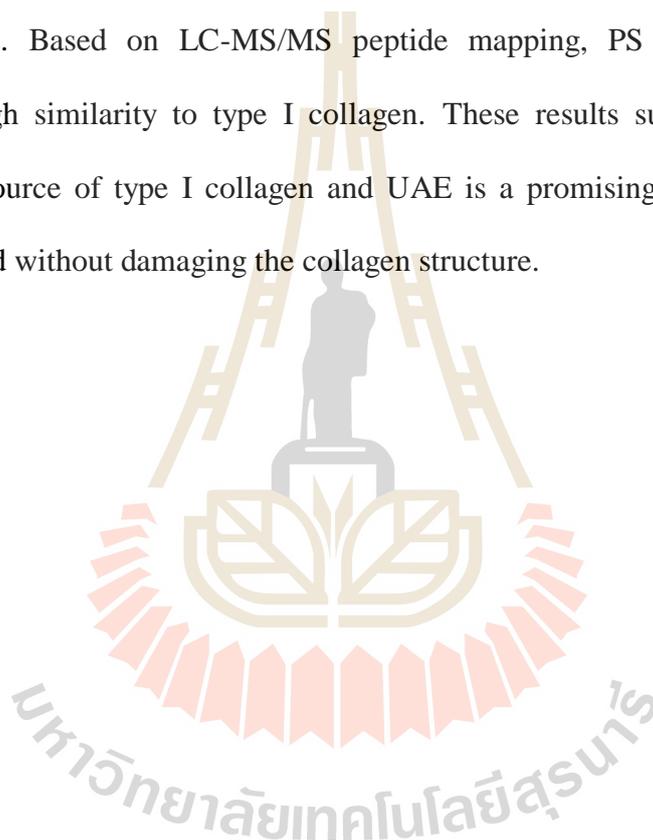
School of Food Technology

Academic Year 2019

Student's Signature_____

Advisor's Signature_____

ACKNOWLEDGEMENTS

Kitsanapong Kaewbangkerd

CONTENTS

CONTENTS (Continued)

CONTENTS (Continued)

CONTENTS (Continued)

CONTENTS (Continued)

CONTENTS (Continued)

LIST OF TABLES

LIST OF TABLES (Continued)

LIST OF FIGURES

LIST OF FIGURES (Continued)

LIST OF FIGURES (Continued)

LIST OF ABBREVIATIONS

Ac = Conventional extraction by acetic acid

Ala (A) = Alanine

Arg (R) = Arginine

AS = Acid-soluble collagen

Asn (N) = Asparagine

Asp (D) = Aspartic acid

cm = Centimeter (10^{-3} cm)

cm^{-1} = Reciprocal centimeter

DI = Deionized water

DW = Dry weight

FT-IR = Fourier transform-infrared spectroscopy

Glu (E) = Glutamic acid

Gln (Q) = Glutamine

Gly (G) = Glycine

g = Gram

HCl = Hydrochloric acid

His (H) = Histidine

h = Hour

Ile (I) = Isoleucine

kDa = kilo Dalton (10^{3} Dalton)

LIST OF ABBREVIATIONS (Continued)

LC-MS/MS	=	Liquid chromatography-mass spectrometry
Leu (L)	=	Leucine
Lys (K)	=	Lysine
M	=	$molL^{-1}$
Met (M)	=	Methionine
Hyl	=	Hydroxylysine
Hyp	=	Hydroxyproline
mg	=	Milligram (10^{-3} gram)
min	=	Minute
mL	=	Milliliter (10^{-3} L)
mM	=	Millimolar (10^{-3} $molL^{-1}$)
mm	=	Millimeter (10^{-3} m)
Mw	=	Molecular weight
MwCO	=	Molecular weight cut off
NaCl	=	Sodium chloride
NaOH	=	Sodium hydroxide
nL	=	Nanoliter (10^{-9} L)
nm	=	Nanometer (10^{-9} m)
ng	=	Nanogram (10^{-9} g)
PAGE	=	Polyacrylamide gel electrophoresis
Pep	=	Conventional extraction by pepsin
PH	=	Proline hydroxylation

LIST OF ABBREVIATIONS (Continued)

Phe (F)	=	Phenylalanine
Pro (P)	=	Proline
PS	=	Pepsin-soluble collagen
p	=	Probability value
RO	=	Reverse osmosis water
Rpm	=	Revolutions per minute
SDS	=	Sodium dodecyl sulfate
SEM	=	Scanning electron microscope
Ser (S)	=	Serine
Std.	=	Standard
sec	=	second
T	=	Chicken trachea
T_d	=	Denaturation temperature
Thr (T)	=	Threonine
Trp (W)	=	Tryptophan
Tyr (Y)	=	Tyrosine
UAE	=	Ultrasound-assisted extraction
U-AS	=	UAE followed by acid extraction
U-PS	=	UAE followed by pepsin extraction
Val (V)	=	Valine
Volt	=	Electrical voltage
v/v	=	Volume per volume

LIST OF ABBREVIATIONS (Continued)

W = Watt

w/v = Weight per volume

$W \cdot cm^{-2}$ = Watt per square centimeter

µDSC = Micro-differential scanning calorimetry

µg = Microgram (10^{-6} gram)

µL = Microliter (10^{-6} L)

µM = Micromolar (10^{-6} molL^{-1})

°C = Degree Celsius

×g = Relative centrifugal fields

α = Alpha

β = Beta

γ = Gamma

λ = Lambda

ΔH = Enthalpy

% = Percent

CHAPTER I

INTRODUCTION

1.1   Introduction

Broiler chicken (*Gallus gallus domesticus*) is one of the important global protein sources with approximate annual production of 23.7 billion chickens worldwide (Shahbandeh, 2020). Chicken meat processing generates abundant coproducts, including viscera, feather, comb, frame bone, cartilages, and etc. Cartilages have been classified as special connective tissue and can also be found in trachea (T). It is constructed by C-shaped cartilaginous rings, as a special structure designed to transport air with high flexibility (Murphy, Kelliher, and Davenport, 2012). It is generally turned into low value animal feed despite of its high collagen content. Collagen is one of extracellular matrix network accounting for about 60% of cartilage dry basis (Eyre, 2004). Collagen extraction would lead to valorization of T coproduct from the chicken meat processing.

Collagen is a natural biopolymer, composing of unique triplet amino acid sequence of Gly-X-Y, interwinding in polyproline II type (PPII) helical conformation or triple-helix structure (Shoulders and Raines, 2009). There are 29 types of collagen, each have different molecular profile, structure, and distribution source. In general, type I-V collagen have been universally studied. Type I collagen has been considerably utilized in various industrial applications, such as food additives, food supplements, food packaging, sausage industry, cosmetics, biomedical implants, and

pharmaceuticals (Martínez-Ortiz et al., 2015; Anandhakumar, Krishnamoorthy, Ramkumar and Raichur, 2017). Due to the abundance of biocompatibility, collagen has a very low immunogenicity and cytotoxicity (Ruszczak, 2003; Zou et al., 2020).

Collagen dressing is a biomedical polymer for chronic wound healing. It contains several potentialities, including matrix metalloproteinases (MMPs) inhibition, increasing type I collagen gene expression, and barrier of harmful environment (Moura et al., 2014; Wahab, Roman, Chakravarthy, Luttrell, 2015). Commercial collagen dressing typically constitutes 55-90% of native type I collagen, which was manufactured from skin or tendon of bovine, equine, porcine, and tilapia (Wiegand et al., 2016; Pallaske, Pallaske, Herklotz, Boese-Landgraf, 2018). Various coproducts were studied as an alternative source of type I collagen, such as jellyfish, hybrid sturgeon skin, sheep bone (Khong et al., 2018; Wei et al., 2019; Vidal, et al. 2020), among others. Nevertheless, utilization of T collagen has not been widely reported thus far. Hence, collagen extraction and characterization from T should be exploited.

Generally, collagen can be extracted by acetic acid (Ac) and pepsin (Pep). Acid can increase electrostatic repulsion between α-helix chains, leading to an increase in swelling and solubilization. High intermolecular cross-linkages via covalent bonds cannot be easily extracted by acid. Another approach is using pepsin to cleave specific peptide bonds on telopeptide region. This can increase yield without damaging triple helix structure (Hong et al., 2017). Yield of collagen extracted by Ac and Pep from various sources ranged 0.1-6.4% and 0.3-36.2%, respectively (Jeevithan et al., 2015; Cheng et al., 2017; Munasinghe, and Schwarz, 2017; Abdollahi, Rezaei, Jafarpour, and Undeland, 2018; Wu et al., 2019). Major disadvantages of these extraction methods are time-consuming, requiring 2-4 days and relatively low yield.

Therefore, alternative approach providing higher yield and time saving should be sought.

Recently, high-intensity ultrasound has been gained enormous attention in food industry because it has several advantages, including, yield enhancement, non-toxic and eco-friendly process (Chemat et al., 2017). The ultrasonic wave is mechanical energy, creating an acoustic cavitation effect that generates high force-pressure and temperature (Chandrapala et al., 2012; Ashokkumar, 2015). This would eventually lead to disintegration of biological tissues. Ultrasound-assisted extraction (UAE) of collagen has been reported to increase yield from various coproducts (Li et al., 2009; Kim et. al., 2012; Song et al., 2018; Ali et al., 2018).

Ultrasound intensity and exposure time would greatly affect yield of extraction, but it seems to vary with sources. Ultrasound power of 150 W for exposure time of 5 min increased collagen yield from chicken lung to 31.25% (Zou et al., 2020). The maximum collagen yield of chicken sternal was increased to 84.14%, after applying ultrasonic intensity of 2,990 $W \cdot cm^{-2}$ for exposure time of 36 min (Akram and Zhang, 2020). These studies indicated that UAE may be an alternative approach for yield improvement and process time reduction for collagen extraction. Consequently, ultrasound intensity, exposure time, and extraction time for collagen extraction by ultrasound should be investigated.

For biomedical application, triple helix structure is vital (Wiegand et al., 2016; Oropallo, 2019). It has been reported in the *ex vivo* study that collagen bundle of human adipose tissue was modified upon exposure to 100% of ultrasound amplitude for 10 min (Palumbo et al., 2011). Long ultrasonication time for 24 h has been reported to damage α-chain collagen from sea bass skin (Kim et. al., 2012). In

addition, exposure time of 36 min disrupted secondary structure of chicken sternal cartilage collagen (Akram and Zhang, 2020). Therefore, modification of structure induced by UAE should be explored that a proper process can be designed to minimize its effect, if any, on the extracted collagen.

1.2   Research objectives

The objectives of this study were:

1.2.1   To extract collagen from T using the conventional method by Ac and Pep.

1.2.2   To extract T collagen by UAE and to study the effect of ultrasound intensity, exposure time and extraction time on the T collagen structure.

1.2.3.   To biochemically characterize the extracted T collagen obtained from the conventional and UAE.

1.3   Research hypotheses

1.3.1   UAE would increase yield and shorten extraction time.

1.3.2   Ultrasound intensity and exposure time might affect biochemical properties of T collagen.

1.4   Scope of this study

Collagen extraction from T was performed by the conventional method using Ac followed by Pep. UAE of T collagen was also applied. Various ultrasound intensity (10.93, 17.87, and 31.27 $W \cdot cm^{-2}$), exposure time (10-30 min), and extraction time (12-48 h) were studied. Scanning electron microscopy (SEM) of extracted collagen was evaluated. Extracted collagen samples were biochemically characterized,

including amino acid composition, protein pattern (SDS-PAGE), secondary structure using Fourier transform infrared spectroscopy (FT-IR), native structure using circular dichroism spectroscopy (CD), and thermal denaturation using micro-differential scanning calorimetry (µDSC). In addition, liquid chromatography-tandem mass spectrometry (LC-MS/ MS) was also carried out to identify type of collagen.
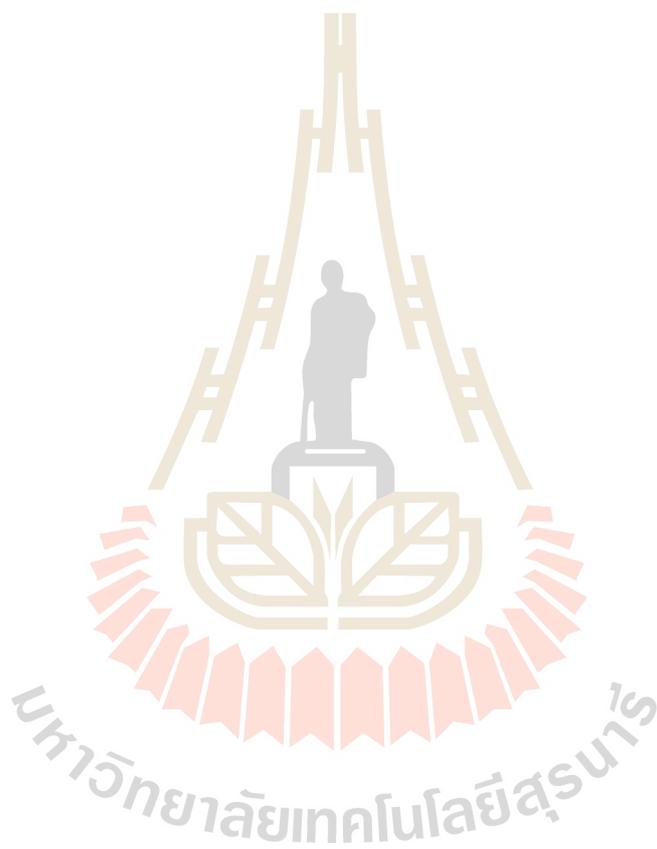
CHAPTER II

LITERATURE REVIEWS

2.1   Trachea

Respiratory organs including lungs and bronchi tubes play a role of gas exchange between external environment with internal organs. There are 2 components that provide function of respirational system. It can be divided into breathing and conducting section (Figure 2.1). Trachea is an important mediator organ of air passageway.
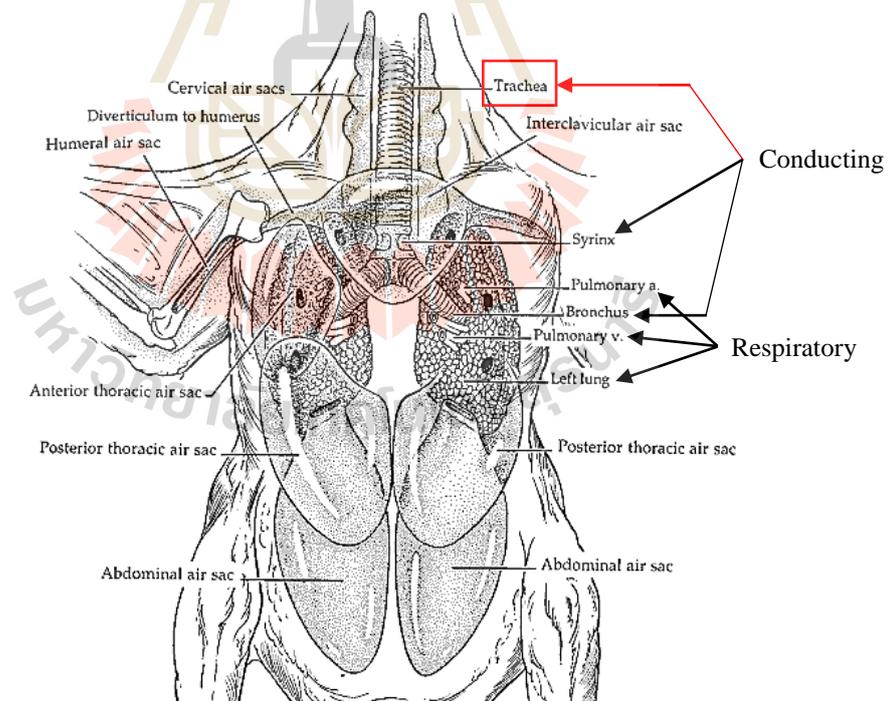
Figure 2.1   Physiology of respiratory system in poultry.
Source: https://www.quakerparakeetsociety.org [on-line].

2.1.1 Trachea physiology

Trachea commonly called windpipe is a long flexible cartilaginous tubular. Trachea has an inside diameter of 12 mm and a length of 10-13 cm in male and tends to be shorter in female (Furlow, and Mathisen, 2018). The trachea is usually incomplete hyaline cartilage, consists of various fibrous cartilages. The characteristic feature of trachea cartilage is relative regular of horseshoe-shaped or C-shaped ring, approximately 15-20 rings (Seelay, Stephens, and Tate, 2003). Moreover, the middle regions between cartilage rings are demonstrated to be H-shaped, which contains multi fibroelastic, elastic ligamentous membrane and bundles of smooth muscle, called trachealis muscle (Mescher, 2016). Contraction of the smooth muscle can narrow the diameter of the trachea for coughing, enunciation, and breathing.
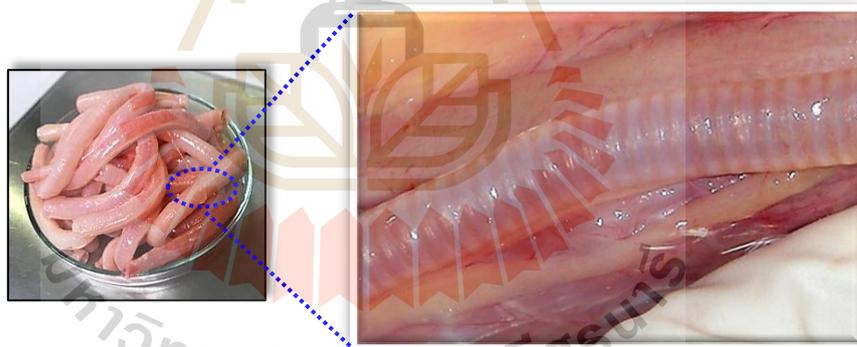
Figure 2.2   Chicken trachea.

Source: Cornell university college of veterinary medicine (2012).

2.1.2 Animal trachea

The number of cartilage ring is not constant in all species. Trachea of ruminants consist of 40-60 cartilage rings (Sisson, Grossman, and Getty, 1975; Byanet, Bosha, and Onoja, 2014; Bello et al., 2017; Prange, 2019), while 13-35 rings

are found in sea lion, porcine, monkey, and mouse trachea (Zeek, 1951; Dyce, Sack, and Wensing, 2017; Valverde and Christe, 2005; Navarro, Ruberte, and Carretero, 2017). Poultry normally comprises of longer and higher number cartilage rings than others, such as 100-130 rings in chicken (Figure 2.2), 120 rings in turkey (120 rings), 114-134 rings in duck, and 115-134 rings in seagull (Doğan and Takaci, 2018). Luo et al., 2017 reported that cartilage was a prolific source of collagen.

2.2 Cartilages

2.2.1 Structure and feature

Cartilages are special connective tissue, which contains resilient but moderate stiffness. It develops at the end of the joint, and is a component structure of the intervertebral discs, nose, ear, epiglottis, rib cages and trachea. Cartilage provides support to bone joints movement and shock absorbing (Alexander, 2017). It also involves to create skeleton preparation in embryo and new bone formation (Setiawati and Rahardjo, 2018). Cartilages have not contained nerve innervation, hence there is no sensation when it is injured or damaged (Grässel, 2014). Importantly, cartilage can also be considered an avascular tissue as does not contain blood vessel.

The extracellular matrix of cartilage contains collagen, interacting with glycosaminoglycan (heparin, hyaluronic acid, chondroitin-, dermatan-, heparan-, and keratan-sulfate) and proteoglycan (Figure 2.5). They are assembled to be a semi-rigid form that is easy to bound water. High content of bound water allows cartilage to serve as a shock absorber with high flexibility. Destruction of collagenous matrix is a major cause of joint disease such as osteoarthritis. (Henao-Murillo, Ito, and van-Donkerlaar, 2018).
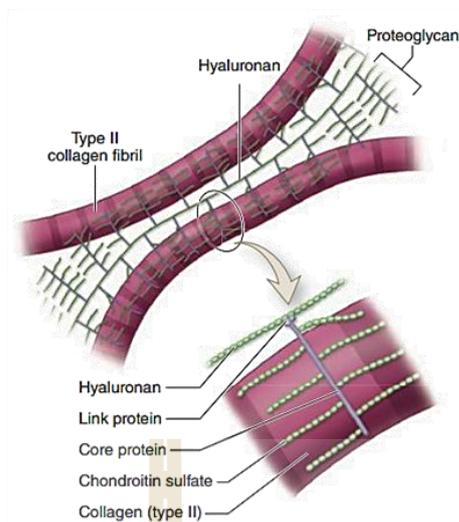
Figure 2.3 Cartilage matrix structure.

Source: Mescher (2016).

2.2.2 Different types of cartilage

Cartilages can be classified into three main types (Figure 2.4), depending on location, major cells, and main functions, as follows:

2.2.2.1 Hyaline cartilage

This cartilage is the most common of the three types. It constitutes homogeneous of collagen type II (Morris, Keene, and Horton, 2002). Hyaline cartilage is generally located in the articular surfaces of movable joints, in the walls of larger respiratory passages (nose, larynx, trachea, bronchi), and costal cartilage. Major functions of this cartilage are providing low friction surfaces in joints.

2.2.2.2 Elastic cartilage

Elastic cartilage is a structural cartilaginous tissue. It comprises an abundant network of elastic fibers, which offers to yellowish color for fresh cartilage, and is more flexible than hyaline cartilage (Pollard et al., 2017). This

cartilage is found in ears, walls of the external auditory canals, auditory tubes, epiglottis, and the upper respiratory tract. Supporting of soft tissues is the main function of elastic cartilage.

2.2.2.3 Fibrocartilage

Fibrocartilage contains a rich source of type I with type II collagen and usually founds in intervertebral discs and pubic symphysis (Maynard and Downes, 2019). Shortage of proteoglycans in the fibrocartilage matrix exhibits more acidophilic than that of hyaline and/or elastic cartilage. Fibrocartilage acts as lubricated cushions, shock absorbers, and compression resistance to prevent damage of intervertebral discs.
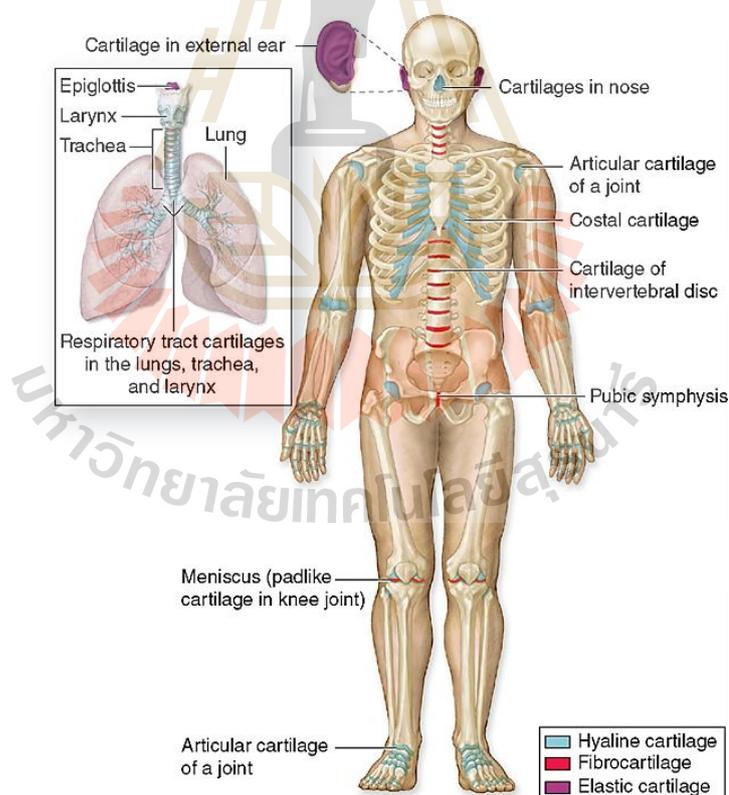
Figure 2.4   Distribution and category of adult cartilage.

Source: Mescher (2016).

2.3   Collagen

The extracellular matrix constitutes several macromolecules and collagen is an exclusive protein in cartilage of trachea. Collagen classifies as the stroma protein (Day, 2016). The word of collagen come from a Greek word, where "kola" means gum and "gen" means production (Khan, Khan, and Bey, 2011). Moreover, collagen is not apparent in unicellular organisms and plants (Silvipriya et al., 2015).

Collagen is the most abundant component in the animal kingdom, composing approximately 30-35% of total body protein and can be found in various organs, such as cornea, bone, cartilage, dentin, desmin, blood vessel, and etc. Most collagens are synthesized by the tendocyte, fibroblast, osteoblast, and a variety of other epithelial cells, whereas the collagens from cartilage are produced by chondrocyte cells (Akkiraju and Nohe, 2015). Collagen molecule has a special conformation, comprises of three α-helix chains, which fold into a triple helix as triple-helical region and telopeptide or non-helical region (Figure 2.5), measuring 9-26 amino acids in length (Sorushanova et al., 2019) and estimating to be 1.0-2.5% of collagen molecule. Collagen molecule can be expressed from a single gene for three chain (homotrimers) or from two or three different genes (heterotrimers).
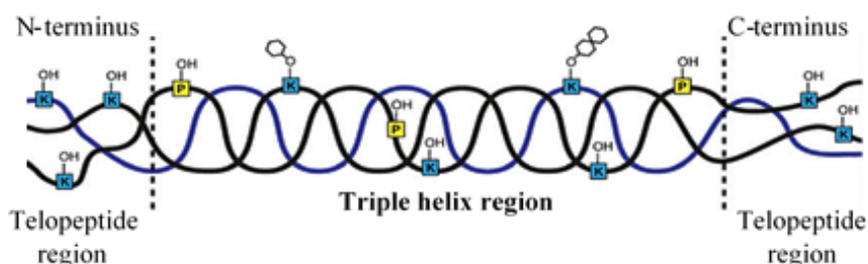
Figure 2.5   Collagen molecule structure.

Modified from: Gjaltema and Bank (2017).

2.3.1 Collagen biosynthesis

The pathway of collagen synthesis occurs in intra- and extra- cellular matrix of the cell. It is a complex multistep process, requiring the coordination of biochemical modifications and intergrades by various enzymes (Figure 2.6).

2.3.1.1 Intracellular events

The initial step, involves transcription of mRNA molecules and alternative splicing. Then, nascent collagen enters into the lumen of the endoplasmic reticulum. Cysteines at C-propeptide will form disulfide bonds and formation triple helix structure, which started at the C-terminus (Raghunath, Bruckner, and Steinmann, 1994).
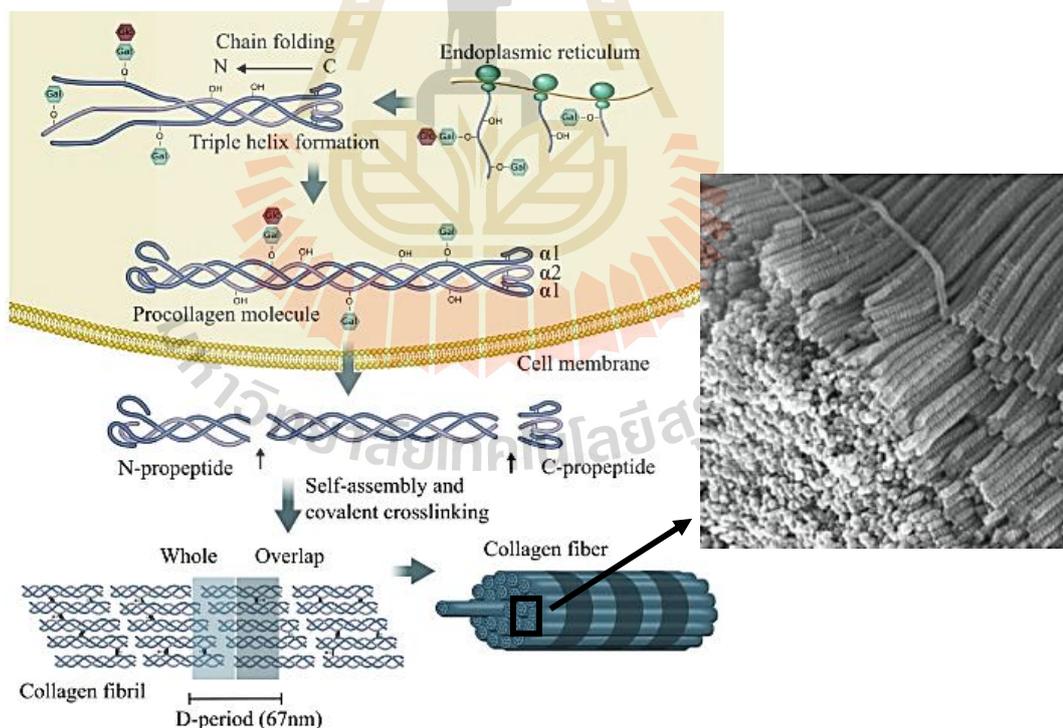
Figure 2.6 Schematic of collagen formation.
Modified from: Mescher (2016); Karsdal, (2019).

2.3.1.2 Post-translational modification

Major post-translational modifications (PTMs) of collagen molecule is hydroxylation. This state occurs before formation to triple helix procollagen. PTMs leads to stability of collagen molecule and assembly conformation via amino acid. Hydroxylation can occur on proline (Pro) and lysine (Lys) residues for forming into hydroxyproline (Hyp) and hydroxylysine (Hyl) on the minimum sequence of Gly-X-Y motif. The lack of that motif on the telopeptides region, lead to low of Pro and Lys hydroxylation (Gjaltema and Bank, 2017).

The signature oxidoreductase enzymes for hydroxylation activity are procollagen lysine dioxygenase (lysyl hydroxylase) and procollagen proline dioxygenase (prolyl hydroxylase). Prolyl hydroxylase can divide into 2 families. There are prolyl 4-hydroxylase (C-P4Hs), which catalyzes proline hydroxylation at Y position, while X position of Gly-X-Hyp motif has been catalyzed by prolyl 3-hydroxylase (C-P3Hs). In addition, both enzymes require 2-oxoglutarate (α-ketoglutarate), O_2, Fe^{2+}, and ascorbate for their hydroxylation activity (Figure 2.7).

2.3.1.3 Extracellular events

When trimerization and PTMs occurres, procollagen transports through the Golgi apparatus, packs in a vesicle, and secrets to extracellular space by exocytosis via microtubules assisting. During secretion, N- and C-propeptides are removed by specific metalloproteinase, called procollagen peptidases, especially are N- and C-proteinase. The N-proteinase cleaves N-terminal propeptides between Pro and Gln residues (Sorushanova et al., 2019), while Ala and Asp or Gly and Asp at C-terminal propeptides have been cleaved by C-proteinase (Li et al., 1996).
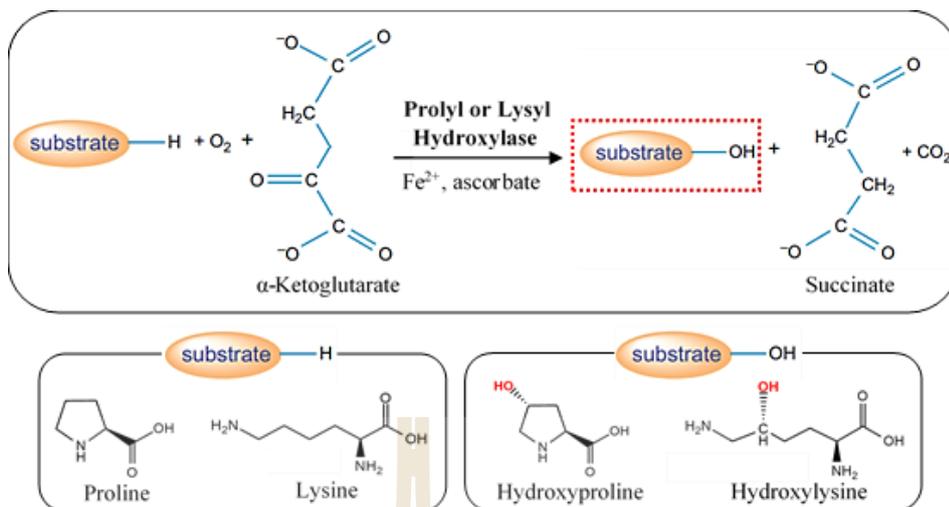
Figure 2.7   Hydroxyproline and hydroxylysine formation of collagen protein.

Modified from: Bhangavan and Ha (2015).

2.3.1.4 Supramolecular assembly

After proteolytic cleavage, procollagen is transformed to tropocollagen (collagen molecule). Tropocollagen procreates to collagen fibrils by self-assembly. Fibril structure is encouraged formation by intermolecular cross-linkages (covalent bond) between the collagen molecules, which is an oxidative deamination by lysyl oxidase (Kumari, Panda, and Pradhan, 2017). Finally, collagen fibrils are formed to collagen fibers.

2.3.2 Collagen diversity and their distribution

The hallmark of collagen molecule is three α-polypeptide chains. The collagen monomer is a cylindrical protein of 300 kDa, 1.4 nm of diameter, and approximate length of 280-300 nm in most types, except for type IV, VI, VII, X, XII, XIV with various lengths (Figure 2.8). Around 29 distinct types of collagen have been

currently identified, which are encoded by 46 distinct types of separate genes. Type I to V collagen are the most ubiquitous with type I is the highest quantity.
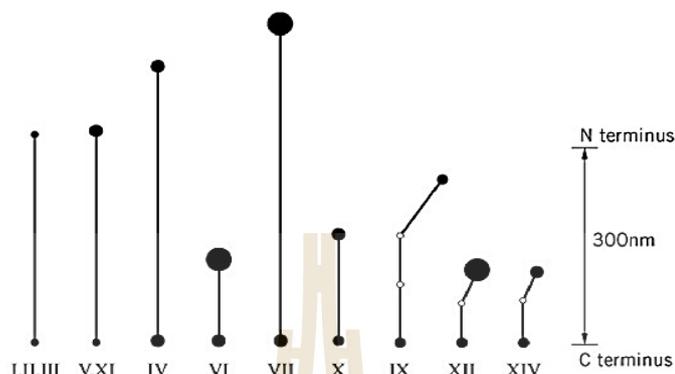
Figure 2.8   Approximate length of triple-helix collagen on various types.
Source: Burgeson and Morris (1987).

Different types of collagen have been grouped into 9 classes, including fibrillar, beaded filament, normal network, hexagonal network, anchoring, fibril-associated collagen with interrupted triple helices (FACITs), membrane-associated collagen with interrupted triple helices (MACITs), multiple triple-helix domains and interruptions (MULTIPLEXIN), and miscellaneous, which are based on their molecular structure, distribution (Table 2.1), and characteristic model (Figure 2.9). Depending on genetic types, the triple-helix structure can be a major or minor portion of molecule, other regions and terminal domains can involve with bioactive molecule, non-collagenous, transmembrane, as well as thrombospondin domains, and etc. (Hulmes, 2008).

As mentioned above, collagen molecules can be homotypic, consists of three identical chains, such as type II or III collagens, while heterotypic collagen as type I, IV, and V, compose of up to two and/or three genetically divergent chains.

Individual chains are identified by the following nomenclature of $\alpha g(N)_n$ model, where g, N, and n are the collagen gene, Roman number (indicating collagen type), and number of the chain, respectively (Linsenmayer, 1981). For example, the chain component of type I collagen, is two $\alpha 1$ chains with one of $\alpha 2$ chain, which is designated as $\alpha 1(I)_2 \, \alpha 2(I)$, while type II collagen as homotypic is three analogous chains, designate to $\alpha 1(II)_3$.

Table 2.1 Type and distribution sources of collagen.

Class	Types	Molecular composition	Distribution
Fibrillar	I	$\alpha 1(I)_2 \, \alpha 2(I)$	Skin/bone/tendon/cornea
	II	$\alpha 1(II)_3$	Cartilages
	III	$\alpha 1(III)_3$	Blood vessels/intestine
	V	$\alpha 1(V)_3$ or $\alpha 1(V)_2 \, \alpha 2(V)$ or $\alpha 1(V) \, \alpha 2(V) \, \alpha 3(V)$	Placenta
	XI	$\alpha 1(XI) \, \alpha 2(XI) \, \alpha 3(XI)$	Cartilages/intervertebral disc
	XXIV	-	Bone/cornea
	XXVII	-	Embryonic cartilage
Beaded filament	VI	$\alpha 1(VI) \, \alpha 2(VI) \, \alpha 3(VI)$	Muscle/lungs
Network	IV	$\alpha 1(IV)_2 \, \alpha 2(IV)$ $\alpha 3(IV) \, \alpha 4(IV) \, \alpha 5(IV)$ $\alpha 5(IV)_2 \, \alpha 6(IV)$	Basement membrane
	X	$\alpha 1(X)_3$	Hypertrophic cartilage
Hexagonal network	VIII	$\alpha 1(VIII)_3$ or $\alpha 1(VIII)_2 \, \alpha 2(VIII)$	Brain/heart/kidneys

Table 2.1   (Continued).

Class	Types	Molecular composition	Distribution
	VII	$\alpha1(VII)_2\,\alpha2(VII)$	Cervix/oral mucous/bladder
	IX	$\alpha1(IX)\,\alpha2(IX)\,\alpha3(IX)$	Vitreous body/cornea/cartilages
Anchoring	XII	$\alpha1(XII)_3$	Tendon/perichondrium
	XIV	$\alpha1(XIV)_3$	Liver/lungs/vessel wall
	XVI	-	Bone/skin
	XIX	-	Human rhabdomyosarcoma
	XX	-	Corneal epithelium/embryonic skin
FACITs	XXI	-	Stomach/kidneys
	XXII	-	Tissue junctions
	XXVI	-	Testis/ovary
	XIII	-	Eyes/heart/hair follicle
MACIT	XVII	$\alpha1(XVII)_3$	Hemidesmosomes in epithelia
	XXIII	-	Heart/retina
	XXV	-	Brain/testis
MULTIPLEXIN	XV	-	Pancreas/smooth muscle
	XVIII	-	Liver/lungs/basement membrane
Miscellaneous	XXVIII	-	Sciatic nerve

Note: Fibril-associated collagen with interrupted triple helices (FACITs); membrane-associated collagen with interrupted triple helices (MACITs); multiple triple-helix domains and interruptions (MULTIPLEXIN);

Source: Shoulders and Raines (2009); Raman and Gopakumar, (2018).
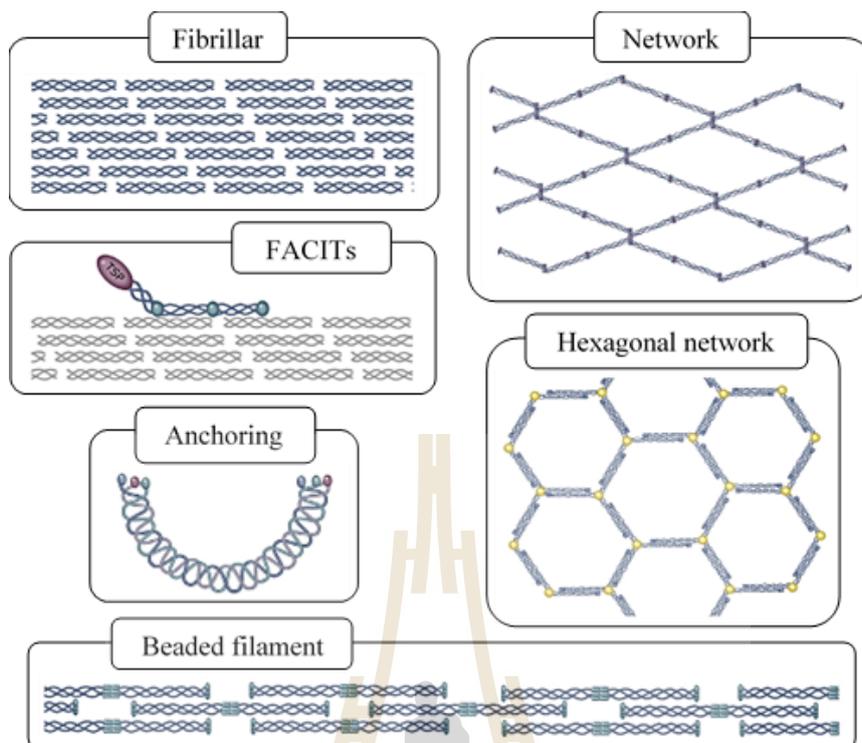
Figure 2.9   Collagen classification model on super molecular structure; FACITs is fibril-associated collagen with interrupted triple helices.

Modified from: Fidler, Boudko, Rokas, and Hudson (2018); Karsdal (2019).

2.3.3   Collagen composition and conformation

2.3.3.1   Primary structure

The individual amino acid subunits are conjugated by amide linkages as peptide bonds. Polypeptides have been arranged on special amino acid triplets. They have a strict building block of Gly-X-Y repeating, where X and Y can be any amino acid but mainly are Pro and Hyp (Figure 2.10). The Gly-X-Y and Gly-Pro-Y motifs constitute approximately 44% in each motif, while 12% remaining is the sequence of Gly-Pro-Hyp (Sorushanova et al., 2019).
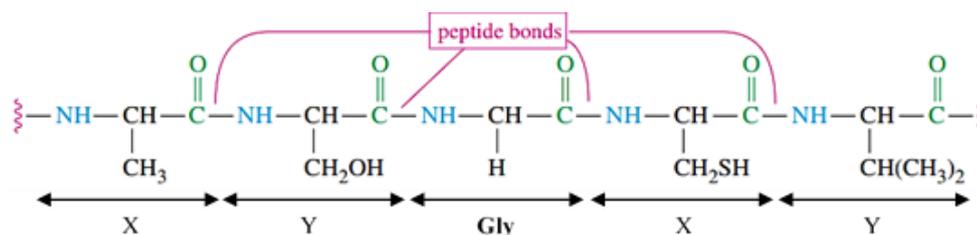
Figure 2.10   Specific Gly-X-Y pattern of collagen primary structure.

Modified from: Wade (2013).

Amino acid composition of collagen is unique compared to other proteins. Major amino acids are Gly, Ala, Pro, and Hyp, whereas histidine (His), hydroxylysine (Hyl), methionine (Met), and tyrosine (Tyr) are relatively low content. Cysteine (Cys) is considered as a minor amino acid in collagen with about 4-8 residues, which discover on procollagen of human fibroblast, type III collagen, and blue shark cartilage (Church and Tanzer, 1975; Brown, Farrell, and Wildermuth, 2000; Bu et al., 2017). Interestingly, tryptophan (Trp) has not been found in collagen (Gorgieva and Kodol, 2011; Gauza-Włodarczyk, Kubisz, and Włodarczyk, 2017). Amino acid profiles of collagen from various coproducts derived from animals are shown in Table 2.2.

Ala is the second highest amino acid after Gly but it does not provide any additional stability (Bhattacharjee and Bansal, 2005). Nevertheless, computational study demonstrated that substituting Gly residues by d-alanine amino acid would stabilize the triple helix (Tsai, Xu, and Dannenberg, 2005). Aspartic acid/asparagine (Asp/Asn), glutamic acid/ glutamine (Glu/Gln), leucine (Leu), and phenylalanine (Phe) are preferred at the X position, whereas arginine (Arg), threonine (Thr) and lysine (Lys) will appear in the Y position (Puri, 2011; Ghosh et al., 2012). The residues at Y

position can promote stability, including assemblies of triple helices through additional interactions. The three repeating of Gly residues, is a critical requirement for molecular structure of collagen. Gly can create a close packing structure along the central axis of the triple helix molecule (Gelse, Pöschl, and Aigner, 2003). Hyp is also an unique amino acid that can only be found in collagen. It is recognized that collagen can be quantified indirectly through Hyp content (Cissell, Link, Hu, and Athanasiou, 2017). Hence, Hyp is an important indicator of collagen purity and possible source for collagen extraction. Meyer (2019) stated that trimerization requires all amino acids in *trans*-configuration. The *cis*-isoform of Pro and Hyp requires more energy for polymerization. In addition, the alignment of cis-isoform for X-Pro and X-Hyp pattern presents 16 and 8% denaturation of telopeptide region, respectively. Therefore, amino acid compositions can be associated with the thermal characteristics of collagen, as described in section 2.6.2.

2.3.3.2 Secondary, tertiary, and quaternary structure

When the primary structure has been constructed, the amount of 1,000 amino acids are folded to be polypeptide chain as α-helix chain with left-handed twisting (Figure 2.11A). An α-helix structure is folded by hydrogen bonds between carbonyl and the amino group in every 3.6-4.0 amino acid residues in each helical turn (Banerjee, Radvar, and Azevedo, 2018). Three α-chains intertwine, resulting in superhelix or triple-helix structure of collagen (Figure 2.11B). Gly residues are arranged in the core center of triple helix structure, while all side chains of other amino acids are aligned to outer positions (Gelse, Pöschl, and Aigner, 2003). Collagen molecules are able to undergo self-assembly into a collagen fibril (supramolecular) by creates quarter-stagger package pattern (Figure 2.11C).

Intermolecular cross-links play an important role in stabilization of this structure as detailed in collagen stability section 2.3.4.2.
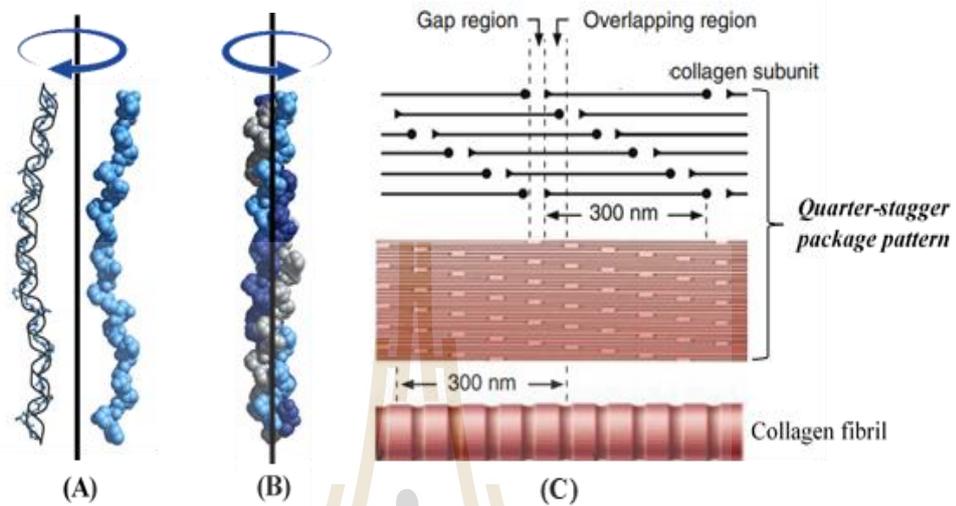
Figure 2.11 Left-handed (A), right-handed (B) helix configuration, and quarter-stagger package pattern (C) of collagen structure.

Modified from: Mescher (2016); Nelson and Cox (2017).

Table 2.2 Amino acid composition of collagen from various animals (residue/ 1,000 residues).

| Tissues/ Animal

Amino Acids | Tail

Rat[1] | Cartilage | | Feet

Chcicken[4] | Scale | | Bone

Alligator[7] | Skin | | | | Tendon

Bovine[11] |
		Hoki[3]	Bester sturgeon[4]		Sea bass[5]	Silver carp[6]		Golden carp[8]	Deer[9]	Porcine[1]	Calf[10]	
Ala	105	89	91	127	133	123	103	120	99	112	119	119
Arg	50	51	51	50	51	51	47	53	19	48	51	52
Asp/ Asn	52	50	51	28	42	43	37	48	39	51	45	46
Glu/ Gln	84	89	92	79	69	66	66	68	66	75	75	65
Gly	**302**	**277**	**324**	**344**	**337**	**344**	**367**	**336**	**339**	**321**	**330**	**330**
His	6	4	6	5	7	5	3	4	12	5	5	5
Hyl	8	15	23	NS	6	7	19	6	NS	6	7	7
Hyp	**91**	**105**	**77**	**99**	**89**	**83**	**87**	**79**	**108**	**130**	**95**	**87**
Ile	13	12	13	11	9	10	11	11	11	12	11	12
Leu	30	41	31	24	19	21	20	22	23	29	23	25
Lys	30	15	16	38	26	26	30	26	30	30	26	28
Met	7	16	8	5	14	14	8	12	7	7	6	6
Phe	15	14	13	12	12	13	12	13	11	14	3	11
Pro	**115**	**123**	**123**	**117**	**106**	**119**	**110**	**120**	**121**	**81**	**121**	**136**
Ser	40	46	35	23	33	32	46	35	34	31	33	30
Thr	23	26	22	19	24	23	22	23	19	19	18	16
Tyr	6	1	4	NS	3	2	2	3	2	4	3	4
Val	24	18	18	19	20	17	15	21	19	25	21	21

NS is data not shown.

Source: [1]Meyer (2019); [2]Cumming, Hall, and Hofman (2019); [3]Meng et al. (2019); Zhou et al. (2016); [5]Chuaychan, Benjakul, and Kishimura (2015); [6]Wu, Kong, Zhang, and Chen (2019); [7]Wood et al. (2008); [8]Ali et al. (2018); [9]Lodhi et al. (2018); [10]Li et al. (2018); [11]Ju et al. (2020).

2.3.4 Stability of collagen

2.3.4.1 Intra-molecular crosslinks

Triple helix of collagen is stabilized by formation of two inter-chain (Figure 2.12A). The individual α-chains are involved to each other by single intra-strand linking with hydrogen bonds between the amino group of Gly N-H and the carbonyl of X residue ($N-H_{(Gly)}\cdots O=C_{(X)}$ model) (Ferreira, Gentile, Chiono, and Ciardelli, 2012).
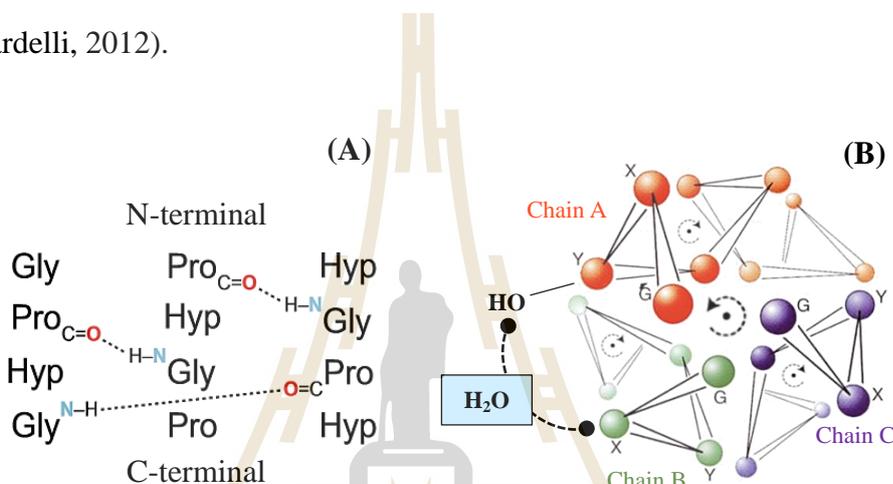
Figure 2.12 Intra-molecular crosslinks (A) and water bridge (B) along triple-helix structure.

Modified from: Beck and Brodsky (1998); Shoulders and Raines (2009).

Moreover, water molecules can form additional hydrogen bonds via hydroxyl (-OH) group of Hyp residues, hydroxyl group of serine (Ser) and Thr (Figure 2.12B). Thus, extra hydrogen bonds via water bridge is a supporter that upholds collagen stability (Ramachandran et al., 1973; Mizuno, Hayashi, and Bachinger, 2003).

2.3.4.2 Inter-molecular crosslinks

Collagen is stabilized through the action of four crosslinks. Two intra-molecular crosslinks (hydrogen bond) initiate in the helical regions.

Furthermore, two more are inter-molecular crosslinks (covalent bond) and occur on the telopeptide regions, such as enzymatic and non-enzymatic crosslinks.

2.3.4.2.1 Enzymatic crosslinks

To stabilize collagen fibril, intermolecular covalent crosslinks between individual collagen molecule has been generated by lysyl oxidase on Lys with Hyl or Lys with Lys residues in collagen telopeptide (Figure 2.13A). The intermolecular crosslinks can be bonded between the telopeptides region with other helical regions of neighbor molecules.
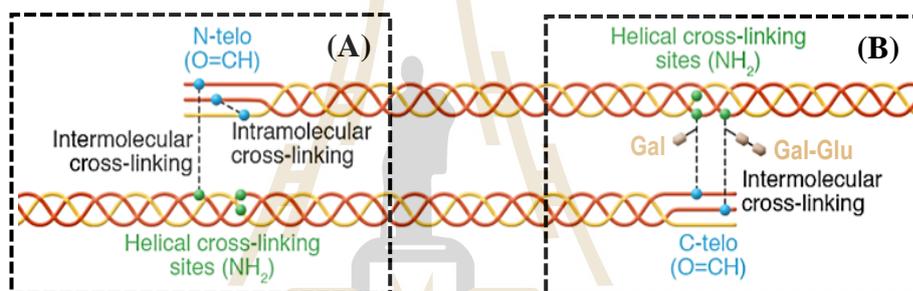
Figure 2.13 Covalent crosslink (A) and O-linked glycosylation (B) between collagen molecule.

Modified from: Yamauchi, Barker, Gibbons, and Kurie (2018).

After deamination, Lys and Hyl residues are converted to aldehydes allysine and hydroxyl-allysine, respectively. When both aldehydes react with Lys and Hyl residues via shift base and amadori arrangement, divalent cross linking continuously occurred, and resulting in crosslink product of pyrroles or pyridinolines, especially lysyl pyridinoline (LP) and hydroxylysyl pyridinoline (HP) (Figure 2.14). Mature cross-linkages ($\geq$ trivalent) are associated with life, species, age, gender, activity, and physical state (Tan et al., 2003). Typical rigid and toughness of connective tissues,

particularly tendons, cartilage and bone, are basic structure formed by many cross-linkages. Additionally, α-chain dimers and/or trimers are produced from intramolecular crosslinks between telopeptide region, which they can be observed by protein pattern on migration of β- and γ- bands.
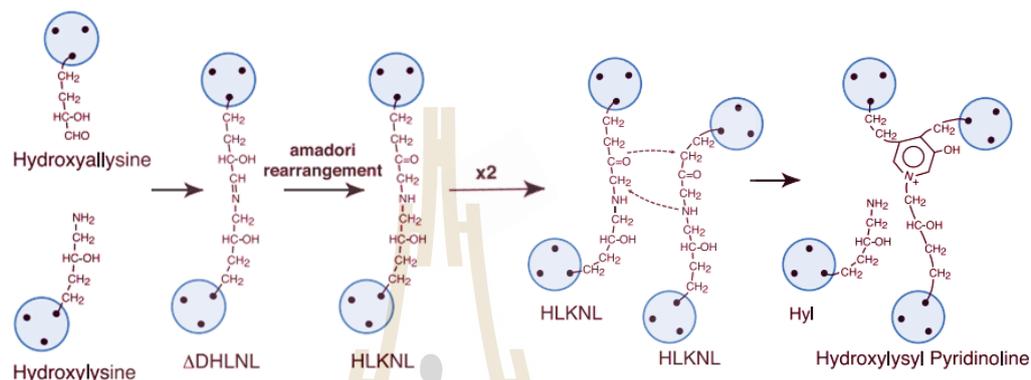
Figure 2.14   Intermolecular crosslinks formation via pyridinoline products; delta-dihydroxylysylnonorleucine (ΔDHLNL); hydroxylysino-ketonorleucine (HLKNL).

Modified from: Eyre, Weis, and Wu (2010).

2.3.4.2.2 Non-enzymatic crosslinks

This crosslink is commonly known as *O*-linked glycosides or sugar-mediated crosslink and specifically modify with Hyl residues (Figure 2.13B). Majority of sugars involved in collagen glycosylation are galactose and/or glucose with mono-and/or disaccharide forms. Collagen glycosylation is catalyzed by glycosyltransferases, producing galactosyl-hydroxylysine (G-Hyl) and glucosyl-galactosyl-hydroxylysine (GG-Hyl) (Figure 2.15). The first carbon atom

(C-1) of galactose is bonded with hydroxyl group of Hyl by β-glycosidic bond, while glucose is linked by α-glycosidic bond (Yamauchi et al., 2019).
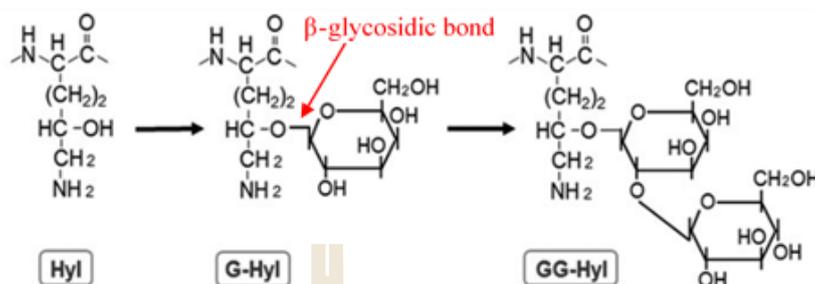
Figure 2.15   Collagen glycosylation with galactose via β-glycosidic bond; galactosyl-hydroxylysine (G-Hyl) and glucosyl-galactosyl-hydroxylysine (GG-Hyl).

Modified from: Yamauchi and Sricholpech (2012).

Sugar plays an important role in the arrangement of collagen fibrils formation (Ruotsalainen et al., 2006). The network forming collagen type IV of basement membrane and type V shows high level of Hyl residues as well as collagen glycosylation, corresponding to disorder structure (Jürgensen et al., 2011). Nevertheless, the highly organized fibrillar collagens as type II has a lower glycosylation level than type VI and V but higher than type I and III collagen in skin and tendon (Sipilä et al., 2007; Yamauchi and Sricholpech, 2012). Glycation typically modulates collagen properties and biomechanical behavior. Enhancing the stability of collagen molecule is an advantage but the most damaging effect is due to glycoside intermolecular crosslinks between the triple helices, which decrease flexibility, permeability and turnover of biological molecule (Sorushanova et al., 2019).

2.4 Source of collagen

Animal slaughter house and fish processing industry generate coproduct materials from varies tissues, such as bones, cartilages, tendons, skins, scales, fins, feet, blood, and internal organs. They are normally produced to animal feed, bio-fuel, and fertilizers (Schmidt et al. 2016), despite of relatively high collagen. Thus, the collagen extraction can add high value and reduces environmental waste.

2.4.1 Land animals

The most common coproduct for collagen extraction is skin, bone, and tendon, obtained from cattle, bovine, buffalo, porcine, caprine, and ovine (Santos et al., 2013; Ran and Wang, 2014; Rizk and Mostafa, 2016; Zhu et al., 2020; Vidal et al., 2020; Ju et al., 2020). Porcine skin is used for manufacture of collagen and gelatin since 1930, and continues to be an important material for industrial production (Gómez-Guillén, Giménez, López-Caballero, and Montero, 2011). However, hoof foot animals have possible risks of disease transmission, such as, bovine spongiform encephalopathy (BSE), transmissible spongiform encephalopathy (TSE), and foot mouth disease (FMD). Additionally, collagen from porcine is prohibited from Muslim and Jewish market (Yamamoto, Uemura, Sawashi, Mitamura and Taga, 2016). For the production process and utilization of collagen, this is the concerning point of safety in the industrial process and commercial trading.

2.4.2 Poultry

Chicken is one of important protein source. Approximately 37% of chicken coproducts are generated (Toldrá, Aristoy, Mora, and Reig, 2012). Skin, sternal, articular cartilage, knee bone, feet and lung from chick, broiler chicken, spent hen and rooster have confirmed as a source of collagen. (Zuo et al., 2016; Munasinghe

and Schwarz, 2017; Hong et al., 2017; Cordeiro et al., 2020; Zhang and Akram, 2020; Zou et al., 2020). Moreover, collagen extraction from bones, tendon, and duck feet has been studied. In addition, emu skin, ostrich trachea and duck larynx have been reported to be a source of collagen (Jaroenviriyapap, 2010; Nagai, Tanoue, Kai, and Suzuki, 2015; Kim et al., 2016; Theng et al., 2018).

2.4.3 Aquatic animals

The extraction of collagen from aquatic animals has been widely studied. Skin, scale, fin, bone, and head are major coproducts, including (1) skin of Nile tilapia, hybrid sturgeon, and bluefin tuna; (2) scale of silver carp and sardine; (3) cartilage of Siberian sturgeon and hoki fish; (4) bone of bigeye tuna; (5) air bladder of striped catfish; (6) body of sea surf clam shell are some sources of collagen (Song et al., 2019; Wei et al., 2019; Tanaka et al., 2018; Wu et al., 2019; Hamdan and Sarbon, 2019; Luo et al., 2018; Cumming Hall and Hofman, 2019; Ahmed, Haq, and Chun, 2019; Divya et al., 2018; Wu et al., 2019). Nevertheless, collagens from aquatic animals contain lower thermal stability than those extracted from land animals (Veeraraj, Arumugam, Ajithkumar, and Balasubramanian, 2017).

2.4.4 Other animals

Collagen extracted from reptiles and amphibians also have been considered. Alligator and leg frog meat are main ingredients in some food, which is popularly consumed in China, France, Belgium, Luxembourg and the south of United States, whereas alligator bone and frog skin are discarded. However, the major composition of these coproducts is type I collagen (Wood et al. 2008; Zhang and Duan, 2017). Soft-shelled turtle meat is considered as a traditional medicine with high nutritional value, especially collagen (Yamamoto et al., 2016).

2.5 Collagen isolation

There is a growing interest in the processes used to produce collagen, including (a) human or animal cells grown in *vitro* tissues, (b) recombinant expression, (c) direct peptide synthesis, and (d) extract from various animal tissues. Advantages and disadvantages of each method of collagen formation are summarized on Table 2.3.

Table 2.3 Advantages and disadvantages of different collagen extraction.

Extraction types	Advantages	Disadvantages
Cell-produced collagen [a]	Autologous	Low yield and many factors handling
Synthetic collagen [a]	Rule out of allogeneic and xenogeneic	Low yield, assembly, and high production cost
Recombinant collagen [a, b]	Low immunogenicity	Low yield and stability
Extracted collagen [a, c]	High yield and antigenic site can be removed by pepsin	Long extraction time and multi steps

Source: (a) Sorushanova et al. (2019); (b) Wang et al. (2017); (c) Lynn,Yannas, and Bonfield (2004).

Tissue extracted collagen has received a lot of attention to study. The extraction process can be described as follows:

2.5.1 Preparation of raw material

Complex biomaterials contain high number of natural polymeric components as proteins, pigments, lipids, and inorganic substances. Before collagen extraction, pre-treatment of raw materials is required to remove these non-collagenous

components. Major pretreatments of raw materials from various animal coproducts are summarized in Table 2.4.

2.5.1.1 Non-collagenous proteins and lipids displacement

Both alkaline and neutral salt solutions were used to eliminate non-collagenous proteins. Nevertheless, uncross-linked collagens can be removed by neutral salt solutions, leading to a low yield of collagen and is not widely practiced. (Regenstein and Zhou, 2007). Diluted solution of sodium hydroxide (NaOH) and calcium hydroxide (Ca(OH)$_2$) are two alkalis that are frequently used for pretreatment (Zhou and Regenstein, 2005; Chinh et al., 2019). NaOH causes a significant swelling of tissue. Previously, 0.05 and 0.1 M NaOH can be successfully used to remove non-collagenous proteins with minimal loss of Hyp and without collagen degradation (Sato, Yoshinaka, Sato, and Shimizu, 1987; Liu et al., 2015). Lipids are contained in various coproducts, especially skin and soft tissues (lung, body, and air bladder). Lipid in raw materials are obstructive of collagen extraction. Solvents like 10% *N*-butyl or ethyl or isopropyl alcohol and hexane can be applied to remove lipids (Zhao, Zhang, Li, and Liu, 2009; Yiin, Huda, Ariffin, and Easa, 2014; Wei et al., 2019; Zhu et al., 2020).

2.5.1.2 Demineralization

Scale, bone, cartilage, and body wall of invertebrate are mineralized materials, constituting calcium, magnesium, ferrous, zinc, hydroxyapatite, and carbonate. Demineralization is therefore necessary. Chelating agents (ethylenediaminetetraacetic acid: EDTA) and/or inorganic solvents (hydrochloric acid: HCl) are mainly applied (Lin et al., 2017; Wu et al., 2019; Akram and Zhang, 2020).

2.5.2 Collagen extraction

Collagen extraction can divide into 2 different methods. The first method is extraction by acid. Collagen contains higher glycine, polar and hydroxylated amino acid residues than hydrophobic residues. Then, collagen can be swelled polar solution (Johnston-Banks, 1990). Therefore, acid solution is regularly used for collagen extraction. In addition, proteinase-aided extraction is the second method that are commonly used, particularly pepsin is widely applied.

2.5.2.1 Acid-solubilized collagen (ASC)

Collagen from any biological tissue can be extracted by organic acids or inorganic acids. Collagen extraction with different acids (HCl, acetic, citric, and lactic acid) has been studied (Cheng et al., 2009; Tan and Chang, 2018). Acetic acid at 0.5 M showed the highest extraction yield. High collagen extractability corresponds with pH 2.0-4.0 (Song et al., 2014; Jeevithan et al. 2015), whereas extremely low pH resulted in collagen digestion and denaturation during extraction.

When the collagenous tissue is treated with acetic acid, hydronium (H_3O^+) ions prefers the accessibility of water to collagen fibers. This water is held by electrostatic forces between charged polar groups (electrostatic swelling) or hydrogen bonding between uncharged polar groups (Gómez-guilloen and Montero, 2001; Hong et al., 2017). Then, it leads to increase repulsion between polypeptide chain (α-helix) and solubilization (Figure 2.16).

Table 2.4 Pretreatment process applied in collagen extraction of various coproducts.

Sources	Pretreatment procedures	References
Sea cucumber	0.1 M Tris-HCl (pH 8.0) at a ratio of 1:20 (w/v) for 72 h 0.1 M NaOH at a ratio of 1:20 (w/v) for 24 h	Lin et al. (2017)
Soft-shelled turtle	0.05 M Tris-HCl (pH 8.0) at a ratio of 1:20 (w/v) for 12 h 0.5 M Na_2CO_3 at a ratio of 1:20 (w/v) for 24 h 0.3 M Na_2EDTA (pH 7.4) at a ratio of 1:20 (w/v) for 24 h 10% isopropyl alcohol at a ratio of 1:20 (w/v) until pH 7.0	Zou et al. (2017)
Silver carp scale	0.1 M NaOH at a ratio of 1:20 (w/v) for 24 h 0.6 M HCl at a ratio of 1:20 (w/v) for 1 h	Wu, Kong, Zhang, and Chen (2019)
Golden carp skin	0.1 M NaOH at a ratio of 1:15 (w/v) for 8 h 10% Butyl alcohol at a ratio of 1:15 (w/v) for 16 h	Ali, Kishimura, and Benjakul (2018)
Puffer fish skin	0.1 M NaOH at a ratio of 1:10 (w/v) for 6 h	Iswariya, Velswamy, and Uma (2018)
Red snapper skin	0.1 M NaOH at a ratio of 1:10 (w/v) for 12 h	Zaelani et al. (2019)
Bester sturgeon notochord	99.5% ethyl alcohol at a ratio of 1:10 (w/v) for 24 h 0.1 M NaOH at a ratio of 1:50 (w/v) for 12 h	Meng et al. (2019)
Clam shell body	0.1 M NaOH at a ratio of 1:10 (w/v) for 24 h	Wu, Guo, Liu, and Chen (2019)
Bigeye tuna bone	0.1 M NaOH at a ratio of 1:10 (w/v) for 24 h	Ahmed, Haq, and Chun (2019)
European Hake bone	0.1 M NaOH at a ratio of 1:10 (w/v) for 24 h	Blanco et al. (2019)
Bovine tendon	50 mM Tris-NaCl (pH 7.5) for 12 h	Ju et al. (2020)
Chicken lung	20% NaCl at a ratio of 1:20 (w/v) for 8 h 0.5 M Na_2CO_3 at a ratio of 1:20 (w/v) for 24 h 0.3 M Na_2EDTA (pH 7.4) at a ratio of 1:20 (w/v) for 24 h 10% isopropyl alcohol for several times	Zou et al. (2020)
Lamp bone with cartilage	0.1 M NaOH at a ratio of 1:20 (w/v) for 48 h 0.5 M Na_2CO_3 (pH 7.5) at a ratio of 1:10 (w/v) for 5 days 10% Butyl alcohol at a ratio of 1:10 (w/v) for 48 h	Vidal et al. (2020)
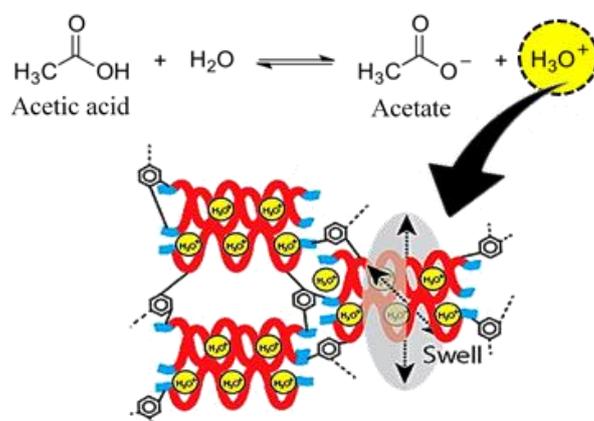
Figure 2.16 Swelling of collagen molecule by hydronium ion repulsion.

Source: Hong et al. (2017).

2.5.2.2 Pepsin-solubilized collagen (PSC)

The number of cross-links in collagen increased with age and habitat of animals, corresponding to its high stability. Furthermore, starvation can increase a greater collagen cross-link (Foegeding et al., 1996). Raw material of high age and land animals comprises of high intermolecular cross-linkages via covalent bonds, resulting in low yield. Only acid solubilization cannot completely solubilize collagen. Thus, they are required more severe process to disrupt the crosslinks and promote collagen solubilization.

To increase collagen extraction, various proteinases have been used, including hyaluronidase, papain, trypsin and pepsin (Liu, Andarawis-Puri, and Eppell, 2016; Khora and Kirti, 2017; Dhakal et al., 2018). Pepsin-aided extraction is universally utilized, because the optimal activity of pepsin is acidic condition. Moreover, high amounts of crosslinks at telopeptide region, were specifically cleaved by pepsin (Figure 2.17). The collagen obtained with pepsin treatment is referred as PSC.
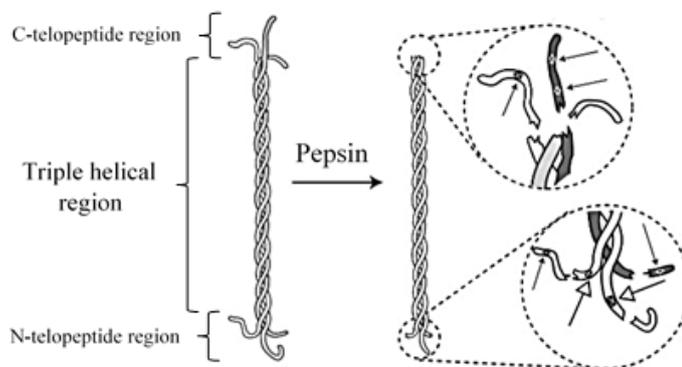
Figure 2.17 Collagen solubilization by cleavage of telopeptide by pepsin.

Modified from: Lynn, Yannas, and Bonfield (2004).

Pepsin initially attacks the N-telopeptide and C-telopeptide is more slowly digested later (Weiss, 1976). At the N-telopeptide region, Gly-Ile position can be cleaved by pepsin (Qian et al., 2017). In contrast, pepsin cleaves on Asp-Phe position at C-telopeptide region (Acton, 2011). It confirms that most inter-molecular crosslinks of collagen originate through the telopeptide region and these crosslinks are interrupted by pepsin digestion (Benjakul, Nalinon, and Shahidi, 2012). Disintegration of non-helical region results in yield improvement without damaging their integrity of triple helix structure (Jongjareonrak et al., 2005; Nalinanon, Benjakul, Visessanguan, and Kishimura, 2007). Yield of acid- and pepsin-soluble collagen from various animal coproducts are shown in Table 2.5.

Table 2.5 Collagen yield from various coproducts obtained from acid and pepsin extraction.

Sources	Extraction time (h)	Yield (%)		References
		ASC	PSC	
Rabbit skin	48	27.0	71.0[a]	Martínez-Ortiz et al. (2015)
Deer skin	72	2.2	9.6[a]	Lodhi et al. (2018)
Bovine tendon	72	64.9	56.8[a]	Ju et al. (2020)
Porcine skin	48	-	64.6[b]	Li et al. (2020)
Porcine lung	72	-	67.0[b]	Lin, Lin, and Su (2011)
Sheep bone with cartilage	72	-	18.0[b]	Vidal et al. (2020)
Lamp bone with cartilage		-	12.5[b]	
Emu skin	96	-	27.3[b]	Nagai et al. (2015)
Rooster skin	48	6.6	36.3[a]	Munasinghe and Schwarz (2017)
Chicken sternal cartilage	96	-	5.12[b]	Akram and Zhang (2020)
Golden carp scale	48	0.4	1.2[a]	Ali, Benjakul, and Kashimura (2017)
Catla scale	48	1.7	1.5[a]	Pal and Suresh (2017)
Jellyfish	72	5.0	8.0[a]	Khong et al. (2018)
Golden carp skin	48	4.1[♦]	7.3[♦a]	Ali et al. (2018)
Tilapia skin	48	19.1	19.6[a]	Song et al. (2019)
Hybrid sturgeon skin	24	5.7[♦]	10.3[♦a]	Wei et al. (2019)
Splendid squid skin	72	-	75.3[b]	Kittiphattanabawon et al. (2015)
Striped catfish air bladder	72	73.4	-	Divya et al. (2018)
Clam shell body	48	-	3.78[a]	Wu et al. (2019)
Sea cucumber body	48	-	72.2[a]	Li et al. (2020)
Turtle lung	12	-	79.3[a]	Song et al. (2014)
Frog skin	72	1.8	19.6[a]	Zhang and Duan (2017)

All coproducts extract by acetic acid 0.5 M and carry out at 4^oC in all steps. ♦ express yield on wet weight basis. Superscript a and b are yield from acid (1st extraction) + pepsin (2nd extraction) and alone pepsin extraction, respectively.

The use of pepsin is an effective method for several reasons as follows: (1) remaining of non-collagenous protein residues are hydrolyzed and are simply removed by salt precipitation; (2) telopeptide region is hydrolyzed, increasing collagen extraction efficiency; (3) elimination of non-helical part, reducing reduce antigenic reactivity, which is problematic in food and pharmaceutical applications (Lyn et al., 2004; Cao and Xu, 2008; Zou et al., 2020).

The lower yield of scale-ASC and bone-ASC from bigeye tuna indicted that the degree of cross-linking among collagen molecules might be stronger in scale and bone than in skin (Ahmed et al., 2019). Differences among these collagen yields have been reported to vary with the species, age, size, starvation condition, and structure ae well as composition of tissue.

Commercial pepsin is mostly isolated from porcine stomach. Major limitation of porcine pepsin is associated with the religious restriction. Another approach is pepsin stomach from other animals. Pepsin from marine fish, including bigeye snapper, albacore-, skipjack- and tongol-tuna have been applied (Nalinanon et al., 2007; Nalinanon, Benjakul, Visessanguan, and Kishimura, 2008; Benjakul et al., 2010).

2.5.3 Collagen recovery

2.5.3.1 Polysaccharide precipitation

Glycosaminoglycans (GAG) and kappa-carrageenan (KCGN) are polysaccharides that structure consists of one or more sulfate groups. Carboxyl and/or sulfate groups of polysaccharides can bind ionic bonds with ε-amino groups of lysine and hydroxylysine residues, guanidyl groups of arginine residues, and α-amino groups at N-terminal of collagens (Sadowska and Kołdziejska, 2005). Collagen can be

precipitated by ratio of protein: KCGN of 1:1 (w/w) (Żelechowska, Sadowska, and Turk, 2010) and ratio of protein: GAG at 1:0.3 (w/w) (Sadowska, Gutowska, and Malesa, 2005). However, this method is uneconomical on a commercial scale because GAG and KCGN is expensive and the dried form of collagen product is a complex with these polysaccharides.

2.5.3.2 Salt precipitation

This is a widely used process for collagen precipitation. This is based on the principle of salting out by the addition of sodium chloride (NaCl). The final concentration at 2.3-2.6 M are generally used (Moreira-Silva et al., 2016). Salt concentration can be adjusted to maximize collagen recovery and removal of impurities. Maximum yield of collagen from snakehead fish skin were obtained by 0.7 M NaCl (Liu, Zhang, Cui, and Wang, 2019). To harvest collagen from jelly fish, red snapper and tilapia skin, 0.9-1.0 M NaCl were applied (Khong et al., 2018; Song et al., 2019; Zaelani et al., 2019), while chicken feet used 3.0 M NaCl (Araújo et al., 2018). Additionally, 1.8-2.6 M NaCl in the presence of 0.05 M trometamol (Tris-base), pH 7.5 has been used for collagen precipitation of yellowfin tuna skin and sheep bone (Nurilmala et al., 2019; Vidal et al., 2020).

2.6 Biochemical characterization of collagen

Several techniques can be used to characterize collagen. These techniques are based on thermal behavior, optical absorption/ spectral characteristics, and proteomics.

2.6.1 Thermal behavior

Calorimetry is a primary technique for measurement thermal properties of materials between temperature and specific physical properties of substances (Gill,

Monghadam, and Ranjbar, 2010). Amongst various types of calorimeters, differential scanning calorimeter (DSC) is a popular technique, which measures energy change that occurs in transition temperature (Haynie, 2008). During a change in temperature, DSC measures heat, which is released (exothermic) or absorbed (endothermic) by the sample, based on a differential temperature between sample and reference material. Protein denaturation is an endothermic process.

DSC is capable of elucidating the factors that contribute to the folding and stability of biomolecules (Van-Holde, Johnson, and Ho, 2006). These factors include pH, buffer, ionic strength, concentration, and weight of sample/ solvent (Cooper, 2000). Where conformational protein has been modified, the force of native protein stability is interrupted, which would reflect on DSC thermogram. The maximal transition temperatures (T_m) or denaturation temperatures (T_d) is considered as the temperature where 50% of the proteins unfold. The thermal behavior of collagen from various sources is demonstrated in Table 2.6, in which it varies with imino acid (Hyp + Pro) content, and animal species.

At acidic condition, lower T_d values of collagen are observed due to electrostatic repulsion of helical structure and destruction of hydrogen bonds in the presence of acid (Sungperm, 2012). In contrast, thermal stability of the collagen triple helix is attributed to the hydrogen bonded networks, mediated by water bridge molecules (Mizuno et al., 2003). Furthermore, higher stability of the triple-helical structure depends on pyrrolidine rings of imino acid and hydrogen bonds via the hydroxy group, leading to nucleation zone as a network structure (Piez and Gross, 1960; Shoulders and Raines, 2009). Thereby, Pro and Hyp greatly effect affect collagen thermal stability. In addition, environmental living and body temperature

contribute to collagen stability. Land animals and poultry have higher T_d than aquatic animals (Khora and Kirti, 2017).

2.6.2 Spectral characterization

Spectroscopic analysis is a universal method in structural characterization of biomolecules because it is rapid, noninvasive, and small amount sample required for measurement (Tsai, 2002). Spectroscopy is defined as the study of interaction between electromagnetic radiation with sample matter. The electromagnetic (EM) spectrum is a very wide range of wavelengths of 1 km-0.01 nm (Figure 2.18). Several spectroscopies for biological characterization including nuclear magnetic resonance (NMR), electron spin resonance (ESR), visible/ fluorescence, X-ray, especially infrared (IR), and ultraviolet (UV) are common technique for collagen characterization.
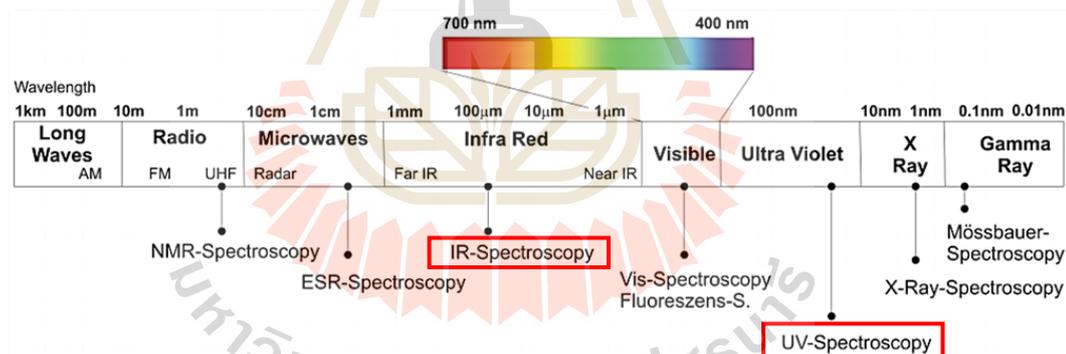
Figure 2.18 The EM spectrum for biochemically characterization.

Source: Glombitza (2010).

Table 2.6 Thermal denaturation (T_d) and enthalpy (ΔH) of collagen in various animals.

Sources	Extraction method	Imino acid content (residue/ 1,000 residues)	T_d (^{o}C)	ΔH (J/ g)	References
In deionized water					
Golden carp skin	ASC	194	36.9	0.87	Ali et al. (2018)
	PSC	197	38.2	1.24	
Golden carp scale	ASC	197	37.8	1.18	Ali et al. (2017)
	PSC	202	37.7	0.86	
Clam shell body	PSC	155	31.3	0.45	Wu et al. (2019)
Chicken sternal cartilage	PSC	204	60.8	NS	Akram and Zhang (2020)
Buffalo skin	ASC	225	51.2	NS	Rizk and Mostafa (2016)
In acetic acid					
Sea cucumber [a]	PSC	141	25.4	NS	Lin et al. (2017)
Siberian sturgeon cartilage [b]	ASC	206	28.3	NS	Luo et al. (2018)
	PSC	206	30.5	NS	
Sea bass scale [b]	ASC	193	38.1	0.72	Chuaychan, Benjakul, and Kishimura (2015)
	PSC	195	39.3	0.91	
Splendid squid skin [c]	PSC	189	34.1	0.66	Kittiphattanabawon et al. (2015)
Chicken articular cartilage [c]	PSC	232	45.6	14.0	Cao et al. (2013)

Noted: ASC and PSC are acid and pepsin soluble collagen, respectively. a, b, and c indicate sample that was rehydrated in 0.5, 0.05, and 0.1 M of acetic acid, respectively. NS denotes data not shown.

2.6.2.1 Ultraviolet (UV) spectroscopy

UV spectral is analyzed at the wavelength regions of 150-400 nm where a compound exhibits functional groups that can absorb UV (Kuball, Höfer, and Kiesewalter, 2017). The chromophores always contain double bond, aromatic ring structure, triple bonds, and double bond of carbonyl group (Field, Li, and Magill, 2020). The UV absorption is related with functional group of ^-COOH, $CONH_2$, and $C=O$ in the polypeptide chains of collagen molecule (Veeruraj, Arumugam, and Balasubramanian, 2013). Triple-helix structure of collagen shows maximum absorption at UV_{230} (Kumar, Nazeer, and Jaiganesh, 2012; Abdollahi, Rezaei, Jafarpour, Undeland, 2018) but it can vary with source of collagen as shown in Table 2.7.

Typical wavelengths of protein absorption and some amino acids are 260, 269, 275, 276, 278, 282, and 284 nm which indicate Phe, Tyr, Trp, heme, elastin, keratin, apoprotein, fibronectin, and glutelin, respectively (Prasad et al., 2017; Sionkowska et al., 2006; Lavrinenko, Vashanov, and Artyukhov, 2015; Zhi, Wang, Li, Yuan, and Shen, 2015; Damodaran, 2017; Sun et al., 2019; Finch, Benson, Donnelly, and Torzilli, 2019). Human serum albumin (HSA) significantly absorbed at $UV_{250-350}$ (Homchaudhuri and Swaminathan, 2004). Therefore, UV absorption of collagen is distinct from amino acids and proteins, thus it can be used for collagen characterization.

Table 2.7 Maximum UV absorption of collagen from various animal tissues.

Animals	Tissues	λ_{max} (nm)	References
Abalone	Muscle	232	Dong et al. (2012)
Silver carp	Entrails	230	Abdollahi et al. (2018)
Sea cucumber	Body wall	237	Li et al. (2020)
Miiuy croaker	Scale	220	Li et al. (2018)
Siberian sturgeon	Skin	230	Luo et al. (2018)
Emu	Skin	235	Nagai et al. (2015)
Buffalo	Skin	231	Rizk and Mostafa (2016)
Porcine	Skin	235	Li et al. (2020)
	Bone	232	Zhu et al. (2020)
Ovine	Bone	231	Gao et al. (2018)

2.6.2.2 Circular dichroism (CD) spectroscopy

CD spectroscopy can monitor integrity and conformational structure change. CD technique is based on absorption of circularly polarized light (Figure 2.19B). Proteins and peptides are sensitive on the far-UV absorption at the wavelength of 170-260 nm (Greenfield 2006; Micsonai et al., 2015). Moreover, this technique can observe the transition of protein structure via thermal modulation at a slower heating and cooling rates (Drzewiecki, Grisham, Parmar, Nanda, and Shreiber, 2016).

CD can be used to characterize protein secondary structure (α-helical, β-sheet, β-turn, and random coil or unordered structure) where molecules have been absorbed right- (E_R) and left-handed (E_L) of circularly polarized light. CD is normally

reported in units of absorbance on ellipticity [θ], which is calculated by equation of

Woody (1996) as [θ] = 32.98 × ΔAbs, where ΔAbs is absorbance of E_L - E_R.
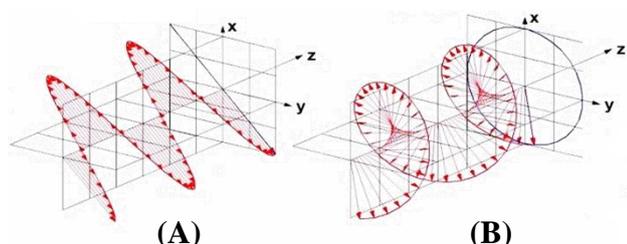
Figure 2.19   Graphical of linear (A) and circular (B) polarization.

Modified from: Elliott (2003).

Different structural elements have specific characteristic CD spectra as shown in Figure 2.20. α-Helix protein has negative ellipticity at 222 and 208 nm and a positive ellipticity at 193 nm. β-Sheets pattern has negative value at 218 nm and positive value at 193 nm, whereas random coil shows low ellipticity around 210 nm and negative band at 195 nm.
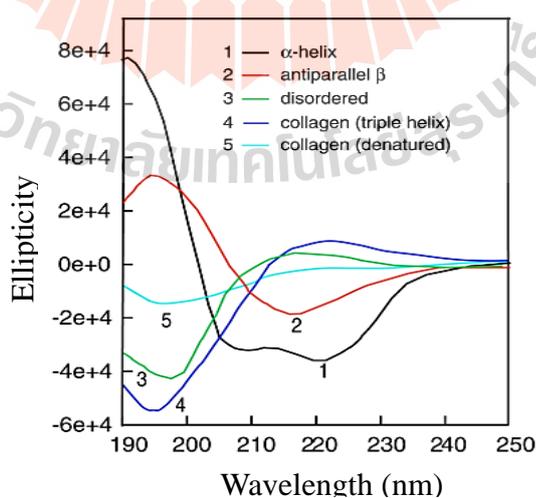
Figure 2.20   Representative CD spectra for secondary structures and collagen.

Source: Greenfield (2006).

Collagen is a unique protein consisting of 3 α-helix chains that twist to a triple helix. Each strand has a conformation resembling that of poly-L-proline (Bovey and Hood, 1967), which all bonds are *trans* configuration, categorizing to poly-L-proline II or PPII (Adzhubei, Sternberg, and Makarov, 2013). The CD profile of supercoil collagen predominantly presented the maximum peak at 222 nm, and the minimum peak at around 196-197 nm, and cross zero rotation at 215 nm (Jeevithan et al., 2014). These CD characteristics are in agreement with previously reported in various extracted collagen from bester sturgeon notochord, soft-shelled turtle, channel catfish skin, chicken sternal cartilage, and bovine tendon (Meng et al., 2019; Zou et al., 2017; Tan and Chang, 2018; Akram and Zhang, 2020; Zhu et al., 2020).

CD spectra indicate that the negative and positive ellipticity are directly related with protein conformation. The unfolding of triple-helix or denatured collagen is shown by a decrease of positive ellipticity along with an increase in negative ellipticity (Pelc, Marion, Pŏzek, and Basletić, 2014), and a redshift of the negative band to 203-210 nm (Cao and Xu, 2008). The complete denaturation of collagen to gelatin results in disappearance of a positive peak at 220-230 nm with remaining of a negative peak at 197-200 nm (Aewsiri et al., 2011; Silva et al., 2016).

In addition, Usha and Ramasami (2005) discovered that CD ellipticity ratio between maximum and minimum (Rpn) value of 0.1, demonstrating triple helix molecule of native collagen. The obtained Rpn values are in agreement with previously informed for collagen of golden carp skin (0.10) and grass carp scale (0.11) (Dhara, Datta, Pal, and Sarkar, 2013; Ali et al., 2018). Hence, the CD profile can be useful to investigate the extracted collagen molecule structure.

2.6.2.3 Fourier transform infrared (FT-IR) spectroscopy

FT-IR spectroscopy observes structural or conformational characterization of chemical compound via molecule vibration of chemical bond. The IR spectrum of a sample is recorded by passing IR light through the sample. When the frequency of IR is the same as the vibration frequency of a bond, absorption of IR radiation occurs. Thus, the specific frequency of the vibrations can be related with a specific bond type as well as characteristic of structure. IR active molecules need to contain dipole moment (Khan et al., 2018).

Vibrational state for many functional groups is located in the mid-IR region (4,000-400 cm^{-1}). Typically, there are four regions that can be used to analyze biological compound from the FT-IR spectra. The single- (O-H, C-H, and N-H), triple- (C≡C and C≡N), double- (C=C, C=O, C=N, and N=O) band, and fingerprint (C-C, C-N, and C-O) are detectable in wavenumber of 4,000-2,500, 2,500-2,000, 2,000-1,500, and 1,500-650 cm^{-1}, respectively (Mohamed et al., 2017).
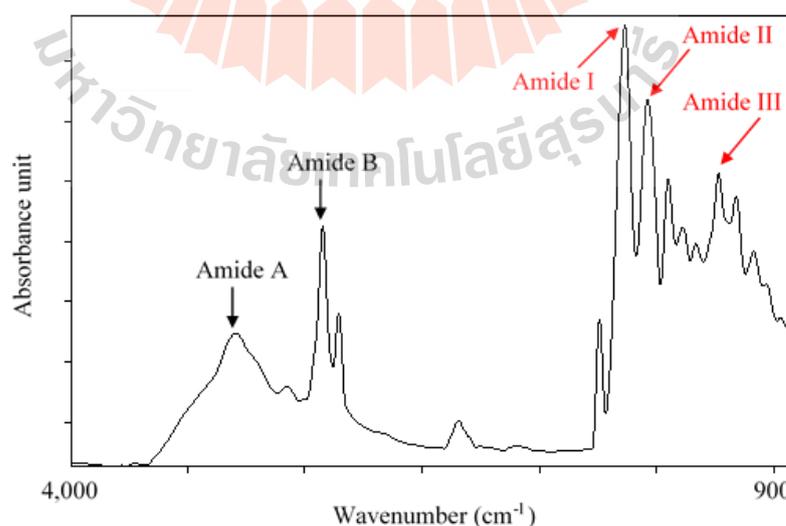
Figure 2.21 Distinctive amide region on FT-IR spectra of collagen sample.

Table 2.8 Characteristic of infrared (IR) absorption for collagen protein.

Amide	Frequency (cm^{-1})	Assignments
A	3,300-3,700	NH stretching, coupled with H bond
B	3,100-2,700	NH stretching and CH_2 asymmetric stretching
		C=O stretching, coupled with H bond;
		β-sheet (anti-parallel): 1,694-1,670
		β-turn: 1,675-1,655
I	1,720-1,600	α-helix: 1,663-1,650
		Random coil: 1,640-1,648
		β-sheet (parallel): 1,626-1,640
		Side chain: 1,629-1,602
II	1,580-1,480	CN stretching and NH bending
III	1,300-1,180	CN stretching and NH bending

Source: Kong and Yu (2007); Belbachir, Noreen, Gouspillou, and Petibois (2009); Carbonaro and Nucara (2010); Tranter (2017).

Collagen exhibits IR absorption between the wavenumber of 4000-900 cm^{-1}. It is normally associated with important regions of amide A, B, I, II, and III, which are demonstrated in Figure 2.21, corresponding to functional groups shown in Table 2.8. The amide I region represented CO stretching vibration, while the amide II and III region featured the CN stretching and NH bending. Bhattacharjee, Nicodemo, Arisawa, and Raniero (2018) reported that, amide I and II regions were indicators for the secondary structure of proteins, while amide III indicated collagen molecule (Cao and Xu, 2008).

2.6.2.3.1 Sample preparation

There are four common FT-IR techniques, including transmission, attenuated total reflection (ATR), diffuse reflectance (DRIFTS), and true specular reflectance/ reflection absorption (Smith, 2011). The DRIFTS and specular mode are suitable for metallic, inorganic polymer, varnish, silicon wafers, and laminated material, whereas organic and biological material are suitable for transmission and ATR mode (Mohamed et al., 2017).

The transmission mode does not require an accessory. IR light will directly pass through the samples but the beam cannot completely pass through very thick and rigid samples. In this situation, sample should be crushed to fine powder, which is mixed with potassium bromide (KBr) and subjected to high pressure of 12,000 psi for 1-2 min (Pavia, Lampman Kriz, and Vyvyan, 2015). KBr is used as the background matrix because it does not absorb IR light (Chen, Zou, Mastalerz, Hu, Gasaway, and Tao, 2015). The main disadvantage of KBr is a hygroscopic chemical, rendering high moisture absorption. This leads to aqueous interference with the IR spectrum. Therefore, sample preparation for a transmission mode is a rather complex task to obtain good results.

Another approach is ATR mode. The beam of IR is directed into an optically dense crystal with a high refractive index (such as diamond, zinc selenide: ZnSe, and germanium: Ge) at a certain angle (Subramanian and Rodriguez-Saona, 2009). Then, light comes in contact with ATR crystal and produced multiple internal reflectance. It will reflect back to the crystal and then exits to the end of the crystal as well as to the detector as shown in Figure 2.21. Therefore, a high resolution is a major advantage of this FT-IR mode, including minimal sample usage, no aqueous

contamination, and ease of cleaning surface crystal (Kazarian and Chan, 2013; Mohamed et al., 2017). Disadvantage and limitation of ATR are expensive crystal accessory.
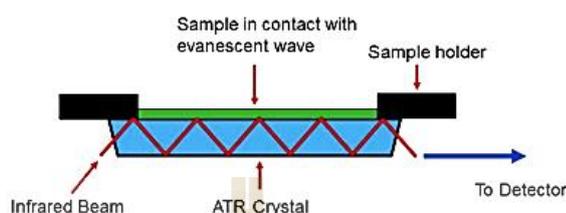
Figure 2.22 Mechanism of IR spectroscopy by ATR mode.

Source: Griffiths and de-Haseth (2007).

2.6.2.3.2   Collagen integrity analysis

FT-IR spectroscopy is applicable for a wide range of materials and it could be utilized for qualitative and quantitative analysis. Amide I region is considered as an indicator of protein. Moreover, their shape and position can determine indicative of the secondary structure (α-Helix, β-Sheet, β-Turn, random coil, and side chain) (Table 2.7; Figure 2.23A). Relative content of secondary structures can be estimated from curve-fitting on Lorentzian/Gaussian spectral line shape. Hong et al. (2017) reported that extracted collagen by conventional method of pepsin (Pep) consisted of 29.1% of α-helix content, respectively. To extract gelatin, thermal treatment at 95°C for 1 h has been applied. The result indicated that α-helix content decreased to 15.4% after thermal treatment. Thus, secondary structure content can be used to monitor protein conformational change.

Amide I, II and III regions are known to be related with the degree of molecular order and involved in triple helical structure of collagen (Sungperm, 2012). Moreover, Liu et al. (2012) found that absorption ratios between 1,454 cm^{-1} and amide III regions (Figure 2.23B) are calculated to be 1.0, representing to integrity triple helix structure. Ratio value of 1.00-1.05 is obtained from collagen of grass carp and golden carp skin (Liu et al., 2015; Ali et al., 2018). Collagen from bigeye snapper skin, is estimated to be 1.24-1.25 (Benjakul et al., 2010).
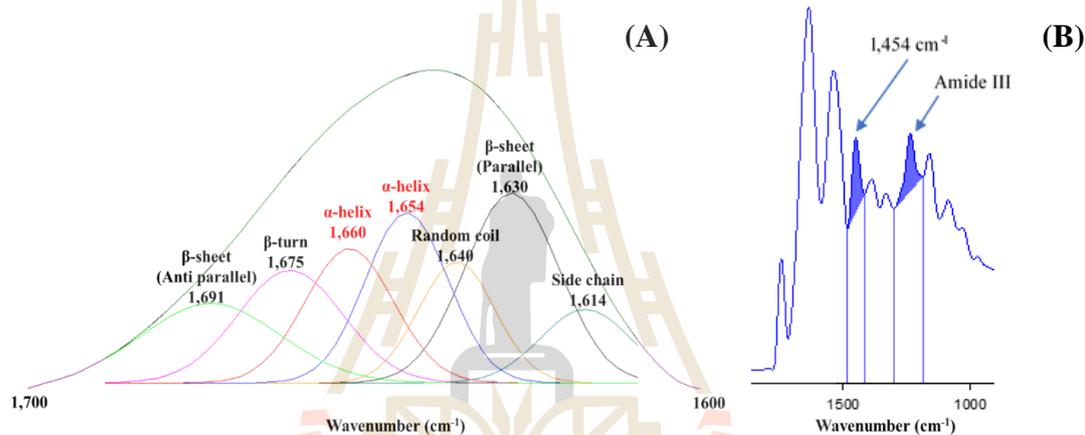
Figure 2.23 Estimation of secondary structures by curve-fitting of amide I region (A) and distinctive 1,454 cm^{-1} and amide III regions for estimation of integrity triple-helix (B).

Shifting of these amide regions are associated with loss of triple helix conformation. Intermolecular cross-linkings result in higher intensity at amide III region (Jakobsen, Hutson, Fink, and Veis, 1983). Collagen extracted by high temperature exhibited a broader amide A region than collagen extracted at low temperature (Muyonga et al., 2004). Dissociated triple helix collagen to gelatin can also be indicated by an absorption ration between 1,454 cm^{-1} and amide III regions of

0.59 value of absorption ratios (Plepis, Goissis, and Das-Gupta, 1996). It can be seen that only normal IR spectra cannot confirm the integrity of triple helix structure of collagen. Analysis of protein secondary structure and absorption ratios between 1,454 cm^{-1} and amide III regions should also be investigated.

2.6.3 Protein patterns

Purity and molecular composition should be monitored after extraction. Sodium dodecyl sulfate-polyacrylamide gel electrophoresis (SDS-PAGE) is widely used for molecular weight (Mw) evaluation. Electrophoresis refers to the movement of charged molecule protein in the presence electric field. Under denaturing condition, proteins are heated with anionic surfactant (SDS) and intermolecular disulfide bonds are diminished by β-mercaptoethanol.

Collagen is composed of γ (trimer), β (dimer), and α (monomer) chain (Jongjareonrak, Benjakul, Visessanguan, and Tanaka, 2005; Tronci, Russell, and Wood, 2013), with Mw of 300, 200, and 100 kDa, respectively. The γ-, and β-molecule indicate high contents of intermolecular crosslinks at the telopeptide region, leading to low-solubility collagen in acid. The Mw of α-chain can be depended on type of collagen. Fibrillar collagen on type I-III and V are consisted α-chain around 100-150 kDa, whereas type IV and VI are larger to 180-240 kDa and type VIII and IX are smaller to 60-85 kDa (Horst, 1991; Deyl and Miksık, 2000; Miner and Nguyen, 2006; Sungperm, 2012; Liang et al., 2014).

Apart of α-chain, heterotrimer as type I collagen from animal skin, scale, bone, and tendon consist of two identical α1-chains and one α2-chain (Liu and Huang, 2016; Fauzi et al., 2016; Wu et al., 2019; Ahmed, Haq, and Chun, 2019), corresponding to disclose two bands on polyacrylamide gel but homotrimer, such as

type II, III, and V collagen from porcine cartilage, skin, and placenta is showed in 1

band (Jongjareonrak, et al., 2005). SDS-PAGE can provide information about purity,

type, specific migration, Mw size, and natural cross-linking of collagen. However, it

still contains obvious limitation as follows: (1) different proteins with similar Mw

cannot be differentiated by this technique; (2) very small proteins (Mw < 10 kDa) are

difficult to determine.

2.6.4 Protein identification

Proteomics is an analytical method for the characterization of proteins.

There are two different means of identifying proteins known as bottom-up and

top-down approach (Figure 2.24).
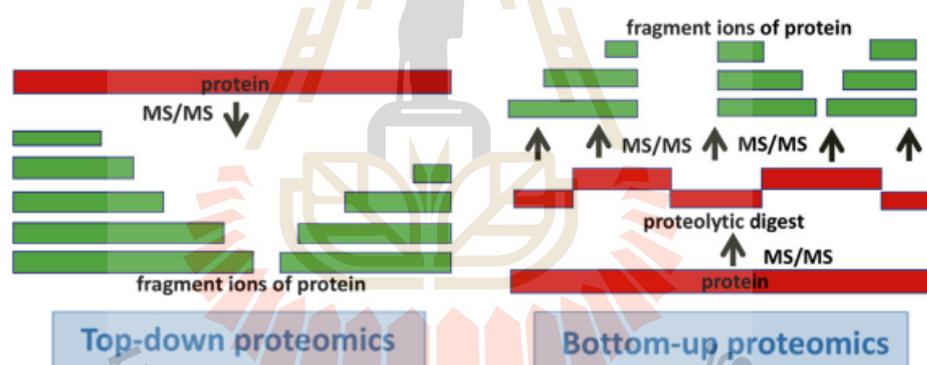
Figure 2.24 Top-down (A) and bottom-up (B) proteomic analysis.

Modified from: Kaczor-Urbanowicz and Wong (2020).

In top-down proteomics, proteins are subjected to ionization and

fragmentation in the intact form without digestion and passed through mass analyzers

(Noor, Mohamedali, and Ranganathan, 2018). The major disadvantage of this method

is the sample treatments required for coupling with mass spectrometry (i.e., formic

acid or trifluoroacetic acid). Therefore, acid insoluble proteins, high Mw proteins, and glycosylated proteins cannot be analyzed (Kaczor-Urbanowicz and Wong, 2020).

Bottom-up proteomics refers to the identification of proteins that are predigested by proteolytic enzymes, usually trypsin, to reduce the large intact protein into peptide fragments (Messana, Cabras, Iavarone, Vincenzoni, Urbani, and Castagnola, 2013; Zhu, Zacharias, Wooding, Peng, and Mechref, 2017). The major advantage of bottom-up is high-resolution separations. In addition, proteins can be separated in a complex mixture before digestion, leading to a good identification (Darville and Sokolowski, 2014). However, low coverage percentages of the protein sequence are obtained in the results (Zhou, 2014). Tryptic digestion can degrade protein, leading to loss of sequence matching (Lazar, Karcini, Ahuja, and Estrada-Palma, 2019).
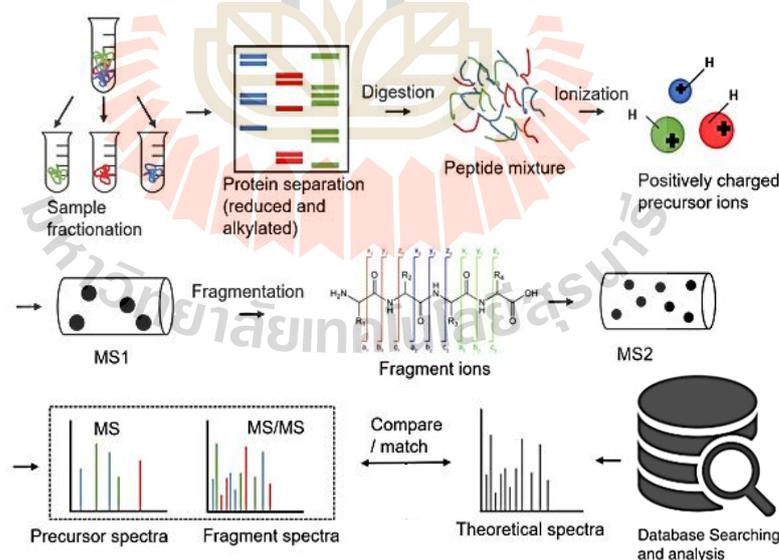
Figure 2.25   Steps of proteomic analysis using mass-spectrometry.

Modified from: Noor et al. (2018).

Protein identification by peptide mapping involves the initial protein preparation by one-dimensional (1D-gel) and two-dimensional (2D-gel) gel electrophoresis (Graves, and Haystead, 2003). Subsequently, protein is digested by trypsin into peptides before MS analysis. All steps of analysis are summarized in Figure 2.25. Once the experimental data and a suitable database of protein sequences have been acquired, protein identifications can be performed. There are several freely available softwares for analyzing peptide mapping as showed in Table 2.9, and Mascot software stands out as the most popular (Veenstra, Van, Fox, and Issaq, 2020).

Table 2.9 Software for protein identification using peptide mass fingerprinting.

Software	Web address/ URL
MultiIdent	https://www.expasy.org
Mascot	http://www.matrixscience.com
MS-Fit	http://prospector.ucsf.edu
PepMAPPER	http://www.nwsr.manchester.ac.uk
MassWiz	http://masswiz.igib.res.in
UniProt	https://www.uniprot.org
ProFound	http://prowl.rockefeller.edu
NCBInr	https://www.ncbi.nlm.nih.gov

Source: Veenstra et al. (2020).

After analysis, proteins are identified, based coverage of protein sequences and number of peptides that matched with database (Chen et al., 2016). Protein identification of the extracted collagen is displayed in Table 2.10. From the result, the

α-chain in each sample are correctly identified to collagen protein but exhibited the disassociation with collagen sample and taxonomy. Bitarte et al., (2007) reported that detection by MS/MS can introduce some errors because species evolution, immigration, and/or mutation of organism, do not correspond with the database. Besides, it lacks sensitivity to detect low abundant protein (Lippolis and Nally, 2018).

Table 2.10 Specific amino acid sequence of α1 and α2 chains obtained from collagen from various sources.

Sample	Band	Peptide sequence hint	Protein identification	Coverage (%)	Taxonomy
Ovine tendon (1)	α1	SGDRGETGPAGPAGPIGPVGAR	Collagen α1 (I) chain	-	*Ailuropoda melanoleuca* (Giant panda)
	α2	GVVGPQGAR GLPGVSGSVGEPGPLGISGPPGAR	Collagen α2 (I) chain	-	*Felis catus* (cat)
Cobia skin (2)	α2	GYTGLDGR GATGPTGLR GNPGAAGSAGPQGPIGPR	Collagen α2 (I) chain	2	*Oreochromis niloticus* (Nile tilapia)
Deer antler (3)	α1	GFSGLDGAK GFPGSDGVAGPK GSPGADGPAGAPGTPGPQGIAGQR	Collagen α1 (I) chain	3	*Ceratotherium simum Simum* (White rhino)
	α1	GETGPAGPAGPIGPVGAR DGEAGAQGPPGPAGPAGER GQAGVMGFPGPK	Collagen α1 (I) chain	4	*Bos grunniens mutus* (Yak)

Source: (1) Fauzi et al. (2016); (2) Zeng et al. (2012); (3) Chen et al. (2014).

2.7   Application of collagen

Collagen has low immune response with excellent biocompatibility and does not contain side effects (Pallask et al., 2018; Zou et al., 2020). Collagen has been applied to many commercial applications, such as sausage industry, food additives, food supplements, food packaging, cosmetic, biomedical implants, tissue engineering, and pharmaceutical (Martínez-Ortiz et al., 2015; Anandhakumar, Krishnamoorthy, Ramkumar and Raichur, 2017). Nowadays, type I collagen has been applied for chronic wound healing.

Burn wounds, dead tissue, inflammation, redness-pain, and diabetic foot ulcer are major symptoms for chronic wound, typically takes a longer curing of more than 3 months, leading to the high expense fee (Tronci, 2019). The global advanced wound care market, negative-pressure wound therapy, wound care biologics are grown in every year and wound dressings account to the largest market. Biological dressing like collagen has become increasingly important. It contains several potentialities, such as extracellular matrix supporting, promote cellular growth, matrix remodeling, tissue regeneration, and barrier against a harmful with external environment. (Wiegand et al., 2016).

Collagen based wound dressing has been successfully manufactured from bovine, equine or porcine tissues. Major commercial wound dressings, typically consists of 80-100% native type I collagen (Table 2.10), which monitored by atomic force microscopy (AFM) and immunoelectron microscopy (IEM). Moreover, 50-55% of denatured or hydrolyzed collagen can also be used for collagen dressing. Developing as dressing pads, have been evolved to control rapid exudate uptake and excessive wound evaporation. In clinical trials, collagen dressing (100% native type I

collagen from bovine) resulted in wound closure of 83% within 90 days from 15 out of 18 patients (Shah and Chakravarthy, 2015). Triple helix is a key component for binding with wound exudate and cytokines. (Qiao et al., 2015). Therefore, extracted collagen from trachea might be a potential source for collagen dressing production and extraction method should be retained integrity of triple helix structure.

Table 2.11 Characteristics of commercial collagen dressings.

Product brand	Characteristic of wound dressings			
	Composition	Collagen form	Collagen content (%)	Format/ shape
Cutimed[®] [(1)]	Type I collagen (Bovine) and calcium alginate	Triple-helix	90	Pad/ Square
Biopad[®] [(2)]	Type I collagen (Equine)	Triple-helix	100	Pad/ Square
Puracol[®] [(2)]	Type I collagen (Bovine) and manuka honey	Triple-helix	88	Pad/ Square
Fibracol[TM] [(3)]	Type I collagen and alginate	Triple-helix	90	Pad/ Square
Helix3[®] [(3)]	Type I collagen (Bovine)	Triple-helix	100	Pad/ Square
Endoform[TM] [(1)]	Type I collagen (Ovine) and extracellular matrix	Triple-helix	90	Pad/ Square
Promogran Prisma[TM] [(2)]	Type I-III collagen (Bovine) and oxidized regenerated cellulose	Hydrolyzed	55	Pad/ Hexagonal
ColActive[®] [(2)]	Gelatin, sodium alginate, carboxymethyl cellulose, and EDTA	Denatured	50	Mesh

Source: (1) Wiegand et al. (2016); (2) Sandri et al. (2020); (3) Pallaske et al. (2018).

2.8 Ultrasound technology

Sound is a mechanical wave that results from the up and down vibration through a medium, which can be air, liquid, and/ or solid. Type of sound wave can be normally classified into 3 groups on vibration frequency (Figure 2.26) as follows;

1. Infrasound or inaudible sound (< 20 Hertz or Hz): Whales, bats and submarines

2. Audible sound (20 Hz - 20 kHz): Human hearing

3. Ultrasound or ultrasonic wave

   - Power ultrasound (> 20 kHz - 1 MHz)

   - Diagnostic ultrasound (> 1 MHz)
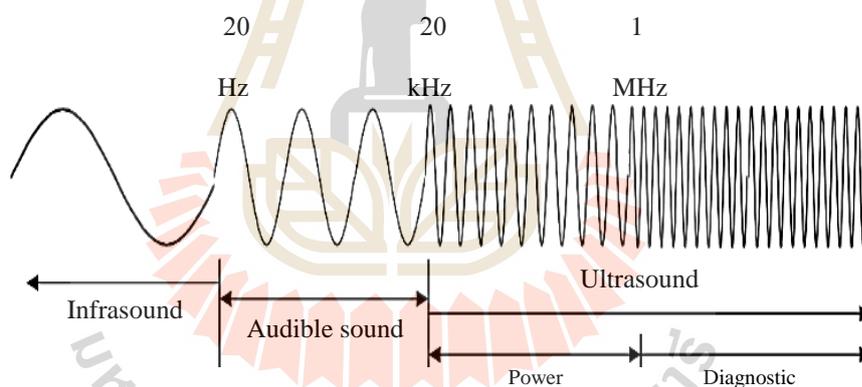
Figure 2.26   Acoustic spectrum on frequency wave.

Modified from: Kentish and Ashokkumar (2011).

2.8.1 Ultrasound feature and phenomenon

Ultrasound is a mechanical energy of longitudinal wave, contributing in a greater than 20 kHz of frequency, which is above the audible limit for humans (Alarcon-Rojo et al. 2019). Ultrasound is a green innovative technology that has been achieved enormous attention in food manufacturing because it has several advantages,

including, rapid, reliable, reproducible, yield enhancement, non-toxic and environmental-friendly process (Soria and Villamiel, 2010; Akram and Zhang, 2020).

Ultrasound in a liquid creates physical force, heating and agitation, causing to acoustic cavitation that generates several effects, such as shear force, shockwaves, macro-turbulences, micro mixing and acoustic streaming with bubble implosion collapse (Figure 2.27). Acoustic cavitation can generate temperature (5,000 K) and pressures (1,000 atm) (Majid, Nayik, and Nanda, 2015; Bashir, Ibrahim, Usmail, and Jaya, 2020). Both intensifications can improve the efficiency of the system by promoting various situations, such as liquid degassing, mass transfer enhancement, and biological cell membrane destruction (Kapustina, 1965; Li et al., 2009; Lentacker et al., 2014; Dong et al., 2015).
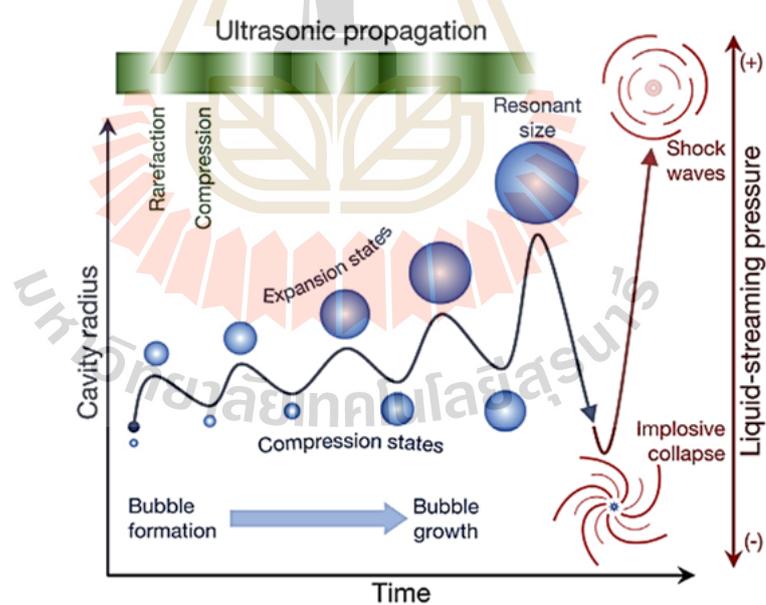
Figure 2.27 Bubbles collapse induced by cavitation effect.

Source: Bui, Ngo, and Tran (2018).

2.8.2 Ultrasound energy

The measurement of the actual applied acoustic power in a process is not clearly reported. Indirect measurement by the physical method has been applied. These methods estimate the transferred energy by measuring either chemical or physical changes on the medium when ultrasound is applied (Chemat et al., 2017). The most common physical method is calorimetric method via thermal acoustic measurement (Margulis and Margulis, 2003).

Ultrasound power can be calculated by calorimetry. Energy is lost in the form of heat, when ultrasound proceeds through the medium (Thompson and Doraiswamy, 1999). Since ultrasonic irradiation produces heat, recording the temperature as a function of time, leads to the power estimation. Ultrasound power in watt (W or J/s) is calculated using the equation (Margulis and Margulis, 2003), as follows;

$$\text{Ultrasound power (P)} \quad = \quad m \times C_p \times \left(\frac{dT}{dt} \right)$$

where, m is the mass of the sonicated medium (g), C_p is heat capacity of medium at a constant pressure ($J \cdot g^{-1} \cdot {}^{\circ}C^{-1}$), and $\frac{dT}{dt}$ is the rate of temperature increase (Jambrak, Lelas, Mason, Krešić, and Badanjak, 2009). Moreover, the ultrasound power can convert to ultrasound intensity, which is expressed in watts per volume of the sonicated medium ($W \cdot cm^{-3}$) or watts per unit of emitting surface ($W \cdot cm^{-2}$) (Mamvura, Iyuke, and Paterson, 2018).

2.8.3 Ultrasound emitter

The emitter is an instrument that radiates ultrasonic wave from transducer into the medium. It plays an important role for amplifying vibrations. Major forms of emitter are baths and horns as shows in Figure 2.28.

2.8.3.1 Emitting baths

Commercial bath system composes of generator, transducer, and treatment tank. The transducers are mounted to the base or sides at the wall of treatment tank. Ultrasound bath is another widely used for decontamination. Advantage of this emitting type is the accommodation of multiple samples. The limitation is relatively low ultrasound intensity (Palma, Zhou, and Feng, 2017). Furthermore, the distribution of ultrasonic intensity is not uniform inside the tank (Mason, 1998).
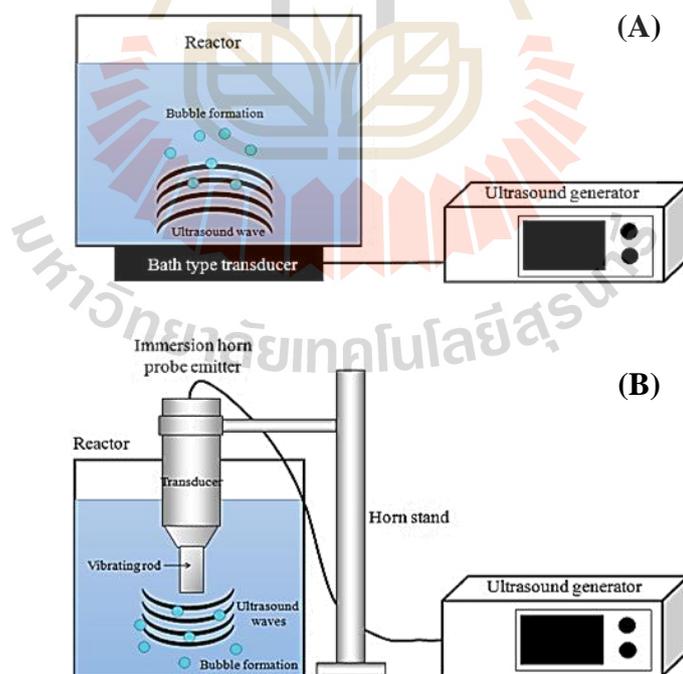
Figure 2.28 Emitter form of ultrasound bath (A) and horn (B).

Source: Thokchoma et al. (2015).

2.8.3.2 Emitting horns (probes)

This emitting type is widely used in laboratory scale. Horn often requires the attachment of a horn tip known as an acoustic horn or sonotrode (Bermúdez-Aguirre, Mobbs, and Barbosa-Cánovas, 2011). Moreover, it can modulate applying with booster for increasing performance of ultrasonication. The sonotrode is a unique part of this system.

Sonotrode is made of titanium alloys, aluminum alloys, steel, and stainless steel (Nad, 2010). They are used in various shapes and sizes, according to the application (Figure 2.29), such as bakery cutting, sealing package, meat tenderizing, compound extraction, and others (McHugh, 2016). Direct radiating ultrasonic waves into the sample is an advantage of this emitting device. However, sonotrode can be deteriorated by acoustic cavitation activity, when extreme and maximum ultrasound intensity are applied (Palma, Zhou, and Feng, 2017).

Figure 2.29 Ultrasound sonotrode for various application.

Source: http://www.bekultrasonics.com/...horns (2020) [On-line].

2.8.4 Types of ultrasound

Ultrasound can be subdivided into three frequency levels, a low- (20-100 kHz), intermediate- (100 kHz-1 MHz), and high-(1-10 MHz) frequency ultrasound (Schoellhammer et al., 2012; Chandrapala, 2015). The frequency level should be suitable for the application since the transducer for a high-level frequency is more expensive than a low frequency. The high- and intermediate-frequency as low intensity ultrasound has not been extensively practiced in food processing but are popularly used for food quality control and assurance. Ferments sugar, eggs, apples, flours (Schöck and Becker, 2010; Aboonajmi et al., 2010; Kim et al., 2009; Alava et al., 2007)

Low frequency or high intensity ultrasound has been typically applied in various applications of bio- and food manufacturing (Ashokkumar, 2015). Application of low-frequencies are shown in Table 2.12. It can be seen that ultrasound-assisted extraction (UAE) is applied to several bioactive compounds (antioxidants, pro-vitamin, plant and animal protein isolates) to increase efficiency and producibility of the extraction. The effectiveness of US in some extraction should be described. Therefore, more efficient collagen extraction method should be developed by UAE as an alternative approach to be a greater extraction method.

2.8.5 Ultrasound-assisted collagen extraction

High amounts of intermolecular cross-links on collagen molecule lead to limited collagen solubilization. Most conventional collagen extraction has been associated with a large volume of organic solvents, low yield, and time consumption, resulting in high incremental cost. Ultrasound technology might be an efficient method that can improve collagen extraction method.

Table 2.12 Applications of low-frequency ultrasound for food industry.

Application	Frequency	Category	References
Tenderization	40 kHz, 300 W	Chicken breast	Li et al. (2015)
Sanitization	45 kHz	Biofilm	São-José, and Vanetti (2012)
Dehydration	25 kHz	Banana	Fernandes and Rodrigues (2007)
Fermentation	20 kHz, 100 W	Milk	Nguyen, Lee, and Zhou (2012)
Emulsification	20 kHz	Palm oil	Pongsawatmanit et al. (2006)
Crystallization	67 kHz, 450 W	Ice	Chow et al. (2003)
Inactivation	45 kHz, 200 W	*Listeria monocytogenes*	Mikš-Krajnik et al. (2017)
	30 kHz	α-Amylase	Kadkhodaee and Povey (2008)
Extraction	20 kHz	Rice proteins	Yang et al. (2018)
	20 kHz, 130 W	Citrus pectin	Polanco-Lugo et al. (2019)
	20 kHz, 130 W	β-carotenes	Bachchhav et al. (2020)
	30 kHz, 100 W	Anthocyanins	Ryu and Koh (2019)
	35 kHz, 100 W	Isoflavones	Fahmi et al. (2014)
	35 kHz, 320 W	Polyphenols	Chmelováa et al. (2020)
	20 kHz, 300 W	Walnut protein	Lv et al. (2019)
	24 kHz, 266 W	Duck liver proteins	Zou et al. (2017)

Ultrasonication enhances the performance of collagen extraction via cavitation phenomena (Akram and Zhang, 2020). Bubbles explosion can disrupt with cell tissue membrane and promotes collagen solubility. Ali et al. (2018) reported that interruption on tissue membrane can enhance the mass transfer of acetic and/ or pepsin to the matrix of raw materials, leading to yield improvement and extraction time reduction. The extracted collagens from various animal coproducts by UAE are presented in Table 2.12. Yield of collagens extracted by US increased in a range of 10-30%. The key factors affecting collagen yield, are exposure time, ultrasound power/ intensity,

and extraction time. Mason and Peters (2002) stated that high extraction yield by UAE was obtained at applying ultrasound intensities more than 10 W·cm^{-2}. Nevertheless, long exposure time for 24 h with 80% amplitude has been reported to dissociate α-chain collagen from sea bass skin (Kim et al., 2012). The secondary structure as well as triple helix structure of collagen is disintegrated when high ultrasound intensity at 2,990 W·cm^{2} for 36 min exposure time was applied (Akram and Zhang, 2020). These studies indicated that long exposure time and extreme intensity ultrasound might disturb collagen structure. Thus, these factors should be investigated to achieve the most efficient collagen extraction.
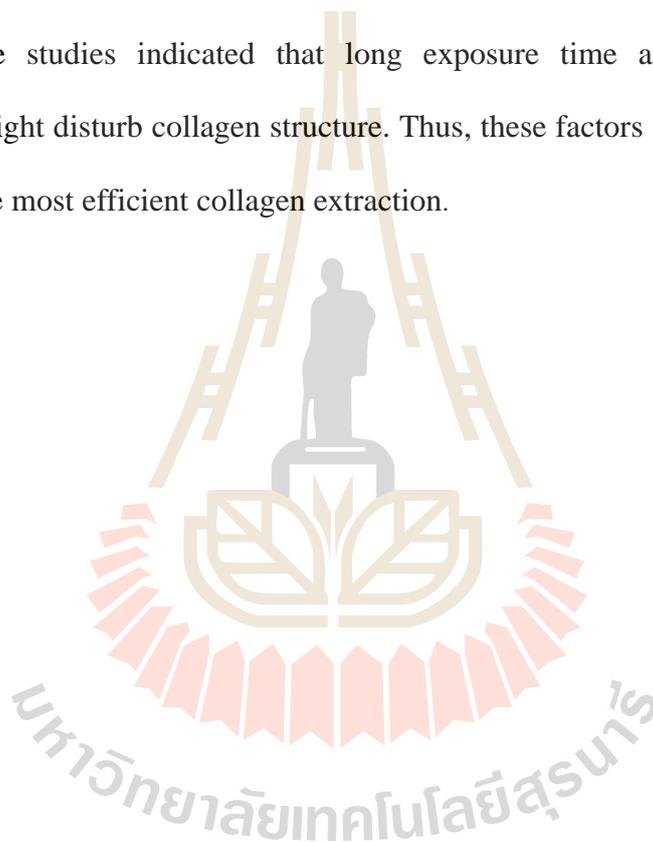
Table 2.13 Ultrasound-assisted extraction (UAE) of collagen from various coproducts.

Sources	Ultrasound parameters				Extraction time (h)	Yield (%)/type extraction				References
	Frequency (kHz)	Power (W)	Intensity	Exposure time		Conventional		UAE		
						ASC	PSC	ASC	PSC	
Bovine tendon [b]	40	120	NA	30 min	24	-	55.4	ND	80.6	Li et al. (2009)
Sea bass skin [h]	20	NA	80% amplitude	12 h	24	18.0	-	90.0	-	Kim et al. (2012)
Soft-shelled turtle [h]	24	200	NA	24 min	24	43.6*	-	50.7*	-	Zou et al. (2017)
Jelly fish bell [b]	NA	NA	NA	15 min	48	5.0	-	38.0	-	Khong et al. (2018)
Golden carp skin [h]	20	750	80% amplitude	30 min	48	51.9	79.3	81.5	94.9	Ali et al. (2018)
Flat fish skin [m]	20	1,500	60% amplitude	3 h	3	20.9**	-	31.3**	-	Song et al. (2018)
Chicken sternal [h]	25	950	2,996 W·cm^{-2}	36 min	96	5.1	-	15.5	-	Akram and Zhang (2020)
Chicken lung [h]	24	200 W	150 W	5 min	24	-	NA	-	31.2	Zou et al. (2020)

ASC and PSC abbreviate acid- and pepsin-soluble collagen. Superscript b, h, and m are extraction by bath, horn transducer, and reactor. NA, not available.

* is collagen content (%). ** calculated from protein content (Biuret method).

CHAPTER III

MATERIALS AND METHODS

3.1   Chemicals

Type I collagen (bovine Achilles tendon), pepsin from porcine gastric mucosa (EC 3.4.23.1: activity of 250 units/mg solid), trans-4-hydroxy-L-proline (hydroxyproline), chloramine-T hydrate, and Folin-ciocalteu's phenol reagent were purchased from Sigma-Aldrich Co. (St. Louis, MO, USA). Ninhydrin used for amino acid analysis was purchased from Biohrom (Cambridge, UK). Protein markers and chemicals used for gel electrophoresis were purchased from Bio-Rad Laboratories (Hercules, CA, USA). All others chemicals of analytical grade were purchased from Carlo Erba (Valde Reuil, France).

3.2   Collection and preparation of raw materials

Chicken trachea (T) samples were donated by Tanaosree Green Food Co., Ltd. (Nakhon Pathom, Thailand). Samples were vacuum-packed in polyethylene bag, packed with dry ice and transported to Suranaree University of Technology. Upon arrival, fat clots and meat residues were removed manually and washed with reverse osmosis (RO) water. Washed materials were stored at -20°C throughout the study.

3.3 Chemical composition analyses

3.3.1 Proximate composition

Frozen samples were thawed at 4°C overnight, cut and homogenized by a food blender (Tefal®, Rumilly, France) for 1 min. Moisture, ash and crude protein were analyzed according to AOAC (AOAC, 2016) according to method No. 925.10, 923.03 and 990.03, respectively. Conversion factor of 6.25 was used for calculation of crude protein content.

3.3.2 Total lipids

Total lipids were analyzed according to Folch et al., 1957 with slight modifications. T samples (6 g) were added chloroform: methanol (2:1) of 36 mL and homogenized using a homogenizer (Nissei AM-8, Nihonseiki Kaisha Ltd., Tokyo, Japan) at 10,000 rpm for 2 min. The homogenates were centrifuged (Sorvall ST16R, Thermo Fisher Scientific Inc., Langenselbold, Germany) at 10,000×g for 5 min. Subsequently, supernatants were collected and filtered through Whatman No. 4 filter paper (Whatman International Ltd., Maidstone, England) into a separation funnel.

Chloroform, deionized (DI) water and 0.58% (w/v) NaCl were added in volumes of 12, 12, and 2 mL, respectively. The mixture was shaken and let stand for 2 h. The bottom layer containing lipids was transferred to an Erlenmeyer flask, and added 2 g of sodium sulfate anhydrous. The extracted lipids were filtered through a Whatman No. 4 and solvents were removed in a 100°C sand bath for 15 min, and further dried in a hot air oven at 60°C for overnight. Total lipids were calculated based on gravity measurement.

3.3.3 Hyp and collagen content

Hyp content was determined according to da-Silva, Spinelli, and Rodrigues (2015) with some modifications. Samples (10 mg) were hydrolyzed in 1 mL of 7.0 M NaOH in an autoclave at 121^oC for 40 min. Hydrolyzed samples were neutralized with 3.5 M sulfuric acid to pH 7 and filtered through Whatman no. 4. Samples (50 µL) were added 450 µL of 0.056 M oxidant reagent (1.38% of Chloramine-T hydrate in acetate-citrate buffer pH 6.5) and mixed well. The mixtures were incubated in the dark at room temperature for 25 min. Subsequently, 500 µL of 1.0 M Ehrlich's aldehyde reagent (15.0% of p-dimethyl aminobenzaldehyde in 2:1 (v/v) isopropanol: perchloric acid) was added. The mixtures were then incubated in a 60^oC water bath for 25 min and cooled at room temperature for 3 min. Absorbance at 550 nm was measured (Genesys 10S UV-VIS, Thermo Fisher Scientific, Madison, WI, USA). Collagen contents were calculated using conversion factors of 8.0 (Venn and Maroudas, 1977).

3.4 Collagen extraction process

3.4.1 Conventional extraction

Non-collagenous proteins, fat and pigments were removed by soaking T in 0.1 M NaOH at a ratio 1:10 (w/v) for 6 h. Fresh alkaline solution was replaced every 2 h. Subsequently, samples were washed with DI water until pH of wash water became neutral.

The alkali-treated samples were added 0.5 M acetic acid at a ratio 1:15 (w/v) and extraction was carried out for 48 h at room temperature (25 ± 2^oC). Subsequently, the mixtures were centrifuged (CR22G-III, Hitachi Ltd., Tokyo, Japan)

at 15,000×g for 20 min. Supernatants were added 4.0 M NaCl to attain final concentration of 2.6 M. Collagen pellets were collected by centrifugation at 17,000×g for 30 min. Then, collagens were dialyzed against RO water using 3.5 kDa molecular weight cut-off (MwCO) dialysis membrane (Thermo Fisher Scientific Inc., Rockford, IL, USA) for 48 h. Dialyzed collagens were lyophilized (GT2-S, GEA Lyophil GmbH, Hürth, Germany) and used for further analysis. Acid-soluble collagen obtained from this process was referred to as AS.

Precipitates remained after acid extraction were further extracted with 0.5 M acetic acid containing pepsin (50 units/ g residue) at a ratio 1:15 (w/v) for 48 h at room temperature ($25\pm2^{o}C$). Soluble collagen was collected and precipitated as described previously. The collagen samples obtained from pepsin solubilization process was referred to as PS. Yield and collagen recovery were calculated, based on dry basis as follows:

$$\text{Yield (\%)} \quad = \left(\frac{\text{weight of lyophilized collagen}}{\text{weight of raw material, dry basis}}\right) \times 100$$

$$\text{Collagen recovery (\%)} \quad = \left(\frac{\text{collagen content of lyophilized collagen}}{\text{collagen content of raw material}}\right) \times 100$$

3.4.2 Ultrasound-assisted extraction

To avoid any metal contamination resulted from cavitation erosion of the titanium alloy probe, the alkali-pretreated T (35 g) was mixed with 100 mL DI water and packed in a polypropylene bag. Subsequently, the filled bag was attached at the bottom and on the wall of a glass beaker containing 300 mL DI water and 200 g ice as shown in Fig. 1. An ultrasonic generator of 20 kHz (Q500, Qsonica LLC., Newtown, CT, USA) equipped with a 25-mm diameter cylindrical titanium alloy

probe connected to a booster was used. The probe was immersed into water in a depth of 5 cm, and a pulse mode of on-time 5 sec with off-time 5 sec were applied. Temperature of the system was monitored by a thermocouple type K (54IIB, Fluke Corporation, Everett, WA, USA) and controlled to be lower than 25°C throughout the ultrasound exposure.

Various ultrasound intensity (10.93, 17.87 and 31.27 W·cm^{-2}) and ultrasound exposure time (10, 20 and 30 min) were studied. The filled sample bags were flipped every 10-min intervals of exposure time to assure uniform ultrasonic treatment. When the exposure time was attained, samples were added acetic acid to contain the final concentration of 0.5 M. Extraction by acid and pepsin was performed as described in 2.4.2, but with various extraction time (12, 18, 24, 30, 36, 42 and 48 h). Optimal condition was determined based on yield and collagen content.
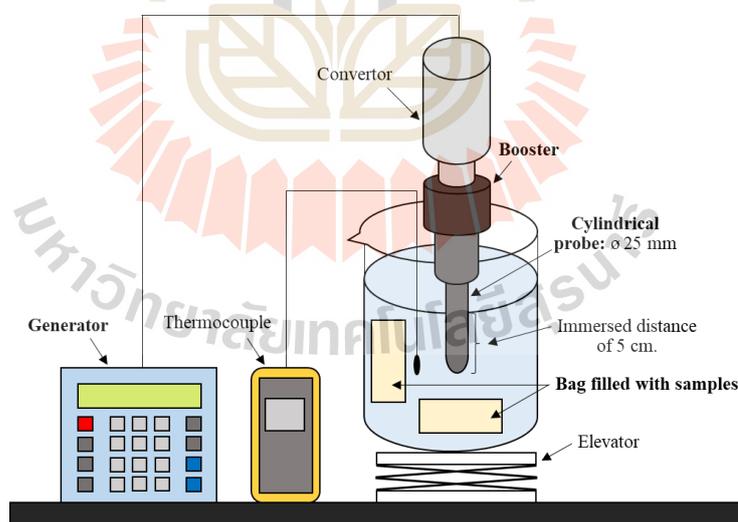
Figure 3.1   Schematic diagram of ultrasound set up.

Ultrasound power was estimated from mechanical energy that is partially lost in the form of heat, when ultrasound waves dissipate through the medium. Ultrasound power in watt (W or J/s) was calculated using the equation (Margulis and Margulis, 2003).

$$\text{Ultrasound power (P)} \quad = \quad m \times C_p \times \left(\frac{dT}{dt} \right)$$

Where, m is the mass of the sonicated medium (g), C_p is specific heat capacity of liquid water at a constant pressure (J·g^{-1}·^{o}C^{-1}), and $\frac{dT}{dt}$ is slope between temperature and time at processing time for 120 sec.

3.5 Scanning electron microscope (SEM)

Microstructure of alkali-pretreated T and ultrasound-treated T, as well as extracted collagen samples were analyzed using a SEM (JSM-6010LV, Japan Electron Optics Laboratory Technics Co. Ltd., Tokyo, Japan). All samples were mounted on specimen stubs with double carbon tape and gold coating was performed using an ion sputtered-coater (JFC-1100E, Japan Electron Optics Laboratory Technics Co. Ltd., Tokyo, Japan) for 1 min. Microstructure of the specimens was evaluated using an electron acceleration voltage of 15 kV at 500X magnification.

3.6 Characterization of collagen

3.6.1 Amino acid composition

Collagen samples (10 mg) were hydrolyzed in 1 mL of 6 M HCl at 115°C for 24 h using a heat block (Boekel Scientific, Feasterville, PA, USA).

Hydrolysates were neutralized with 3.5 M NaOH, and filtered through Whatman No. 4. Norleucine was added as an internal standard. Amino acid profiles were analyzed using an amino acid analyzer (Biochrom 30 plus, Biochrom Ltd., Cambridge, UK) equipped with a cation exchange column (u-3183 High resolution, 200 mm of bed length and 4.6 mm of diameter, Biochrom Ltd., Cambridge, UK). Mobile phases were lithium citrate buffer (pH 2.80-3.55) and lithium hydroxide buffer (pH 14.0). Analysis system was performed using a post-column derivatization by ninhydrin. Mobile phases and ninhydrin were operated at 20 mL/h. Amino acid profiles were analyzed using an EZChrom Elite software, version 3.3 (Biochrom Ltd., Cambridge, UK) and expressed as amino acid residues/1,000 residues.

3.6.2 Micro-differential scanning calorimetry (μDSC)

Thermal denaturation of collagen sample was determined, according to Carsote and Badea (2019) with slight modifications. Collagen samples (5 mg) were accurately weighed into a Hastelloy C crucible and added 500 mg of either DI water or 0.5 M acetic acid. The mixtures were allowed to rehydrate in a $4^{o}C$-refrigerated incubator (KB240, Binder GmbH, Tuttlingen, Germany) for 24 h. Thermal analysis was performed using a μDSC (7 evo micro calorimetry, Setaram Instrumentation, Caluire-et-Cuire, France). Instrument was calibrated using a naphthalene standard. Samples were scanned from 20 to $70^{o}C$ at a heating rate of $1^{o}C$/min. DI water and 0.5 M acetic acid were used as references for the respective solubilizing medium. Denaturation temperature (T_{d}) and enthalpy (ΔH) were estimated using Calisto software, version 1.0 (Setaram Instrumentation, Caluire-et-Cuire, France).

3.6.3 Spectral characterization

3.6.3.1 Ultraviolet (UV) spectroscopy

Collagen samples (5 mg) were dissolved in 5 mL 0.5 M acetic and shaken at 150 rpm at 4°C for 12 h. Debris was removed by centrifugation at 10,000×g for 10 min. Solubilized samples were diluted to obtain 0.5 mg protein/ mL as quantified by the Biuret method (Gornall, Bardawill, David, 1949). Samples were placed in a 1-cm quartz cell and absorbance was measured using a UV spectrophotometer (Libra S22, Biochrom Ltd., Cambridge, UK). All spectra were scanned between 200 and 400 nm at a scan speed of 4 nm/s, and the maximum absorption peak was analyzed using a Biochrom acquire software, version 1.01 (Biochrom Ltd., Cambridge, UK).

3.6.3.2 Circular dichroism (CD) spectroscopy

Collagen samples were prepared as described in 3.6.3. Protein content was diluted to 0.1 mg/mL as quantified using a NanoDrop UV-vis spectrophotometer (OneC, Thermo Fisher Scientific, Madison, WI, USA) at 205 nm described by Loughrey, Mannion, and Matlock (2016). Samples were placed in a 1-mm quartz cell and analyzed using a CD spectrophotometer (Jasco J-815, Jasco International Co., Ltd., Tokyo, Japan). Spectra were recorded between 260 and 190 nm at a scan speed of 50 nm/min. Measurements were performed at 25°C using a peltier type cell holder. Acetic acid solution (0.5 M) was used as a reference for subtraction. All spectra were recorded using a Spectra manager[®] software, version 2.0 (Jasco International Co., Ltd., Tokyo, Japan).

3.6.3.3 Fourier transform infrared (FT-IR) spectroscopy

Collagen samples were placed on the crystal cell (Pike Technology Inc., Madison, WI, USA) and compressed on a FT-IR spectrometer (Tensor 27, Bruker Co., Ettlingen, Germany). Samples were performed on an attenuated total reflectance (ATR) mode. The IR spectra were recorded over the wavelength range of 4,000-900 cm^{-1}. Spectra were collected for 64 scans with a resolution of 4 cm^{-1} against background spectra which was measured from the clean empty cell at 25°C. Spectra preprocessing was carried out by smoothing, baseline correction and normalization (X_{start} to $X_{end\ point}$: 1,700-1,600 cm^{-1}). Curve fitting of protein secondary structure was analyzed at the amide I region, using Lorentzian/Gaussian spectral line shape. The β-sheet, random coil, α-helix, and β-turn were observed at 1,626-1,639, 1,640-1,649, 1,650-1,663, and 1,675-1,696 cm^{-1}, respectively (Tranter, 2017). Moreover, absorption intensity of 1,454 region (1,415-1,485 cm^{-1}) and amide III region (1,200-1,300 cm^{-1}) was determined. All spectral data were collected and analyzed using the OPUS software, version 7.2 (Bruker Co., Ettlingen, Germany).

3.6.4 Protein pattern

Collagen samples (5 mg) were dissolved in 1 mL of 10% sodium dodecyl sulfate (SDS), and shaken at 150 rpm at room temperature for 6 h. Debris was removed by centrifugation at 10,000×g for 10 min. Solubilized samples were mixed with a treatment buffer (0.5 M Tris-HCl, pH 6.8, containing 4% (w/v) SDS, 20% (v/v) glycerol, 10% (v/v) β-mercapthoethanol and 0.02% (w/v) bromophenol blue) to obtain 12 µg of protein as quantified by the Lowry method (Lowry, 1951). Samples were boiled at 90°C for 3 min, and separated on polyacrylamide gel electrophoresis made

from 7.5% running gel, and 4% stacking gel. Electrophoresis was carried out at 80 Volt. Subsequently, gels were stained with Coomassie brilliant blue R-250 for 30 min and followed by de-staining with 10% (v/v) acetic acid in 25% (v/v) methanol for 2 h. SDS-PAGE image was recorded using a gel document system (Fire reader V4, Uvitec Ltd., Cambridge, UK) and molecular weight (Mw) was estimated using UV1-ID software, version 16.0 (Uvitec Ltd., Cambridge, UK).

3.6.5 Protein identification

Type of collagen was identified according to Sharma et al. (2014) with some modifications. Collagen samples were separated on SDS-PAGE using 7.5% running and 4.0% stacking gel. Protein bands were excised from the gel using a scalpel. Gel pieces were washed with 20 mM ammonium bicarbonate (AmB), followed by 20 mM AmB: acetonitrile (ACN) at a ratio 1:1, and lastly by ACN for 10 min in each step. Gels were then treated with 10 mM dithiothreitol (DDT) in 20 mM AmB at 56°C for 45 min, followed by 55 mM iodoacetamide (IAA) in 20 mM AmB in the dark at room temperature for 30 min, and washed with 20 mM AmB: ACN (1:1) and ACN for 10 min in each step.

In-gel digestion was carried out in 20 mM AmB containing 20 ng/μL of sequencing-grade modified trypsin (V5111, Promega Corp., Madison, WI, USA) at 4°C for 30 min. Gel pieces were incubated with 25 mM AmB at 37°C overnight. Peptides were extracted with 1% formic acid (FA) in 50% ACN and followed by 1% FA in 85% ACN. Samples were dried using a refrigerated centrifugal vacuum concentrator (CentriVap, Labconco Corp., Kansas City, MO, USA) for 2 h, and reconstituted with 0.1% FA in 2% ACN. Undissolved debris was removed by centrifuging at 10,000 rpm for 10 min.

Digested samples were analyzed using a nano-liquid chromatography system (EASY-nLC II, Bruker Daltonik GmbH, Bremen, Germany) coupled with an ion trap mass spectrometer (Amazon Speed ETD, Bruker) equipped with an ESI nano-sprayer. The ESI-TRAP instrument was calibrated in the m/z range 50-3,000 using an internal calibration standard. Digested samples (3 μL) were loaded by an autosampler onto an EASY-Column (10 cm, ID 75 μm, 3 μm, C18-A2, Thermo Fisher Scientific, Madison, WI, USA). Mobile phase A (0.1% FA) and B (0.1% FA in ACN) were used at a flow rate of 500 nL/min with a linear gradient from 5-35% B for 50 min, and 80% B for 10 min. Tryptic-digested bovine serum albumin (50 fmol) was used as a control. LC–MS/MS spectra were analyzed using Compass Data Analysis version 4.0.

Collagen identification was performed by searching against the NCBI's protein database on Metozoa (animals) using the Mascot MS/MS ion search program (http://www.matrixscience.com) with the initial searching parameters; Enzyme: Trypsin; carbamidomethylation (C) as fixed modification, and oxidation (HW) and oxidation (M) as variable modification; peptide mass tolerance of 0.5 Da and fragment mass tolerance of 0.5 Da; a peptide charge state of +1, +2, +3; instrument type: ESI-TRAP; and report top (Auto).

3.7 Statistical analysis

All experiments were performed in triplicates. Mean values of chemical composition of raw material and alkali-treated samples were compared by student's *t*-test for independent samples model with 95% confidence level ($p<0.05$). Others studies, analysis of variance was performed with a completely randomized design

model and mean comparisons were analyzed by Duncan's multiple range test with 95% confidence level ($p<0.05$). Statistical analyses were performed using IBM SPSS Statistics for Windows, version 24.0 (IBM Corp., Armonk, NY, USA).
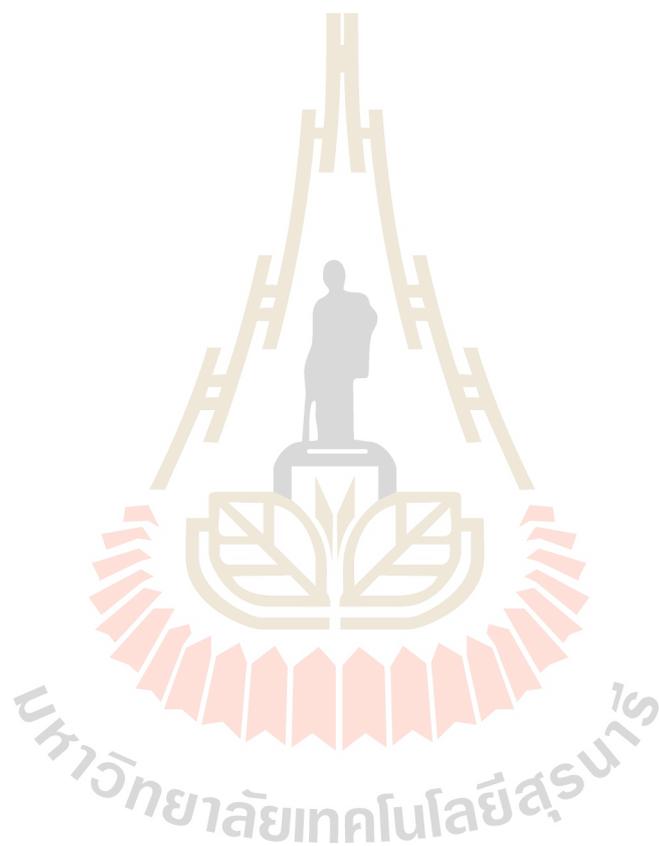
CHAPTER IV

RESULTS AND DICUSSIONS

4.1　Chemical composition

Major component of T was protein, accounting for 68.0% dry basis (Table 4.1). Collagen was estimated to be 37.6% based on the amount of hydroxyproline (Hyp) content. This was higher than that reported in duck trachea (32.9%), turkey head (19.9%), sheep cartilage (12.3%), and lamb cartilage (8.9%) (Vittayanont and Jaroenviriyapap, 2014; Vidal et al., 2020; Blanco, Sotelo, and Pérez-Martín, 2019).

Table 4.1 Chemical composition of broiler chicken trachea (T).

Composition	Content (%)	
	Raw material	Alkali-pretreated
Moisture	82.6±0.05	83.8±0.04
Protein	68.0[b]±0.84	89.3[a]±0.27
- Hyp	4.7[b]±0.05	6.5[a]±0.52
- Collagen	37.6[b]±0.39	52.3[a]±3.98
Ash	3.3[a]±0.01	0.8[b]±0.03
Total lipid	14.4[a]±0.42	3.0[b]±0.05
Carbohydrate	14.3[a]±0.07	7.0[b]±0.09

All are in dry basis except for moisture content; Carbohydrate content was calculated by 100 - (ash + total fat + protein); Different superscripts in row indicate significant difference ($p<0.05$) with row.

However, T also contained relatively high total lipid (14.4%) and carbohydrate (14.3%). After alkali pretreatment, collagen content of T increased to 52.3% because, non-collagenous proteins and fat were removed. Moreover, minerals and carbohydrates were leached out by after alkali-pretreatment. Alkali pretreatment is required for T collagen extraction.

4.2   Yield of collagen

UAE increased yield of collagen extraction with the applied power up to 17.87 $W \cdot cm^{-2}$ (Figure 4.1A) .Further increase the intensity to 31.27 $W \cdot cm^{-2}$ did not increase yield of collagen extraction .It should be noted that ultrasound at intensity of 10.93 $W \cdot cm^{-2}$ showed comparable yield with the conventional methods, AS and PS. Hydrodynamic oscillation of 17.87 $W \cdot cm^{-2}$ could increase tissue disruption, leading to enhancement of acid and/or pepsin accessibility. However, tissue membrane was not sufficiently disrupted at applied power of 31.27 $W \cdot cm^{-2}$, resulting in comparable yield with 17.87 $W \cdot cm^{-2}$.

When UAE at intensity of 17.87 $W \cdot cm^{-2}$ was applied for 20 min, yield improvement was clearly noticed (Figure 4.1B). Extended exposure time of ultrasound, enhanced tissue disruption, allowing more acid/ pepsin solubilization. Nevertheless, further increase of exposure time to 30 min did not further increase yield ($p>0.05$).

When the ultrasound-treated samples were extracted by either acid or acid/ pepsin, collagen yield slowly increased with acid extraction and reached the maximum at 1.58% at 42 h, while 36 h extraction time resulted in the maximum yield in pepsin-solubilization process ($p<0.05$, Figure 4.4C). In the conventional process, extraction time of collagen is about 48 h (Li et al., 2009; Liang et al., 2014; Ali et al., 2018; Luo et al., 2018). UAE

reduced extraction time by 12.5% in U-AS and 25% in U-PS. In addition, both yields of U-AS and U-PS increased up to 2times, when compared to the respective conventional process. UAE in combination with pepsin appeared to be the most effective process for T collagen extraction, enabling 6.28% yield and 25% time-reduction. Ultrasonic cavitation can open-up structure of collagen fibrils (Li et al., 2009), thus improving the pepsin solubilization of collagen.

Yield of collagen from the conventional extraction by Ac and Pep were 0.7 and 3.1%, corresponding to 1.3 and 6.9% recovery of collagen (Figure 4.2). Acid extraction showed lower yield and collagen recovery than did acid-pepsin extraction. Crosslinks at telopeptide region, were specifically cleaved by pepsin, resulting in an increased yield. In contrast, hydronium ion (H_3O^+) from acetic acid could increase the swelling of collagen molecule, enhancing repulsion between α-helix, and solubilizations. Yields of AS and PS were much lower than that reported from skin and tendon at 24 h extraction (Iswariya, Velswamy, and Uma, 2018; Tang et al., 2018; Ju et al., 2020). Collagen on cartilage coproducts were a complex form, which could not be extracted with ease, in comparison with skin coproduct (Kittiphattanabawon et al., 2010). They reported that yield of shark cartilage collagen extracted by Ac and Pep for 48 h was 1.0-1.3 and 9.5-10.3%, respectively. Yield of chicken sternum collagen extracted by Pep for 96 h was 5.1% yield (Akram and Zhang, 2020).
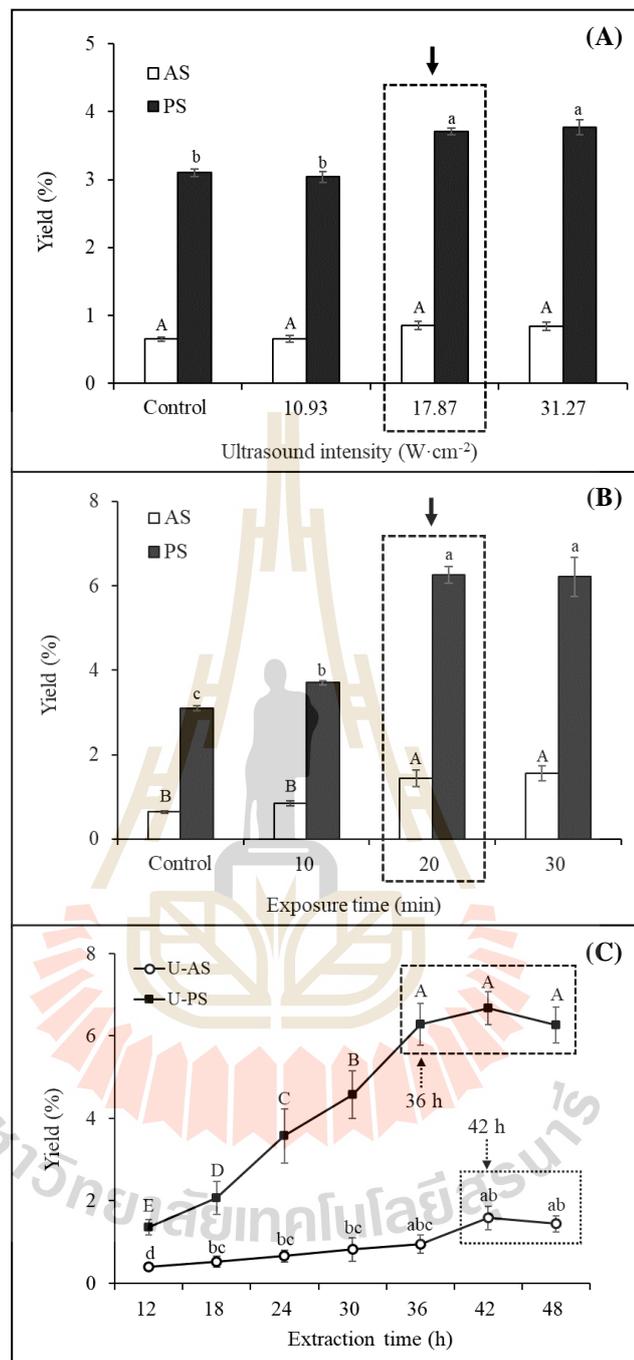
Figure 4.1 Extraction yield of ultrasound-treated T by various ultrasound intensities at 10-min exposure time (A), various exposure times at ultrasound intensity of 17.87 W·cm^{-2} (B), and various extraction times at ultrasound intensity of 17.87 W·cm^{-2} for exposure time of 20 min (C).

U-AS and U-PS showed higher yield than collagens extracted by the conventional extraction reported in various sources, including bigeye tune skin, body of surf clam shell carp scale, and gutted silver carp (Tanaka et al., 2018; Wu, Guo, Liu, and Chen, 2019; Pal and Suresh, 2017; Abdollahi, Rezaei, Jafarpour and Undeland, 2018). However, yield of T collagen obtained from this study was lower than that of flatfish skin collagen extracted by UAE at 60% amplitude for 3 h (Song et al., 2018) and chicken sternal collagen extracted by UAE at intensity of 2,990 $W \cdot cm^{-2}$ for 36 min (Akram and Zhang, 2020). This study demonstrated that ultrasound treatment was effective in disrupting T membrane, resulting in high yield.

In this study, contamination of metal carrion was prevented by avoiding direct contact between probe and sample. This would somewhat lower ultrasound intensity exposing to the sample. In addition, exposing ultrasound simultaneously with acid extraction might facilitate the extraction compared to exposing ultrasound alone prior to extraction. Ultrasound promoted dispersal of bulky enzyme aggregates (Li et al., 2009). Moreover, ultrasound enhanced mass transfer of acid and/or pepsin towards the matrix of raw material (Ali et al., 2018).

Yield of collagen extracted by acid (AS and U-AS) was lower than that of collagen extracted by pepsin (PS and U-AS) as shown in Figure 4.2. More individual collagen molecules from pepsin solubilization would lead to higher amount of Hyp as well as collagen purity. PS and U-PS collagen exhibited high purity about 82-86%, whereas collagen content of AS and U-AS samples were 73-74%. Collagen content from both U-AS and U-PS under -48h extraction time was comparable ($p>0.05$, data not shown). These results revealed that high purity of T collagen can be obtained through pepsin extraction. Moreover, purity of all collagens was much higher than that

reported in soft-shelled turtle collagen. Acid extraction showed 43.6% of collagen purity and 50.7% was obtained in the sample subjected to ultrasonic power of 200 W for 24 min (Zou et al., 2017). Therefore, ultrasound intensity of 17.87 W·cm^{-2} with exposure time of 20 min in conjunction with pepsin provided the highest yield, recovery, and collagen purity.
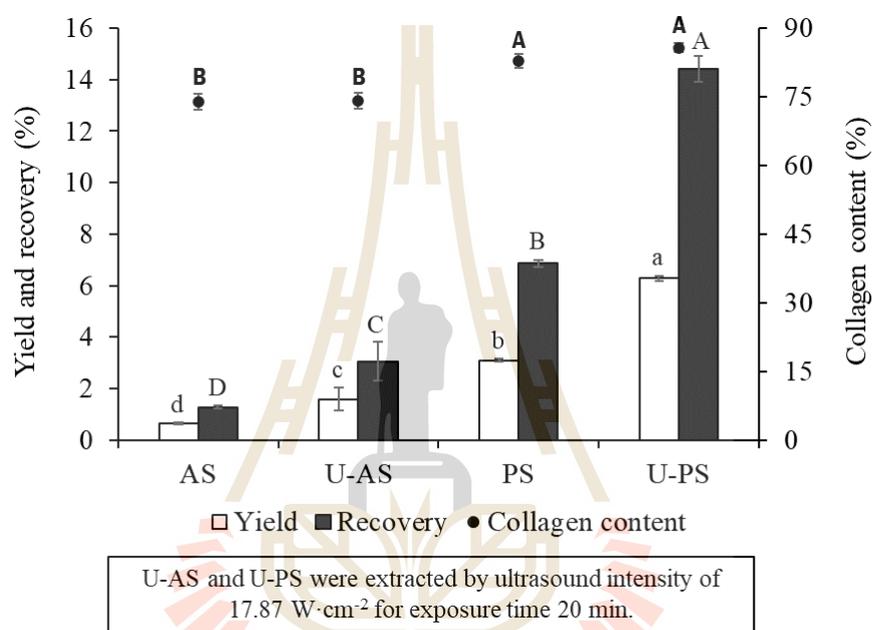
Figure 4.2 Extraction yield, recovery, and collagen content obtained from the conventional and ultrasound-assisted extraction method.

4.3   Scanning electron microscopy (SEM)

SEM images of residues obtained after alkali-pretreatment and ultrasound treatment are shown in Figure 4.3 The images revealed that ultrasound treatment for 10 min disrupted surface of T tissues (Figure 4.3B) and greater extent of tissue disintegration was observed after 20 min exposure (Figure 4.3C). Ultrasound treatment for 30 min also showed severe rupture of T tissue (data not shown). The implosion bubbles from acoustic

cavitation, resulted in high shear stress of compression and decompression pressure $(1.0 \times 10^5$ kPa) (Soria and Villamiel, 2010), leading to tissue rupture. This would allow more accessibility to acid and pepsin, rendering higher yield in ultrasound at 20 min.

Ultrasound intensity of 17.87 W·cm^{-2}
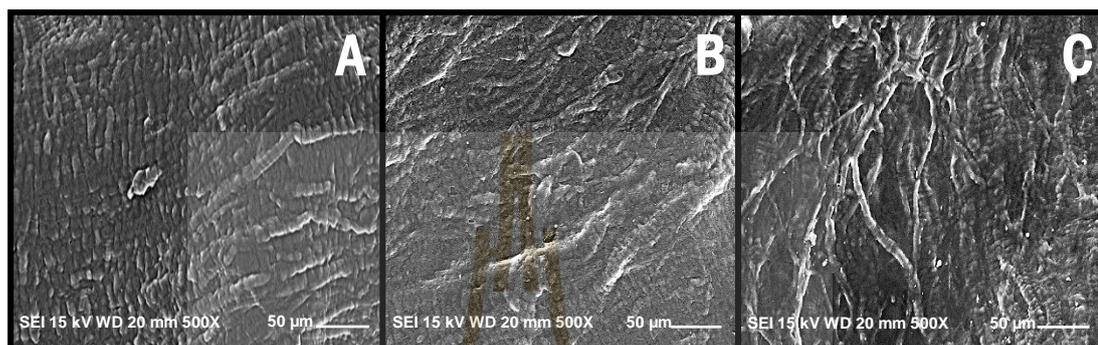
Figure 4.3 SEM images of residues obtained after alkali-pretreatment (A), ultrasound treatment for 10 min (B) and 20 min (C) at 500 magnifications.

All extracted collagen samples exhibited fibrous structure (Figure 4.4). This was in agreement with previous studies (Zou et al. 2017; Song et al., 2019; Akram and Zhang, 2020). AS and U-AS collagen showed a fine fibrous structure. However, PS and U-PS presented a dense multi-layered sheet-like structure.

These microscopic results suggested that microstructure of acid-solubilized collagen and pepsin-solubilized collagen was different. Ultrasonic processing did not affect microstructure of the extracted collagen. Yang, Leong, Du, and Chua (2001) reported that architectural features of cavities and interconnectivities were important for biological activities of collagen, including cell adhesion, growth, proliferation, and new tissue formation. The use of collagen for wound healing application relies on dense sheet-like film

structures (Ge et al., 2020). These results indicated that T collagen extracted by ultrasound technology showed potential to be used in biomedical applications.

Conventional method

Ultrasound intensity of 17.87 W·cm⁻²
for exposure time 20 min
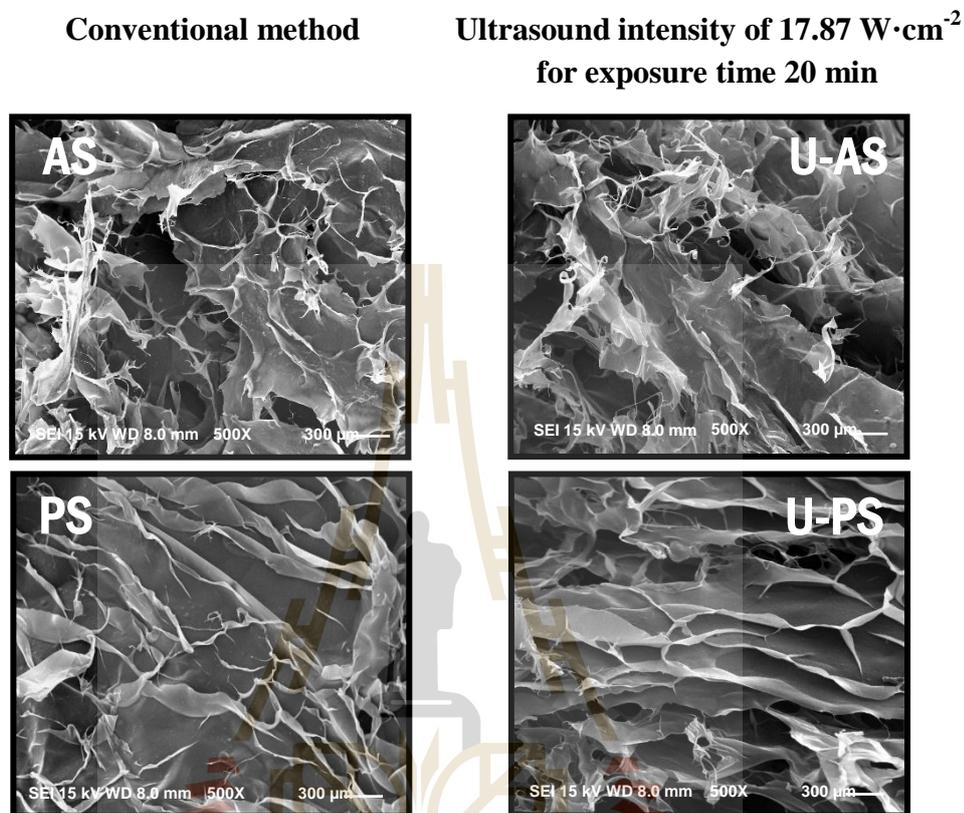
Figure 4.4   SEM images of T collagen extracted by various methods at 500 magnifications; AS (acid-soluble collagen), PS (pepsin-soluble collagen), U-AS (UAE followed acid extraction) and U-PS (UAE followed pepsin extraction).

4.4   Amino acid composition

Distinct amino acids of all collagen samples were glycine (Gly), proline (Pro), hydroxyproline (Hyp), whereas histidine (His), hydroxylysine (Hyl), methionine (Met), phenylalanine (Phe), and tyrosine (Tyr) were present in low amounts (Table 4.2). These AA profiles were similar to those previously reported in type I collagen extracted from

various sources, including chick sternal, chicken feet, Siberian sturgeon cartilage, and bigeye tuna bone (Cao, et al. 2013; Zhou et al., 2016; Luo et al., 2018; Ali et al., 2018, Ahmed, Haq and Chun, 2019).

Cysteine (Cys) and tryptophan (Trp) were not determined in this study as they were destroyed during acid hydrolysis. Trp has not been found in collagen (Gauza-Włodarczyk, Kubisz, Włodarczyk, 2017), while only about 2-6 Cys residues have been reported in collagen (Brown, Farrell, and Wildermuth, 2000). Cartilages sources normally composed of 80% type II collagen, containing relatively high amount of Hyl (18 residues), Glu/Gln (88 residues) (Aigner and Stöve, 2003; Cao et al., 2013; Liang et al., 2014; Cumming, Hall, and Hofman, 2019). However, T collagen exhibited amino acid profiles of type I collagen with relatively low Hyl and Glu/Gln, but high Ala. This profile was similar to silver carp scale, golden carp skin, and bovine tendon (Wu et al., 2019; Ali et al., 2018; Ju et al., 2020).

Hyp was derived from post-modification through hydroxylation of Pro by prolyl-hydroxylase. This amino acid is associated with thermal stability of collagen triple helix. Collagens extracted by pepsin (PS and U-PS) exhibited higher imino acids (Pro+Hyp) than acid soluble collagens (AS and U-AS). This result suggested that T contained high intermolecular cross-links at telopeptide region via imino acids, which are cleaved by pepsin. Moreover, the degree of proline hydroxylation (PH) for collagen extracted by pepsin was also higher than the acid-soluble collagen. Hydroxylation is a critical process regulating collagen stability via imino acid rings (Rappu, Salo, Myllyharju, Heino, 2019). Pyrolidine ring on Hyp and Pro led to nucleation zone to generate network structure, exerting high stability of triple helix. The results revealed that pepsin-soluble collagen exhibited higher stability than acid-soluble collagen. This was in agreement with those

previously reported in collagens extracted from whale shark cartilage, sea bass scale, and golden carp skin (Jeevithan et al., 2015; Chuaychan et al., 2015; Ali et al., 2018).

Acid-solubilized collagen showed different amino acid profiles with those collagens extracted by pepsin extraction. Some amino acids, namely Ala, Arg, Ile, Leu, Thr, and Val of pepsin soluble collagen were obtained lower content than acid-solubilized collagen ($p<0.05$). This could be because of the removal of the telopeptide region during pepsin hydrolysis. Similar findings were also reported in collagens from skin of eel-fish, blue shark and deer (Veeruraj, Arumugam, and Balasubramanian, 2013; Elango et al., 2018; Lodhi et al., 2018). Additionally, collagens obtained from UAE showed similar amino acid profiles from those extracted from the conventional process. These results demonstrated that amino acid compositions of all collagens have not been affected by the ultrasonic process.

4.5 Micro-differential scanning calorimetry (μDSC)

T_d and ΔH values of collagen rehydrated in 0.5 M acetic acid were lower than those rehydrated in deionized (DI) water (Table 4.3). Lower T_d values in acetic acid were likely due to electrostatic repulsion of helical structure and destruction of hydrogen bonds in the presence of acid. In addition, T_d and ΔH values of collagen extracted by pepsin were higher than those of sample extracted by acid. Higher imino acid content in PS might explain its higher thermal stability via pyrolidine rings (Shoulders and Raines, 2009). Moreover, the collagen extracted by UAE exhibited comparable T_d and ΔH values with those extracted by the conventional method, regardless of the rehydration solvent ($p>0.05$). These results revealed that ultrasound treatment did not damage with triple helix structure of T collagen.

Table 4.2 Amino acid composition of collagen extracted by conventional and ultrasound-assisted extraction methods.

Amino acid	Content (residues/ 1,000 total residues)			
	AS	U-AS	PS	U-PS
Ala	116[a]±1.96	112[a]±2.70	97[b]±3.47	101[b]±0.88
Arg	58[a]±3.16	57[a]±2.83	52[b]±2.57	51[b]±4.05
Asp/ Asn	48±2.67	47±1.20	42±3.46	46±1.62
Glu/ Gln	72±3.10	73±3.11	74±1.31	73±3.25
Gly	308±3.23	311±4.89	310±2.26	308±2.30
His	6±2.57	10±1.20	11±0.57	8±0.52
Hyl	7±1.02	7±0.83	8±2.81	9±0.65
Hyp	76[b]±1.03	77[b]±1.31	105[a]±0.88	104[a]±3.81
Ile	20[a]±2.60	17[a]±1.00	15[b]±0.19	14[b]±1.11
Leu	47[a]±2.18	45[a]±3.69	42[b]±1.61	42[b]±1.19
Lys	28±1.08	26±3.12	25±1.59	27±0.51
Met	11±1.35	9±4.71	9±0.63	8±1.05
Phe	11±1.49	10±0.62	15±0.85	13±1.72
Pro	112[ab]±3.75	108[b]±0.93	115[ab]±4.10	118[a]±1.27
Ser	29±1.53	29±2.42	27±1.27	28±1.82
Thr	26[a]±0.92	25[a]±2.52	20[b]±2.25	19[b]±1.56
Tyr	6±0.37	7±4.62	5±0.57	4±0.52
Val	32[a]±1.92	30[ab]±2.22	29[b]±0.83	27[b]±0.66
Imino acid	188[b]±2.48	186[b]±0.72	220[a]±4.89	222[a]±1.51
PH (%)	41.0[b]±0.72	42.0[b]±0.60	47.7[a]±0.72	46.9[a]±2.02

PH was degree of proline hydroxylation and calculated from [Hyp residue/ (Hyp residue + Pro residue)] × 100. Different superscripts in a row indicate significant difference.

Table 4.3 Denaturation temperature (T_d) and enthalpy (ΔH) values of collagen samples by different rehydration.

Sample	T_d (^{o}C)		ΔH (J/g)	
	DI Water	0.5 M Acetic acid	DI Water	0.5 M Acetic acid
AS	35.1[b]±0.48	32.6[b]±0.32	0.11[b]±0.02	0.09[b]±0.03
U-AS	34.3[b]±0.34	31.9[b]±0.41	0.13[b]±0.01	0.09[b]±0.01
PS	45.6[a]±0.17	42.1[a]±0.11	0.26[a]±0.03	0.21[a]±0.01
U-PS	45.0[a]±0.22	41.8[a]±0.28	0.23[a]±0.03	0.18[a]±0.06

Different superscripts in column indicate significant difference ($p < 0.05$).

The habitat and body temperature of animal greatly affected thermal stability of collagen. Collagen from body of surf clam shell, frog skin, and hybrid sturgeon skin exhibited T_d of 26.5-33.5^{o}C (Wu et al., 2019; Zhao, Wang, Zhang, and Su, 2018; Wei, Zheng, Shi, Li, and Xiang, 2019), whereas collagen from chicken lungs, porcine lungs, cattle tendon, ovine bone, calf skin, and rabbit skin showed T_d values of 35.3-45.6^{o}C (Zou et al., 2020; Lin et al., 2011; Gao et al., 2018; Ran and Wang, 2014; Martínez-Ortiz et al., 2015). T_d value of collagen from land animals generally was higher than that of collagens extracted from amphibian, reptile and aquatic animals. Collagens derived from land animals also contained higher imino acid content of approximately 215-225 residues/1,000 residues, while imino acid content of collagens extracted from other sources ranged 155-180 residues/1,000 residues. T collagen extracted by pepsin showed higher T_d value than 40°C, corresponding to 220-222 imino acid residues/1,000 residues. These results indicated that PS and U-PS collagen

revealed higher thermal stability than that collagen from other animals as mentioned above.

Lys and Hyl residues are crucial for intermolecular crosslink via covalent bond by lysyl oxidase between the collagen telopeptide and helical region (Yamauchi and Sricholpech, 2012). Thus, Lys and Hyl cross-linking would provide stability to collagen structure. PS and U-PS collagen comprised similar contents of Lys and Hyl of 33 and 36 residues/ 1,000 residues (p>0.05), corresponding to higher T_d values (> 42°C). Luo et al. (2018) reported that pepsin-solubilized and acid-solubilized collagen from Siberian sturgeon cartilage contained Lys and Hyl of 27 and 34 residues/1,000 residues, estimating to be 28.3 and 30.5°C of T_d, respectively. Additionally, Lys and Hyl of collagen from Amur sturgeon cartilage extracted by acid and pepsin were 28 and 33 residues/ 1,000 residues, whose T_d value was 32.9 and 35.7°C, respectively (Liang et al., 2014). These results confirmed that high content of Lys and Hyl residues lead to high thermal stability. Collagen extracted by pepsin showed higher thermal stability than that extracted by acid. Hence, imino acids, Lys, and Hyl residues contributed to thermal characteristic of collagen and this is the first study elucidating thermal behavior of T collagen.

4.6   Ultraviolet (UV) spectroscopy

Triple-helix structure of collagen reveals an individual absorption peak at approximately 230 nm (Zhu et al., 2020). UV-spectrum of all extracted collagen samples exhibited the maximum peak at approximately 231 nm (Figure 4.5). Maximum absorption of collagen extracted from fresh water carp scale, catfish

air-bladder, porcine skin and bluefin tuna skin was found at 192, 224, 235, and 238 nm (Chinh et al., 2019; Divya et al., 2018; Tanaka et al., 2018; Li et al., 2020).
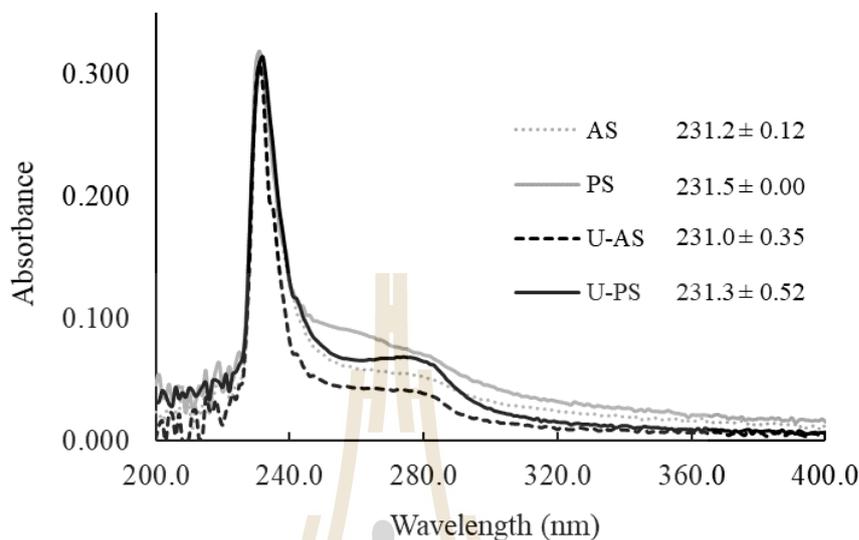
Figure 4.5 UV spectrum of collagen samples extracted by different methods.

The UV-absorption was related with C=O, $CONH_2$, and ^-COOH in the polypeptide chains of collagen molecule (Abdollahi et al., 2018). Contamination of non-collagenous proteins would be minimal due to low absorbance of UV_{280}, a typical wavelength of protein absorption. The sensitive chromophores between $UV_{210-220}$ and $UV_{260-280}$ were minimal in all spectra, confirming low amount of His, Tyr, and Phe residues, as well as lack of Trp in all extracted collagen samples. In addition, collagen extracted by ultrasound showed comparable UV absorption with those extracted by the conventional method ($p>0.05$). Hence, these results suggested that super-helix structure of extracted collagen was not damaged through UAE treatment.

4.7   Circular dichroism (CD) spectroscopy

Changes of triple helix conformation was evaluated by CD spectra (Figure 4.6). Spectra of all samples showed a cross zero rotation at 215 nm, the maximum peak was observed at 222 nm, and the minimum peak was approximately 196-197 nm. These are characteristics of supercoil structure of collagen characteristic (Drzewiecki, Grisham, Parmar, Nanda, Shreiber, 2016).

Both negative and positive ellipticity were correlated with protein conformation (Greenfield, 2006). Unfolding of triple helix can be seen by a decrease in positive ellipticity in concomitant with an increase of negative ellipticity as well as a red shift of negative band to 203-210 nm (Cao and Xu, 2008; Silva et al., 2016; Drzewiecki et al., 2016). Akram and Zhang (2020) reported that chicken sternal collagen extracted by UAE at intensity of 2,990 $W \cdot cm^{-2}$ with exposure time of 36 min exhibited more negative ellipticity value, and the negative band shifted to 202.2 nm, indicating partial loss of triple helix structure. This study revealed that ultrasound treatment of 17.87 $W \cdot cm^{-2}$ for 20 min did not significantly disturb triple helical structure.

Most collagens showed similar values of negative ellipticity, while U-PS exhibited the lowest value ($p<0.05$). Dynamic force by acoustic pressure disrupted T cellular membrane and might simultaneously enhance mass transfer pepsin towards the collagen fibril, resulting in shorter extraction time. Then, collagen extracted by Pep followed UAE led to high order collagen structure. It demonstrated that U-PS revealed the highest integrity of triple-helical structure.

The ratio of positive and negative ellipticity or Rpn value of all samples was about 0.1 (Table 4.4), indicating triple helix for native conformation of collagen (Usha

and Ramasami, 2005). These results confirmed that T collagen retained triple helix integrity even under high intensity ultrasound treatment applied.
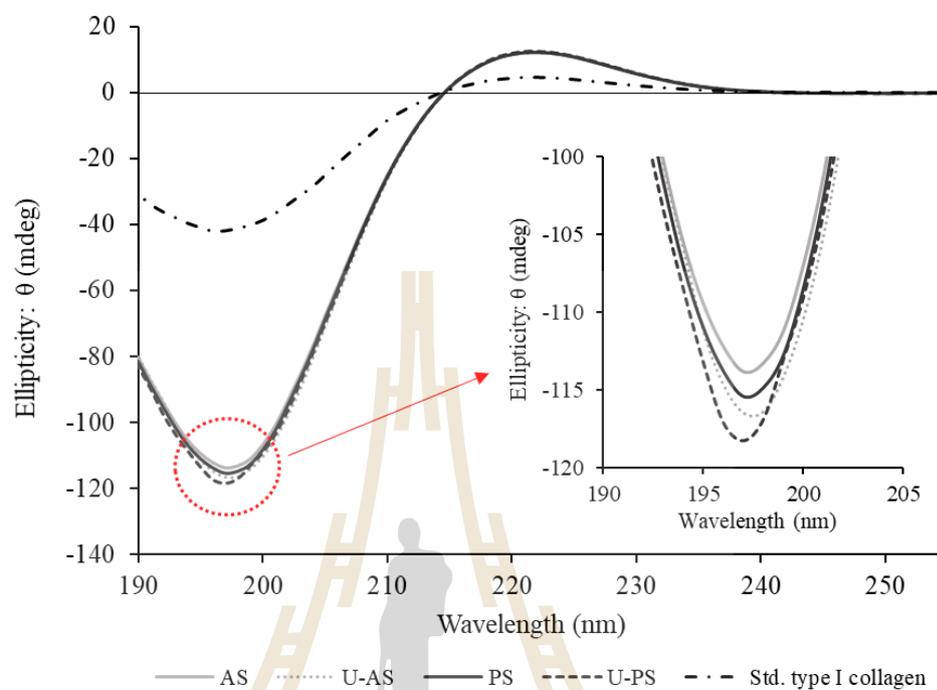
Figure 4.6 CD spectra of all extracted collagen samples.

Table 4.4 Absorption ratio obtained from FT-IR spectra and Rpn ratio calculated from CD spectra of collagens extracted by various methods.

Sample	Absorption ratio (Amide III/ 1,454 cm^{-1})	Rpn*
AS	1.03±0.12	0.11±0.01
U-AS	1.07±0.03	0.10±0.20
PS	1.06±0.16	0.11±0.00
U-PS	1.04±0.07	0.10±0.43
Std. type I collagen	1.01±0.01	0.11±0.00

*Rpn was CD ellipticity ratio between maximum and minimum value .

4.8   Fourier transform infrared (FT-IR) spectroscopy

FT-IR spectra of all collagens showed peaks related to amide A, B, I, II and III regions (Figure 4.7A). Collagen typically shows 3 distinct regions, the amide I region representing C=O stretching vibration along the polypeptide backbone, while the amide II and III region featured the C-N stretching and N-H bending (Carbonaro and Nucara, 2010; Bunchu, Fleschin, and Aboul-Enein, 2014). Amide I and II regions are indicators of the secondary structure of proteins, whereas amide III is a sensitive fingerprint of collagen molecule (Cao and Xu, 2008).

Spectra of all collagen samples exhibited similar pattern with wavenumbers of amide I, II and III regions at 1,635-1,637, 1,539-1,547, and 1,236-1,239 cm^{-1}, respectively. Furthermore, most collagen contained weak vibration at 1,743 cm^{-1}. This region represented C=O stretching band from ester bond of cholesterols, including high-density, low-density, and very low-density lipoprotein, which vibrated at 1,737-1,744 cm^{-1} (Krilov, Balarin, Kosovic, Gamulin, and Brnjas-Kraljevic, 2009). These results indicated that T collagen from this study likely contained lipoproteins. Further pretreatment should be developed to remove fat and lipoproteins to obtain high purity collagen.

The α-helix is a major structure in all collagen samples (Figure 4.7B), estimating to be 30-32% ($p>0.05$), whereas the β-turn and random coil were minor structure. This result demonstrated that ultrasound intensity of 17.87 $W \cdot cm^{-2}$ for 20 min exposure time did not disturb secondary structure of T collagen. Akram and Zhang (2020) stated that chicken sternal collagen extracted by ultrasound intensity of 2,990 $W \cdot cm^{-2}$ for exposure time 36 min resulted in disruption of secondary structure

of collagen. Hence, extremely high intensity and long exposure time might induce structural changes of intact collagen structure.

Figure 4.7 FT-IR spectra (A) and protein secondary structure estimated from amide I region (B) of collagen samples extracted by different methods.

The α-helix is a major structure in all collagen samples (Figure 4.7B), estimating to be 30-32% ($p>0.05$), whereas the β-turn and random coil were minor structure. This result demonstrated that ultrasound intensity of 17.87 W·cm^{-2} for 20 min exposure time did not disturb secondary structure of T collagen. Akram and Zhang (2020) stated that chicken sternal collagen extracted by ultrasound intensity of 2,990 W·cm^{-2} for exposure time 36 min resulted in disruption of secondary structure of collagen. Hence, extremely high intensity and long exposure time might induce structural changes of intact collagen structure.

Intensity ratio between amide III (1,237 cm^{-1}) and 1,454 cm^{-1}, indicates integrity of the triple helix structure. When the ratio is lower than 0.59, it implies dissociation of triple helix (Plepis, Goissis, and Das-gupta, 1996). All collagen samples exhibited the ratio value approximately 1.01-1.07 (Table 4.3, $p>0.05$), confirming integrity of collagen triple helix. These results were similar with those previously reported from collagen extracted from channel catfish and golden carp skin, which were estimated to be 1.00-1.05 (Liu et al., 2015; Ali et al., 2018). Therefore, this study confirmed that UAE at intensity of 17.87 W·cm^{-2} for 20 min was not detrimental to triple helix structure as well as the secondary structure of the extracted T collagen.

4.9 Protein patterns

All collagen comprised of α1(I)$_2$ and α2(I) chains as major components (Figure 4.8). High molecular weight γ-chains (trimer) and β-chains (dimer) were evident, indicating that extracted collagen contained high amount of covalent inter-molecular cross-linkages. The α1(I)$_2$ and α2(I) bands exhibited molecular weight (Mw) of 135

and 116 kDa, respectively, corresponding to the Mw observed from the standard type I collagen of bovine Achilles tendon with α1(I) and α2(I) at 130 and 113 kDa, respectively. This is the first study classifying the collagen extracted from T as type I collagen.
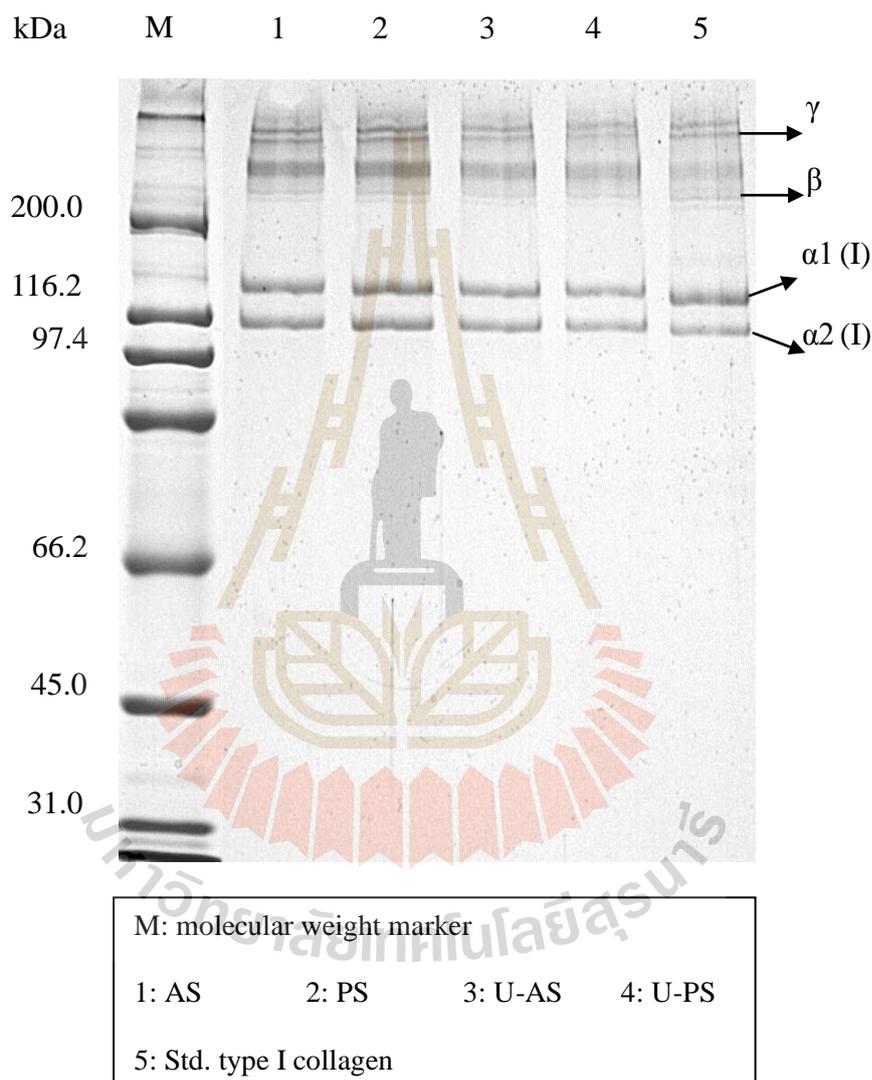
Figure 4.8   Protein pattern of all collagen samples on 7.5% acrylamide gel.

Collagen samples extracted from the conventional and UAE method showed comparable pattern. Low Mw proteins (<100 kDa) were not obviously noticed in the UAE sample. Therefore, the disruption with T tissue membrane by UAE at intensity

of 17.87 W·cm^{-2} for 20 min did not cause severe hydrolysis of collagen. Collagen obtained from sea bass skin subjected to 80% amplitude of ultrasound (power or intensity was not reported) for long exposure time of 24 h showed degradation of α_1- and α_2- chains (Kim et al., 2012). Additionally, collagen extracted from chicken sternal cartilage by UAE at intensity of 2,990 W·cm^{-2} for exposure time of 36 min exhibited resulted in partial degradation of the β- and α-chain structure (Akram and Zhang, 2020). Thus, extreme ultrasound intensity might cause detrimental effect on collagen structure. It should be noted that disruption of polypeptide chain (α-helix) was not observed under the studied ultrasound treatment.

4.10   Protein identification

Proteomic results of α1 and α2-chains of PS and U-PS are illustrated in Table 4.5. Gly and Pro were found in all matched peptides, corresponding to Gly-Pro-X. Both α-subunits of PS and U-PS presented similar peptide sequences that showed high similarity with type I collagen.

Matched peptides, GFSGLDGAK and GQAGVMGFPGPK, corresponded with type I collagen of Nile tilapia (*Oreochromis niloticus*), donkey (*Equus asinus*), and sheep (*Ovis aries*) (Zheng et al., 2012; Chen, Hsiang, Lin, and Ho, 2014). In addition, SAGVAVPGPMGPAGPR and DGEAGAQGPPGPTGPAGER were matched with peptide of α1 for type I collagen, which found in the broiler chicken. The α2 (I) chain of PS and U-PS exhibited the 8 matched peptides (Table 4.5) that corresponded with peptide α2 of type I collagen in the broiler chicken.

It has been reported that, T cartilage was a rich source of type II collagen (Mescher, 2016). However, T collagen revealed type I characteristic from both

SDS-PAGE pattern and LC-MS/MS. Therefore, this study suggested that T is an alternative source of type I collagen. In addition, this is the first study demonstrating that PS and U-PS of T collagen was type I collagen.

Table 4.5 Specific amino acid sequence of α1 and α2 chains obtained from collagen extracted by the conventional and ultrasound-assisted extraction methods.

Band	Peptide sequence hint	Coverage (%)	Protein Identification	Taxonomy
α1PS and α1U-PS	SAGVAVPGPMGPAGPR GFSGLDGAK GQAGVMGFPGPK DGEAGAQGPPGPTGPAGER	3.85	Collagen α1 (I) chain	*Gallus gallus*
α2PS and α2U-PS	AADFGPGPMGLMGPR GEIGPAGNYGPTGPAGPR VGPIGPAGNR GNVGLAGPR GEGGPAGPAGPAGAR GDPGPVGPVGPAGAFGPR GLAGPQGPR GPPGPSGPPGK	7.70	Collagen α2 (I) chain	*Gallus gallus*

Coverage values were calculated by comparing between numbers of amino acids obtained from LC-MS/MS and total amino acids of α1 and α2, which were 1,453 and 1,363 residues.

CHAPTER V

CONCLUSION

Chicken trachea (T) was a rich source of protein for collagen extraction. Conventional extraction by pepsin resulted in 3.1% yield. T collagen yield was increased to 6.28%, after ultrasound intensity of 17.87 $W \cdot cm^{-2}$ for exposure time 20 min, followed pepsin extraction for 36 h was applied. T collagen extracted by pepsin contained more than 80% collagen. UAE did not affect collagen microstructure, and did not damage triple helix, as well as protein secondary structure. Collagen extracted by pepsin showed higher thermal denaturation than that extracted by acid in both DI water and 0.5 M acetic acid. T collagen contained high imino acid content but low amount of essential amino acids (His, Met, Phe and Trp). T collagen composed of α_1 with α_2-chain indicated characteristic of type I collagen, which has been confirmed by LC-MS/MS peptide matching. Therefore, this study revealed that high-intensity ultrasound improves collagen extraction without disturbing collagen structure. Valorization of T can be achieved by collagen extraction. This is the first study classifying T collagen as a type I collagen.

REFERENCES

Abdollahi, M., Rezaei, M., Jafarpour, A., and Undeland, I. (2018). Sequential extraction of gel-forming proteins, collagen and collagen hydrolysate from gutted silver carp (*Hypophthalmichthys molitrix*), a biorefinery approach. **Food Chemistry**. 242: 568-578.

Aboonajmi, M., Akram, A., Nishizu, T., Kondo, N., Setarehdan, S. K, and Rajabipour, A. (2010). An ultrasound-based technique for the determination of poultry egg quality. **Research in Agricultural Engineering**. 56: 26-32.

Abid, M., Jabbar, S., Wu, T., Hashim, M. M., Hu, B., Lei, S., Zhang, X., and Zeng, X. (2013). Effect of ultrasound on different quality parameters of apple juice. **Ultrasonics Sonochemistry**. 20: 1182-1187.

Acton, Q. A. (2011). **Sclerproteins: Advances in research and application** (pp. 1-310). Atlanta, Georgia: Scholarly Editions.

Adzhubei, A. A., Sternberg, M. J. E., and Makarov, A. A. (2013). Polyproline-II Helix in Proteins: Structure and Function. **Journal of Molecular Biology**. 425: 2100-2132

Aewsiri, T., Benjakul, S., Visessanguan, W., Wierenga, P. A., and Gruppen, H. (2011). Improvement of foaming properties of cuttlefish skin gelatin by modification with N-hydroxysuccinimide esters of fatty acid. **Food Hydrocolloids**. 25: 1277-1284.

Ahmed, R., Haq, M., and Chun, B. (2019). Characterization of marine derived collagen extracted from the byproducts of bigeye tuna (*Thunnus obesus*).

International Journal of Biological Macromolecules. 135: 668-676.

Aigner, T. and Stöve, J. (2003). Collagens-major component of the physiological cartilage matrix, major target of cartilage degeneration, major tool in cartilage repair. **Advanced Drug Delivery Reviews**. 55: 1569-1593.

Akkiraju, H. and Nohe, A. (2015). Role of chondrocytes in cartilage formation, progression of osteoarthritis and cartilage regeneration. **Journal of Developmental Biology**. 3: 177-192.

Akram, A. A., and Zhang, C. (2020). Effect of ultrasonication on the yield, functional and physicochemical characteristics of collagen-II from chicken sternal cartilage. **Food Chemistry**. 307: 125544.

Alarcon-Rojo, A. D., Carrillo-Lopez, L. M., Reyes-Villagrana, R., Huerta-Jimenez, M., and Garcia-Galicia, I. A. (2019). Ultrasound and meat quality: a review. **Ultrasonics Sonochemistry**. 55: 369-382.

Alava, J. M., Sahi, S. S., García-Alvarez, J., Turó, A., Chávez, J. A., García, M. J., and Salazar, J. (2007). Use of ultrasound for the determination of flour quality. **Ultrasonics**. 46: 270-276.

Alexander, D. E. (2017). Nature's machines: **An introduction to organismal biomechanics**. Oxford, UK: Academic Press.

Ali, A. M. M., Benjakul, S., and Kishimura, H. (2017). Molecular characteristics of acid and pepsin soluble collagens from the scales of golden carp (*Probarbus jullieni*). **Emirates Journal of Food and Agriculture**. 29: 450-457.

Ali, A. M. M., Kishimura, H., and Benjakul, S. (2018). Extraction efficiency and characteristics of acid and pepsin soluble collagens from the skin of golden carp (*Probarbus Jullieni*) as affected by ultrasonication. **Process Biochemistry**.

66: 237-244.

Anandhakumar, S., Krishnamoorthy, G., Ramkumar, K. M., and Raichur, A. M. (2017). Preparation of collagen peptide functionalized chitosan nanoparticles by ionic gelation method: An effective carrier system for encapsulation and release of doxorubicin for cancer drug delivery. **Materials Science and Engineering C**. 70: 378-385.

Ashokkumar, M. (2015). Applications of ultrasound in food and bioprocessing. **Ultrasonics Sonochemistry**. 25: 17-23.

Association of official agricultural chemists (AOAC). (2016). **Official methods of analysis of AOAC international** (20th ed.). Rockville, MD: AOAC international.

Astráin-Redín, L., Ciudad-Hidalgo, S., Raso, J., Condón, S., Cebrián, G., and Álvarez, I. (2019). Application of high-power ultrasound in the food industry. **Sonochemical Reactions**. 1-24.

Araújo, Í. B. S., Bezerra, T. K. A., do-Nascimento, E. S., Gadelha, C. A. de A., Santi-Gadelha, T., and Madruga, M. S. (2018). Optimal conditions for obtaining collagen from chicken feet and its characterization. **Food Science and Technology**. 38: 167-173.

Bachchhav, M. B., Kulkarni, M. V., and Ingale, A. G. (2020). Process-intensified extraction of phycocyanin followed by β-carotene from Spirulina platensis using ultrasound-assisted extraction. **Separation Science and Technology**. 55: 932-944.

Bunchu, A. A., Fleschin, S., and Aboul-Enein, H. Y. (2014). Evaluation of the protein secondary structures using Fourier transform infrared spectroscopy. **Gazi University Journal of Science**. 27: 637-677.

Banerjee, J., Radvar, E., and Azevedo, H. S. (2018). Chapter 10 self-assembling peptides and their application in tissue engineering and regenrative medicine, In: M. A. Barbosa and M. C. L. Martins (eds.), **Peptides and proteins as biomaterials for tissue regeneration and repair** (pp. 245-281). Cambridgeshire. UK: Woodhead.

Bashir, M. J. K., Ibrahim, N., Usmail, M. N., and Jaya, M. A. T. (2020). Chapter 34 physical treament technologies for landfill leachate: performance and limitation, In: Information resources management association USA (ed.), **Waste management: Concepts, methodologies, tools, and applications** (pp. 717-753). Hershey, PA: IGI Global.

Beck, K. and Brodsky, B. (1998). Supercoiled protein motifs: the collagen triple-helix and the a-helical coiled coil. **Journal of structural biology**. 122: 17-29.

Belbachir, K., Noreen, R., Gouspillou, G., and Petibois, C. (2009). Collagen types analysis and differentiation by FTIR spectroscopy. **Analytical and Bioanalytical Chemistry**. 395: 829-837.

Bello, A., Shuaibu, I., Onu, J. E., Umaru, M. A., Shehu, S. A., Onyeanusi, B. I., Suleiman, M. H., Nzalak, J. O., and Baki, A. S. (2017). Anatomical study of the trachea of an adult donkey (*Equus asinus*): A histomorphometric study. **Multidisciplinary Advances in Veterinary Science**. 1: 89-99.

Benjakul, S., Thiansilakul, Y., Visessanguan, W., Roytrakul, S., Kishimura, H., Prodpran, T., and Meesane, M. (2010). Extraction and characterisation of pepsin-solubilised collagens from the skin of bigeye snapper (*Priacanthus Tayenus* and *Priacanthus Macracanthus*). **Journal of the Science of Food and Agriculture**. 90: 132-138.

Benjakul, S., Nalinon, S., and Shahidi, F. (2012). Part 3 meat, poultry, and seafoods: Fish collagen, In: B. K. Simpson, L. M. L. Nollet, F. Toldrá, S. Benjakul, G. Paliyath, and Y. H. Hui (eds.), **Food biochemistry and food processing** (2nd ed.) (pp. 365-387). Danvers, MA: John Wiley & Sons.

Bermúdez-Aguirre, D., Mobbs, T., and Barbosa-Cánovas, G. V. (2011). Chapter 3 ultrasound applications in food processing, In: H. Feng, G. V. Barbos-Canovas, and J. Weiss (eds.), **Ultrasound Technologies for Food and Bioprocessing** (pp. 65-105). New York, NY: Springer.

Bhangavan, N. V. and Ha, C. (2015). **Essentials of medical biochemistry with clinical cases**. Waltham, MA: Academic Press.

Bhattacharjee, A. and Bansal, M. (2005). Collagen structure: the madras triple helix and the current scenario. **International Union of Biochemistry and Molecular Biology Life**. 57: 161-172.

Bhattacharjee, T., Nicodemo, M., Arisawa, E. L. S., and Raniero, L. (2018). FTIR study of Achilles tendinopathy: protein secondary structure changes in tendon post injury. **Research on Biomedical Engineering**. 34: 350-355.

Bitarte, N., Bandrés, E., Zárate, R., Ramirez, N., and Garcia-Foncillas, J. (2007). Moving forward in colorectal cancer research, what proteomics has to tell. **World Journal of Gastroenterology**. 13: 5813-5821.

Blanco, M., Sotelo, C. G., and Pérez-Martín, R. I. (2019). New strategy to cope with common fishery policy landing obligation: collagen extraction from skins and bones of undersized Hake (*Merluccius merluccius*). **Polymers**. 11: 1-16.

Bovey, F. A. and Hood, F. P. (1967). Circular dichroism spectrum of poly-L-proline. **Biopolymers**. 5: 325-326.

Brown, E. M., Farrell, H. M., and Wildermuth, R. J. (2000). Influence of neutral salts on the hydrothermal stability of acid-soluble collagen. **Journal of Protein Chemistry**. 19: 85-92.

Bu, Y., Jeevithan, E., Zhang, J., Bao, B., Guo, R., Palaniyandi, K., Robinson, J. S., Geevaretnam, J., Regenstein, J. M., and Wu, W. (2017). Immunological effect of collagen and collagen peptide from blue shark cartilage on 6T-CEM cells. **Process Biochemistry**. 57: 219-227.

Bui, T. Q., Ngo, H. T. M., and Tran, H. T. (2018). Surface-protective assistance of ultrasound in synthesis of superparamagnetic magnetite nanoparticles and in preparation of mono-core magnetite-silica nanocomposites. **Journal of Science: Advanced Materials and Devices**. 3: 323-330.

Burgeson, R. E. and Morris, N. P. (1987). The collagen family of proteins, In: J. Uitto and A. J. Perejda (eds.), **Connective tissue disease, molecular pathology of the extracellular matrix** (pp. 3-28). Oxford: Marcel Dekker.

Byanet, O., Bosha, J. A., and Onoja, B. O. (2014). A quantitative study on the trachea of the red Sokoto (*Maradi*) goat (*Capra hircus*). **Veterinary Medicine International**. 2014: 1-5.

Carbonaro, M. and Nucara, A. (2010). Secondary structure of food proteins by Fourier transform spectroscopy in the mid-infrared region. **Amino Acids**. 38: 679-690.

Cárcel, J. A., Benedito, J., Rosselló, C., and Mulet, A. (2007). Influence of ultrasound intensity on mass transfer in apple immersed in a sucrose solution. **Journal of Food Engineering**. 78: 472-479.

Carsote, C. and Badea, E. (2019). Micro differential scanning calorimetry and micro hot table method for quantifying deterioration of historical leather. **Heritage Science**.

7: 1-13.

Cao, H. and Xu, S. (2008). Purification and characterization of type II collagen from chick sternal cartilage. **Food Chemistry**. 108: 439-445.

Cao, H., Shi, F. X., Xu, F., and Yu, J. S. (2013). Molecular structure and physicochemical properties of pepsin-solubilized type II collagen from the chick sternal cartilage. **European Review for Medical and Pharmacological Sciences**. 17: 1427-1437.

Chandrapala, J., Oliver, C., Kentish, S., and Ashokkumar, M. (2012). Ultrasonics in food processing. **Ultrasonics Sonochemistry**. 19: 975-983.

Chandrapala, J. (2015). Low intensity ultrasound applications on food systems. **International Food Research Journal**. 22: 888-895.

Chemat, F., Rombat, N., Sicaire, A., Meullemiestre, A., Fabiano-Tixier, A., and Abert-Vian, M. (2017). Ultrasound assisted extraction of food and natural products. Mechanisms, techniques, combinations, protocols and applications. **Ultrasonics Sonochemistry**. 34: 540-560.

Chen, J., Hsiang, C., Lin, Y., and Ho, T. (2014). Deer antler extract improves fatigue effect through altering the expression of genes related to muscle strength in skeletal muscle of mice. **Evidence-Based Complementary and Alternative Medicine**. 2014: 1-10.

Chen, y., Zou, C., Mastalerz, M., Hu, S., Gasaway, C., and Tao, X. (2015). Applications of micro-Fourier transform infrared spectroscopy (FTIR) in the geological sciences: A review. **International Journal of Molecular Sciences**. 16: 30223-30250.

Chen, J., Yi, L. L. R., Xu, N., Gao, R., and Hong, B. (2016). Extraction and characterization of acid-soluble collagen from scales and skin of tilapia (*Oreochromis niloticus*). **LWT- Food Science and Technology**. 66: 453-459.

Cheng, F. Y., Hsu, F. W., Chang, H. S., Lin, L. C., and Sakata, R. (2009). Effect of different acids on the extraction of pepsin-solubilised collagen containing melanin from silky fowl feet. Food Chemistry. 113: 563-567.

Cheng, X., Shao, Z., Li, C., Yu, L., Raja, M. A., and Liu, C. (2017). Isolation, characterization and evaluation of collagen from jellyfish *Rhopilema esculentum* kishinouye for use in hemostatic applications. **PloS ONE**, 12: 1-21.

Chinh, N. T., Manh, V. Q., Trung, V. Q., Lam, T. D., Huynh, M. D., Tung, N. Q., Trinh, N. D., and Hoang, T. (2019). Characterization of collagen derived from tropical freshwater carp fish scale wastes and its amino acid Sequence. Natural Product Communications. 1-12.

Chmelováa, D., Škulcováa, D., Legerskáa, B., Horníkb, M., and Ondrejovič, M. (2020). Ultrasonic-assisted extraction of polyphenols and antioxidants from *Picea abies* bark. **Journal of Biotechnology**. 314-315: 25-33.

Chow, R., Blindt, R., Chivers, R., and Povey, M. (2003). The sonocrystallisation of ice in sucrose solutions: primary and secondary nucleation. **Ultrasonics**. 41: 595-604.

Chuaychan, S., Benjakul, S., and Kishimura, H. (2015). Characteristics of acid- and pepsin-soluble collagens from scale of sea bass (*Lates calcarifer*). **LWT-Food Science and Technology**. 63: 71-76.

Church, R. L. and Tanzer, M. L. (1975). Isolation and amino acid composition of human procollagen [Pro α1 (I)]₂ Pro α2 from skin fibroblasts in culture. **Federation of European Biochemical Societies Letters**. 53: 105-109.

Cissell, D. D. Link, J. M., Hu, J. C. and Athanasiou, K. A. (2017). A modified hydroxyproline assay based on hydrochloric acid in Ehrlich's solution accurately measures tissue collagen content. **Tissue Engineering Part C**. 23: 243-250.

Cooper, A. (2000). Microcalorimetry of protein-DNA interactions, In: A. Travers and M. Buckle (eds.), **DNA-Protein Interactions.** Oxford, UK: Oxford University Press. 125-139.

Cumming, M.H., Hall, B., and Hofman, K. (2019). Isolation and characterization of major and minor collagens from hyaline cartilage of hoki (*Macruronus novaezelandiae*). **Marine Drugs**. 17: 1-17.

Damodaran, S. (2017). Amino acids, peptides, and proteins, In: S. Damodaran, K. L. Parkin (Eds.), **Fennema's food chemistry**, (5ᵗʰ ed.) (pp. 235-356). Boca Raton, FL: CRC Press.

Darville, L. N. F. and Sokolowski, B. H. A. (2014). Bottom-up and shotgun proteomics to identify a comprehensive cochlear proteome. **Journal of Visualized Experiments**. 85: 1-10.

Deyl, Z. and Miksık, I. (2000). Advanced separation methods for collagen parent a-chains, their polymers and fragments. **Journal of Chromatography B**. 739: 3-31.

Dhakal, D., Koomsap, P., Lamichhane, A., Sadiq, M. B., and Anal, A. K. (2018). Optimization of collagen extraction from chicken feet by papain hydrolysis

and synthesis of chicken feet collagen based biopolymeric fibres. Food Bioscience. 23: 23-30.

Dhara, S., Datta, P., Pal, P., and Sarkar, S. D. (2013). Chapter 30 processing and industrial aspects of fish scale collagen: A biomaterials perspective, In: S. K. Kim (ed.), **Marine proteins and peptides: Biological activities and applications** (pp. 589-622). John Wiley & Sons.

Divya, K. V., Sreerekha, P. R., Tejpal, C. S., Asha, K. K., Mathew, S., Ravishankar, C. N., and Anandan, R. (2018). Extraction and characterization of acid soluble collagen (ASC) from airbladder of striped cat fish (*Pangasius hypophthalmus*). **International Journal of Fisheries and Aquatic Studies**. 6: 310-318.

Dong, Z., Yao, C., Zhang, X., Xu, J., Chen, G., Zhao, Y., and Yuan, Q. (2015). A high-power ultrasonic microreactor and its application in gas-liquid mass transfer intensification. **Lab on a Chip**. 15: 1145-1152.

Doǧan, G. K. and Takaci, I (2018). Anatomy of respiratory system in poultry. **Veterinary Journal of Mehmet Akif Ersoy University**. 3: 141-147.

Drzewiecki, K. E., Grisham, D. R., Parmar, A. S., Nanda, V., and Shreiber, D. I. (2016). Circular dichroism spectroscopy of collagen fibrillogenesis: a new use for an old technique. **Biophysical Journal**. 111: 2377-2386.

Dyce, K. M., Sack, W. O., Wensing, C. J. G. (2017). **Textbook of veterinary anatomy**. Philadelphia, PA: Saunders.

da-Silva, C. M. L., Spinelli, E., Rodrigues, S. V. (2015). Fast and sensitive collagen quantification by alkaline hydrolysis/ hydroxyproline assay. **Food Chemistry**. 173: 619-623.

Elango, J., Lee, J. W., Wang, S., Henrotin, Y., Sanchez-de-Val, J. E., Regenstein, J. M., Lim, S. Y., Bao, B., and Wu, W. (2018). Evaluation of differentiated bone cells proliferation by blue shark skin via biochemical for bone tissue engineering. **Marine Drugs**. 16: 1-15.

Elliott, R. S. (2003). **Antenna Theory and Design**. Piscataway, NJ: IEEE Press.

Eyre, D. R. (2004). Collagens and cartilage matrix homeostasis. **Clinical Orthopaedics and Related Research**. 427S: S118-S122.

Eyre, D. R., Weis, M. A., and Wu, J. J. (2010). Maturation of collagen ketoimine cross-links by an alternative mechanism to pyridinoline formation in cartilage. **Journal of Biological Chemistry**. 285: 16675-16682.

Fahmi, R., Khodaiyan, F., Pourahmad, R., and Emam-Djomeh, Z. (2014). Effect of ultrasound assisted extraction upon the Genistin and Daidzin contents of resultant soymilk. **Journal of Food Science and Technology**. 51: 2857-2861.

Fauzi, M. B., Lokanathan, Y., Aminuddin, B. S., Ruszymah, B. H. I., and Chowdhury, S. R. (2016). Ovine tendon collagen: Extraction, characterisation and fabrication of thin films for tissue engineering applications. **Materials Science and Engineering C**. 68: 163-171.

Fernandes, FA. N. and Rodrigues, S. (2007). Ultrasound as pretreatment for drying of fruits: dehydration of banana. **Journal of Food Engineering**. 82 261-267.

Ferreira, A. M., Gentile, P., Chiono, V., and Ciardelli, G. (2012). Collagen for bone tissue regeneration. **Acta Biomaterialia**. 8: 3191-3200.

Fidler, A. L., Boudko, S. P., Rokas, A., and Hudson, B. (2018). The triple helix of collagens-an ancient protein structure that enabled animal multicellularity and tissue evolution. **Journal of Cell Science**. 131: 1-15.

Finch, A. J., Benson, J. M., Donnelly, P. E., and Torzilli, P. A. (2019). Light absorptive properties of articular cartilage, ECM molecules, synovial fluid, and photo initiators as potential barriers to light-Initiated polymer scaffolding procedures. **Cartilage**. 10: 82-93.

Folch, J., Less, M., and Sloane, S. G. H. (1957). A simple method for the isolation and purification of total lipids from animal tissues. **Journal of Biological Chemistry**. 226: 497-509.

Foegeding, E. A., Lanier, T. C., and Hultin, H. O. (1996). Characteristics of edible muscle tissue, In: O. R. Fennema (ed.), **Food chemistry**. New York, NY: Marcel Dekker. 902-906.

Furlow, P. W. and Mathisen, D. J. (2018). Surgical anatomy of the trachea. **Annals of Cardiothoracic Surgery**. 7: 255-260.

Gao, L., Wang, Z., Li, Z., Zhang, C., and Zhang, D. (2018). The characterization of acid and pepsin soluble collagen from ovine bones (*Ujumuqin sheep*). **Journal of Integrative Agriculture**. 17: 704-711.

Gauza-Włodarczyk, M., Kubisz, L., and Włodarczyk, D. (2017). Amino acid composition in determination of collagen origin and assessment of physical factors effects, **International Journal of Biological Macromolecules**. 104: 987-991.

Ge, B., Wang, H., Li, J., Liu, H., Yin, Y., Zhang, N., and Qin, S. (2020). Comprehensive assessment of Nile tilapia skin (*Oreochromis niloticus*) collagen hydrogels for wound dressings. **Marine Drugs**. 18: 1-16.

Gelse, K., Pöschl, E., and Aigner, T. (2003). Collagens-structure, function, and biosynthesis. **Advanced Drug Delivery Reviews**. 55: 1531-1546.

Ghosh, N., McKillop, T. J., Jowitt, T. A., Howard, M., Davies, H., Holmes, D. F., Roberts, I. S., and Bella, J. (2012). Collagen-like proteins in pathogenic *E. coli* strains. **PLoS ONE**. 7: 1-21.

Gill, P., Monghadam, T. T., and Ranjbar, B. (2010). Differential scanning calorimetry techniques: applications in biology and nanoscience. **Journal of Biomolecular Techniques**. 21: 167-193.

Gjaltema, R. A. F. and Bank, R. A. (2017). Molecular insights into prolyl and lysyl hydroxylation of fibrillar collagens in health and disease. **Critical Reviews in Biochemistry and Molecular Biology**. 52: 74-95.

Glombitza, C. (2010). **New Zealand coals-A potential feedstock for deep microbial life**, Ph. D. dissertation. Technical University of Berlin, Berlin, Germany. 337.

Gorgieva, S. and Kodol, V. (2011). Chapter 2 collagen-vs. gelatine-based bomaterials and their biocompatibility: review and perspectives, In R. Pignatello (ed.), **Biomaterials applications for nanomedicine**. Rijeka, Croatia: Intech. 17-52.

Graves, P. R. and Haystead, T. A. J. (2003). Chapter 1 Proteomics and the molecular biologist, In: P. M. Conn (ed.), **Handbook of proteomic methods**. New York, NY: Springer. 3-16.

Greenfield, N. J. (2006). Using circular dichroism spectra to estimate protein secondary structure. **Nature Protocols**. 1: 2876-2890.

Griffiths, P. R. and de-Haseth, J. A. (2007). **Fourier transform infrared spectrometry.** Hoboken, NJ: John Wiley & Sons. 57-74.

Griffiths, P. R. and de-Haseth, J. A. (2007). Fourier transform infrared spectrometry. Hoboken, NJ: John Wiley & Sons. 57-74.

Gómez-guilloen, M. C. and Montero, P. (2001). Extraction of gelatin from megrim (*Lepidorhombus boscii*) skins with several organic acids. **Journal of Food Science**. 66: 213-.216

Gómez-Guillén, M. C., Giménez, B., López-Caballero, M. E., and Montero, M. P. .(2011)Functional and bioactive properties of collagen and gelatin from alternative sources: A review. **Food Hydrocolloid**. 25: 1813-1827.

Haynie, D. T. (2008). **Biological Thermodynamics**. Cambridge, UK: Cambridge University Press. 58-80.

Hamdan, F. S. and Sarbon, N. M. (2019). Isolation and characterisation of collagen from fringescale sardinella (*Sardinella fmbriata*) waste materials. **International Food Research Journal**. 26: 133-140.

Henao-Murillo, L., Ito, K., and van-Donkerlaar, C. C. (2018). Collagen damage location in articular cartilage differs if damage is caused by excessive loading magnitude or rate. **Annals of Biomedical Engineering**. 46: 605-615.

Hong, H., Chaplot, S., Chalamaiah, M., Roy, B. C., Bruce, H. L., and Wu, J. (2017). Removing cross-linked telopeptides enhances the production of low-molecular-weight collagen peptides from spent hens. **Journal of Agricultural and Food Chemistry**. 65: 7491-7499.

Homchaudhuri, L. and Swaminathan, R. (2004). Near ultraviolet absorption arising from lysine residues in close proximity: A probe to monitor protein unfolding and aggregation in lysine-rich proteins. **Bulletin of the Chemical Society of Japan**. 77: 765-769.

Horst, A. (1991). **Molecular pathology**. Boca Raton, FL: CRC Press.

Hulmes, D. J. S. (2008). Chapter 2 collagen diversity, synthesis and assembly, In: P. Fratzl (ed.), **Collagen structure and mechanics**. New York, NY: Springer. 15-41.

Iswariya, S., Velswamy, P., Uma, T. S. (2018). Isolation and characterization of biocompatible collagen from the skin of puffer fish (*Lagocephalus inermis*). **Journal of Polymers and the Environment**. 26: 2086-2095.

Jakobsen, R. J., Hutson, B. L., Fink, D. J., and Veis, A. (1983). Intermolecular interactions in collagen self-assembly as revealed by Fourier transform infrared spectroscopy. **Science**. 220: 1288-1290.

Jambrak, A. R., Lelas, V., Mason, T. J., Krešić, G., and Badanjak, M. (2009). Physical properties of ultrasound treated soy proteins. **Journal of Food Engineering**. 93: 386-393.

Jongjareonrak, A., Benjakul, S., Visessanguan, W., Nagai, T., and Tanaka, M. (2005). Isolation and characterisation of acid and pepsin-solubilised collagens from the skin of brownstripe red snapper (*Lutjanus vitta*). **Food Chemistry**. 93: 475-484.

Jongjareonrak, A., Benjakul, S., Visessanguan, W., and Tanaka, M. (2005). Isolation and characterization of collagen from bigeye snapper (*Priacanthus macracanthus*) skin. **Journal of the Science of Food and Agriculture**. 85: 1203-1210.

Jaroenviriyapap, T. (2010). **Production of chondroitin sulfate and collagen hydrolysate containing product from poultry trachea**, M.S. thesis,. Prince of Songkla University, Sonkla, Thailand. 99.

Jeevithan, E., Bao, B., Bu, Y., Zhou, Y., Zhao, Q., and Wu, W. (2014). Type II collagen and gelatin from silvertip shark (*Carcharhinus albimarginatus*) cartilage: isolation, purification, physiochemical and antioxidant properties. **Marine Drugs**. 12: 3852-3873.

Jeevithan, E., Jingyi, Z., Wang, N., He, L., Bao, B., and Wu, W. (2015). Physio-chemical, antioxidant and intestinal absorption properties of whale shark type-II collagen based on its solubility with acid and pepsin. **Process Biochemistry**. 50: 463-472.

Johnston-Banks, F.A. (1990). Gelatin, In: P. Harris (ed.), Food gels. London, UK: Elsevier applied science. 233-289.

Ju, H., Liu, X., Zhang, G., Liu, D., and Yang, Y. (2020). Comparison of the structural characteristics of native collagen fibrils derived from bovine tendons using two different methods: modified acid-solubilized and pepsin-aided extraction. **Materials**. 13: 1-13.

Jürgensen, H. J., Madsen, D. H., Ingvarsen, S., Melander, M. C., Gårdsvoll, H., Patthy, L., Engelholm, L. H., and Behrendt, N. (2011). A novel functional role of collagen glycosylation: Interaction with the endocytic collagen receptor uPARAP/ENDO180. **Journal of Biological Chemistry**. 286: 32736-32748.

Kaczor-Urbanowicz, K. E. and Wong, D. T. W. (2020). Chapter 4 proteomics, In: S. T. Spnis and A. Villa (eds.), **Translational systems medicine and oral disease**. Oxford, UK: Academic Press. 93-118.

Kadkhodaee, R. and Povey, M. J. W. (2008). Ultrasonic inactivation of Bacillus α-amylase. I. Effect of gas content and emitting face of probe. **Ultrasonics Sonochemistry**. 15: 133-142.

Karsdal, M.A. (2019). Introduction, In: M. A. Karsdal, D. J. Leeming, K. Henriksen, A. Bay-Jensen, S. H. Nielsen, and C. L. Bager (eds.), **Biochemistry of collagens, laminins, and elastin: Structure, function, and biomarkers** (2nd ed.). San Diego, CA: Academic press. xxiii-xliv.

Kapustina, O. A. (1965). Kinetics of the ultrasonic degassing of a liquid below the cavitation threshold. **Soviet Physics Acoustics**. 10: 376-379.

Kazarian, S. G. and Chan, K. L. A. (2013). ATR-FTIR spectroscopic imaging: recent advances and applications to biological systems. **Analyst**. 138: 1940-1951.

Kentish, S. and Ashokkumar, M. (2011). Chapter 1: The physical and chemical effects of ultrasound, In: H. Feng, G. V. Barbosa-Canovas, and J. Weiss (eds.), **Ultrasound technologies for food and bioprocessing**. New York, NY: Springer. 1-12.

Khan, S. A., Khan, S. B., Khan, L. U., Farooq, A., Akhtar, K., and Asiri, A. M. (2018). Chapter 9 Fourier transform infrared spectroscopy: fundamentals and application in functional groups and nanomaterials characterization, In: S. K. Sharma, D. S. Verma, L. U. Khan, S. Kumar, and S. B. Khan (eds.), **Handbook of materials characterization.** Zug, Switzerland: Springer. 317-344.

Khong, N. M. H., Yusoff, F. M., Jamilah, B., Basri, M., Maznah, I., Chan, K. W., Armania, N., and Nishikawa, J. (2018). Improved collagen extraction from jellyfish (*Acromitus hardenbergi*) with increased physical-induced solubilization processes. **Food Chemistry**. 251: 41-50.

Khora, S. S. and Kirti ((2017. Chapter 12recent trends in bioprospecting of marine collagen, In: S. Kim (ed.), **Marine glycobiology: Principles and applications**. Boca Raton, FL: CRC Press. 178-169.

Kim, H. K., Kim, Y. H., Kim, Y. J., Park, H. J., and Lee, N. H. (2012). Effects of ultrasonic treatment on collagen extraction from skins of the sea bass *Lateolabrax japonicus*. **Fisheries Science**. 78: 485-490.

Kim, K.B., Lee, S., Kim, M.S., and Cho, B.K. (2009). Determination of apple firmness by nondestructive ultrasonic measurement. **Postharvest Biology and Technology**. 52: 44-48.

Kim, H., Yeo, I., Hwang, K., Song, D., Kim, Y., Ham, Y., Jeong, T., Choi, Y. and Kim, C. (2016). Isolation and characterization of pepsin-soluble collagens from bones, skins, and tendons in duck feet. **Korean Journal for Food Science of Animal Resources**. 36: 665-670.

Kittiphattanabawon, P., Benjakul, S., Visessanguan, W., and Shahidi, F. (2010). Isolation and characterization of collagen from the cartilages of brownbanded bamboo shark (*Chiloscyllium punctatum*) and blacktip shark (*Carcharhinus limbatus*). **LWT- Food Science and Technology**. 43: 792-800.

Kittiphattanabawon, P., Nalinanon, S., Benjakul, S., and Kishimura, H. (2015). Characteristics of pepsin-solubilised collagen from the skin of splendid squid (*Loligo formosana*). **Journal of Chemistry**. 2015: 1-8.

Kong, J. and Yu, S. (2007). Fourier transform infrared spectroscopic analysis of protein secondary structures. **Acta Biochimica et Biophysica Sinica**. 39: 549-559.

Krilov, D., Balarin, M., Kosović, M., Gamulin, O., and Brnjas-Kraljević, J. (2009). FT-IR spectroscopy of lipoproteins-A comparative study. **Spectrochimica Acta Part A: Molecular and Biomolecular Spectroscopy**. 73: 701-706.

Kumari, S., Panda, T. K., and Pradhan, T. (2017). (Lysyl oxidase: its diversity in health and diseases. **Indian Journal of Clinical Biochemistry**. 32: 141-132.

Kuball, H. G. Höfer, T., and Kiesewalter, S. (2017). Chiroptical spectroscopy, general theory. **Encyclopedia of Spectroscopy and Spectrometry**. 217-231.

Kumar, N. S., Nazeer, R. A., and Jaiganesh, R. (2012). Wound healing properties of collagen from the bone of two marine fishes. **International Journal of Peptide Research and Therapeutics**. 18: 185-192.

Lavrinenko, I. A., Vashanov, G. A., and Artyukhov, V. G. (2015). Decomposition of the hemoglobin UV absorption spectrum into the absorption spectra of a prosthetic group and apoprotein using an additive model. **Biophysics**. 60: 197-204.

Lazar, L. M., Karcini, A., Ahuja, S., and Estrada-Palma, C. (2019). Proteogenomic analysis of protein sequence alterations in breast cancer cells. **Scientific Reports**. 9: 1-13.

Lentacker I., De Cock I., Deckers R., Smedt S. C. D., and Moonen C. T. W. (2014). Understanding ultrasound induced sonoporation: Definitions and underlying mechanisms. **Advanced Drug Delivery Reviews**. 72: 49-64.

Li, S., Sieron, A. L., Fertala, A., Hojima, Y., Arnold, W. V., and Prockop, D. J. (1996). The C-proteinase that processes procollagens to fibrillar collagens is identical to the protein previously identified as bone morphogenic protein-1. **Proceedings of the National Academy of Sciences of the United States of**

America. 93: 5127-5130.

Li, D., Mu, C., Cai, S., and Lin, W. (2009). Ultrasonic irradiation in the enzymatic extraction of collagen. **Ultrasonics Sonochemistry**. 16: 605-609.

Li, K., Kang, Z.-L., Zou, Y.-F., Xu, X.-L., Zhou, G.-H. (2015). Effect of ultrasound treatment on functional properties of reduced-salt chicken breast meat batter. **Journal of Food Science and Technology**. 52: 2622-2633.

Li, L., Zhao, Y., He, Y., Chi, C., and Wang, B. (2018). Physicochemical and antioxidant properties of acid and pepsin-soluble collagens from the scales of Miiuy croaker (*Miichthys Miiuy*). **Marine Drugs**. 16: 1-19.

Li, P., Lu, W., Chan, Y., Ko, W., Jung, C., Huynh, D. T. L., and Ji, Y. (2020). Extraction and characterization of collagen from sea cucumber (*Holothuria cinerascens*) and its potential application in moisturizing cosmetics. **Aquaculture**. 515: 734590.

Liang, Q., Wang, L., Sun, W., Wang, Z., Xu, J., and Ma, H. (2014). Isolation and characterization of collagen from the cartilage of Amur sturgeon (*Acipenser schrenckii*). **Process Biochemistry**. 49: 318-323.

Lin, Y., Lin, T., and Su, H. (2011). Extraction and characterisation of telopeptide-poor collagen from porcine lung. Food Chemistry. 124: 1583-1588.

Lin, S., Hue, Y., San, E., Keong, T. C., Chen, L., and Zhang, Y. (2017). Extraction and characterization of pepsin soluble collagen from the body wall of sea cucumber *Acaudina leucoprocta*. **Journal of Aquatic Food Product Technology**. 26: 502-515.

Linsenmayer, T. F. (1981). Chapter 1 collagen, In: E. D. Hay (ed.), **Cell biology of extracellular matrix** (2nd ed.). New York, NY: Springer. 7-40.

Lipopolis, J. D. and Nally, J. E. (2018). Considerations for farm animal proteomic experiments: An introductory view gel-based versus non-gel-based approaches, In: A. M. de-Almeida, D. Eckersall, and I. Miller (eds.), **Proteomics in domestic animals: from farm to systems biology**. Zug, Switzerland: Springer. 7-16.

Liu, D. S., Liang, L., Regenstein, J. M., and Zhou, P. (2012). Extraction and characterization of pepsin-solubilised collagen from fins, scales, skins, bones and swim bladders of bighead carp (*Hypophthalmichthys nobilis*). **Food Chemistry**. 133: 1441-1448.

Liu, D., Wei, G., Li, T., Hu, J., Lu, N., Regenstein, J. M., and Zhou, P. (2015). Effects of alkaline pretreatments and acid extraction conditions on the acid-soluble collagen from grass carp (*Ctenopharyngodon idella*) skin. **Food Chemistry**, 172: 836-843.

Liu, Y., Andarawis-Puri, N., and Eppell, S. J. (2016). Method to extract minimally damaged collagen fibrils from tendon. **Journal of Biological Methods**. 3: 1-9.

Liu, H. and Huang, K. (2016). Structural characteristics of extracted collagen from tilapia (*Oreochromis mossambicus*) bone: Effects of ethylenediaminetetraacetic acid solution and hydrochloric acid treatment. **International Journal of Food Properties**. 19: 63-75.

Liu, W., Zhang, Y., Cui, N., and Wang, T. (2019). Extraction and characterization of pepsin-solubilized collagen from snakehead (*Channa argus*) skin: effects of hydrogen peroxide pretreatments and pepsin hydrolysis strategies. **Process Biochemistry**. 76: 194-202.

Lodhi, G., Kim, Y., Kim, E., Hwang, J., Won, H., Kim, W., Moon, S., Jeon, B. and Park, P. (2018). Isolation and characterization of acid- and pepsin-soluble collagen from the skin of Cervus Korean TEMMINCK var. mantchuricus swinhoe. **Animal Production Science**. 58: 585-594.

Lottspeich, F. and Engels, J. (2018). **Bioanalytics: Analytical methods and concepts in biochemistry**. Weinheim, Germany: Wiley-VCH. 131-180.

Loughrey, S., Mannion, J., and Matlock, B. (2016). Using the nanodrop one to quantify protein and peptide preparations at 205 nm. **Thermo Fisher Scientific Application Note**. 52774: 1-3.

Lowry, O. H., Rosebrough, N. J., Farr, A. L., and Randall, R. J. (1951). Protein measurement with the Folin phenol reagent. **Journal of Biological Chemistry**, 193: 265-275.

Luo, Y., Sinkeviciute, D., He, Y., Karsdal, M., Henrotin, Y., Mobasheri, A., Önnerfjord, P., and Bay-Jensen, A. (2017). The minor collagens in articular cartilage. **Protein Cell**. 8: 560-572.

Luo, Q., Chi, C., Yang, F., Zhao, Y., and Wang, B. (2018). Physicochemical properties of acid- and pepsin-soluble collagens from the cartilage of Siberian sturgeon. **Environmental Science and Pollution Research**. 25: 31427-31438.

Lv, S., taha, A., Hu, H., Lu, Q., and Pan, S. (2019). Effects of ultrasonic-assisted extraction on the physicochemical properties of different walnut proteins. **Molecules**. 24: 1-16.

Lynn, A. K., Yannas, I. V., and Bonfield, W. (2004). Antigenicity and immunogenicity of collagen. **Journal of Biomedical Materials Research**. 71: 343-354.

McHugh, T. (2016). **Putting Ultrasound to Use in Food Processing** [On-line]. Available: https://www.ift.org/news-and-publications/...food-processing.

Majid, I., Nayik, G.A., and Nanda, V. (2015). Ultrasonication and food technology: A review. **Cogent Food & Agriculture**. 01: 1-11.

Mamvura, T. A., Iyuke, S. E., and Paterson, E. A. (2018). Energy changes during use of high-power ultrasound on food grade surfaces. **South African Journal of Chemical Engineering**. 25: 62-73.

Margulis, M. A., Margulis, I. M., (2003). Calorimetric method for measurement of acoustic power absorbed in a volume of a liquid. **Ultrasonics Sonochemistry**. 10: 343-345.

Mason, T. J. and Peters, D. (2002). **Practical sonochemistry: Power ultrasound uses and applications**. Cambridge. UK: Woodhead.

Martínez-Ortiz, M. A., Hernández-Fuentes, A. D., Pimentel-González, D. J., Campos-Montiel, R. G., Vargas-Torres, A., and Aguirre-Álvarez, G. (2015). Extraction and characterization of collagen from rabbit skin: partial characterization. **CyTA-Journal of Food**. 13: 253-258.

Mason, T. J. (1998). Chapter 6 power ultrasound in food processing, In: M. J. W. Povey and T. J. Mason (eds.), **Ultrasound in Food Processing** (pp. 105-125). London. UK: Blackie academic & professional.

Maynard, R. L. and Downes, N. (2019). **Anatomy and histology of the laboratory rat in toxicology and biomedical research**. Oxford, UK: Academic Press.

Meng, D., Tanaka, H., Kobayashi, T., Hatayama, H., Zhang, X., Ura, K., Yunoki, S., and Takagi, Y. (2019). The effect of alkaline pretreatment on the biochemical characteristics and fibril-forming abilities of types I and II collagen extracted

from bester sturgeon by-products. **International Journal of Biological Macromolecules**. 131: 572-580.

Mescher, A. L. (2016). **Junqueira's: basic histology text and atlas** (14th ed.). New York, NY: McGraw-Hill.

Messana, I., Cabras, T., Iavarone, F., Vincenzoni, F., Urbani, A., and Castagnola, M. (2013). Unraveling the different proteomic platforms. **Journal of Separation Science**. 36:128-139.

Meyer, M. (2019). Processing of collagen-based biomaterials and the resulting materials properties. **Biomedical Engineering Online**. 18: 1-74.

Micsonai, A., Wien, F., Kernya, L., Lee, Y., Goto, Y., Réfrégiers, M., and Kardos, J. (2015). Accurate secondary structure prediction and fold recognition for circular dichroism spectroscopy. **Proceedings of the National Academy of Sciences**. 112: E3095-E3103.

Mikš-Krajnik, M., Feng, J. L. X., Bang, W. S., and Yuk, H. G. (2017). Inactivation of *Listeria monocytogenes* and natural microbiota on raw salmon fillets using acidic electrolyzed water, ultraviolet light or/and ultrasounds. **Food Control**. 74: 54-60.

Miner, J. H. and Nguyen, N. M. (2006). Extracellular matrix: Basement membranes, In: G. J. Laurent and S. D. Shapiro (eds.), **Encyclopedia of Respiratory Medicine**. St Louis, MO: Academic press. 157-162.

Mizuno, K., Hayashi, T., and Bachinger, H. P. (2003). Hydroxylation-induced stabilization of the collagen triple helix. **Journal of Biological Chemistry.** 278: 32373-32379.

Mohamed, M. A., Jaafar, J., Ismail, A. F., Othman, M. H. D., and Rahman, M. A. (2017). Chapter 1 Fourier transform infrared (FTIR) spectroscopy, In: N. Hilal, A. F. Ismail, T. Matsuura, and D. Oatley-Radciffe (eds.), **Membrane characterization**. Amsterdam, Netherlands: Elsevier. 3-29.

Moreira-Silva, J., Diogo, G. S., Marques, A. L. P., Silva, T. H., Reis, R. L. (2016). Marine collagen isolation and processing envisaging biomedical applications, In: N. M. Neves and R. L. Reis (eds.), **Biomaterials from nature and advanced devices and therapies**. New Jersey, NJ: John Wiley & Sons. 16-34.

Morris, N. P., Keene, D. R., and Horton, W. A. (2002). Chapter 1 morphology and chemical conposition of connective tissue; Part II cartilage, In: P. M. Royce and B. Steinmann (eds.), **Connective tissue and it's heritable disorders: Molecular, genetic, and medical aspects (2nd ed.).** New York, NY: Willey-Liss. 41-66.

Morris, N. P., Keene, D. R., and Horton, W. A. (2002). Chapter 1 morphology and chemical conposition of connective tissue; Part II cartilage, In: P. M. Royce and B. Steinmann (eds.), Connective tissue and it's heritable disorders: Molecular, genetic, and medical aspects (2nd ed.). New York, NY: Willey-Liss. 41-66.

Munasinghe, K. A. and Schwarz, J. G. (2017). Rooster collagen extracts from rooster by-products. **Journal of Nutritional Health & Food Engineering**. 7: 296-299.

Murphy, C., Kelliher, D., and Davenport, J. (2012). Shape and material characteristics of the trachea in the leatherback sea turtle promote progressive collapse and reinflation during dives. **Journal of Experimental Biology**. 215: 3064-3071.

Muyonga, J. H., Cole, C. G. B., and Duodu, K. G. (2004). Characterization of acid soluble collagen from skins of young and adult Nile perch (*Lates niloticus*). **Food Chemistry**. 85: 81-89.

Nad, M. (2010). Ultrasonic horn design for ultrasonic machining technologies. **Applied and Computational Mechanics**. 4: 79-88.

Nagai, T., Tanoue, Y., Kai, N., and Suzuki, N. (2015). Characterization of collagen from emu (*Dromaius novaehollandiae*) skins. **Journal of Food Science and Technology**. 52: 2344-2351.

Nalinanon, S., Benjakul, S., Visessanguan, W., and Kishimura, H. (2007). Use of pepsin for collagen extraction from the skin of bigeye snapper (*Priacanthus tayenus*). **Food Chemistry**. 104: 593-601.

Nalinanon, S., Benjakul, S., Visessanguan, W., and Kishimura, H. (2008). Tuna pepsin: Characteristics and its use for collagen extraction from the skin of threadfin bream (*Nemipterus* spp.). **Journal of Food Science**. 73: C413-C419.

Navarro, M., Ruberte, J., and Carretero, A. (2017). Chapter 6 respiratory apparatus, In: J. Ruberte, A. Carretero, and M. Navarro (eds.), **Morphological mouse phenotyping: Anatomy, histology and imaging**. Madrid, Spain: Academic Press. 147-178.

Nelson, D.L. and Cox, M.N. (2017). **Lehgninger principles of biochemistry** (7th ed.). New York, NY: Freeman.

Nguyen, T. M. P., Lee, Y. K., and Zhou, W. (2012). Effect of high intensity ultrasound on carbohydrate metabolism of bifdobacteria in milk fermentation. **Food Chemistry**. 130: 866-874.

Noor, Z., Mohamedali, A., and Ranganathan, S. (2018). Identification of proteins from proteomic analysis. **Reference Module in Life Science**. 3: 855-870.

Nurilmala, M., Pertiwi, R. M., Nurhayati, T., Fauzi, S., Batubara, I., and Ochiai, Y. (2019). Characterization of collagen and its hydrolysate from yellowfin tuna *Thunnus albacares* skin and their potencies as antioxidant and antiglycation agents. **Fisheries Science**. 85: 591-599.

Oropallo, A. R. (2019). Use of native type I collagen matrix plus polyhexamethylene biguanide for chronic wound treatment. **Plastic and Reconstructive Surgery**. 7: 1-6.

Pal, G. K., and Suresh, P. V. (2017). Comparative assessment of physico-chemical characteristics and fibril formation capacity of thermostable carp scales collagen. **Materials Science and Engineering C**. 70: 32-40.

Pallaske, F., Pallaske, A., Herklotz, K., and Boese-Landgraf, J. (2018). The significance of collagen dressings in wound management: a review. **Journal of Wound Care**. 27: 692-702.

Palma, S., Zhou, B., and Feng, H. (2017). Fresh produce treated by power ultrasound, In: Bermudez-Aguirre, D. (ed.), **Ultrasound advances in food processing and preservation**. Oxford, UK: Academic Press. 201-211.

Palumbo, P., B.g.-Miconi, C. L. A. Torre, G. Zoccali, N. Vrentzos, A. R. Vitale, P. Leocata, D. Lombardi, C. Lorenzo, B. D'angelo, G. Macchiarelli, A. Cimini, M.G. Cifone, M. Giuliani, (2011). Biological effects of low frequency high intensity ultrasound application on ex vivo human adipose tissue. **International Journal of Immunopathology and Pharmacology**. 24: 411-422.

Pavia, D. L., Lampman G. M., Kriz, G. S., and Vyvyan, J. A. (2015). **Introduction to spectroscopy**. Stamford, CT: Cengage learning. 14-106.

Pelc, D., Marion, S., Pŏzek, M., and Basletić, M. (2014). Role of microscopic phase separation in gelation of aqueous gelatin solutions. **Soft Matter**. 10: 348-356.

Piez, K. A. and Gross, J. (1960). The amino acid composition of some fish collagens: the relation between composition and structure. **Journal of Biological Chemistry**. 235: 995-998.

Plepis, A. M. G., Goissis, G., and Das-gupta, D.K. (1996). Dielectric and pyroelectric characterization of anionic and native collagen. **Polymer Engineering & Science**. 36: 2932-2938.

Polanco-Lugo, E., Martínez-Castillo, J. I., Cuevas-Bernardino, J. C., González-Flores, T., Valdez-Ojeda, R., Pacheco, N., and Ayora-Talavera, T. (2019). Citrus pectin obtained by ultrasound-assisted extraction: Physicochemical, structural, rheological and functional properties. **CYTA-Journal of Food**. 17: 463-471.

Pollard, T. D., Earnshaw, W. C., Lippincott-Schwartz, J., and Johnson, G. T. (2017). **Cell Biology**. Philadelphia, PA: Elsevier.

Pongsawatmanit, R., Harnsilawat, T. and McClements, D. J. (2006). Influence of alginate, pH and ultrasound treatment on palm oil-in-water emulsions stabilized by β-lactoglobulin. **Colloids and Surfaces A**. 287: 59-67.

Prange, T. (2019). Chapter 48 trachea, In: J. A. Auer, J. A. Stick, J. M. Kümmerle, and T. Prange (eds.), **Equine Surgery** (5th ed.). St. Louis, MO: Saunders. 797-804.

Prasad, S., Mandal, I., Singh, S., Paul, A., Mandal, B., Venkatramani, R., and Swaminathan, R. (2017). Near UV-Visible electronic absorption originating

from charged amino acids in a monomeric protein. **Chemical Science**. 8: 5416-5433.

Puri, D. (2011). **Textbook of medical biochemistry**. Delhi, India: Elsevier. 75-99.

Qian, J., Ito, S., Satoh, J., Geng, H., Tanaka, K., Hattori, S., Kojima, K., Takita, T. and Yasukawa, K. (2017). The cleavage site preference of the porcine pepsin on the N-terminal α1 chain of bovine type I collagen: A focal analysis with mass spectrometry. **Bioscience, Biotechnology, and Biochemistry**. 81: 514-522.

Qiao, X., Russell, S. J., Yang, X., Tronci, G., and Wood, D. J. (2015). Compositional and in vitro evaluation of nonwoven type I collagen/poly-dl-lactic acid scaffolds for bone regeneration. **Journal of Functional Biomaterials**. 6: 667-686.

Raghunath, M., Bruckner, P., and Steinmann, B. (1994). Delayed triple helix formation of mutant collagen from patients with osteogenesis imperfecta. **Journal of Molecular Biology**. 236: 940-949.

Ran, X. and Wang, L. (2014). Use of ultrasonic and pepsin treatment in tandem for collagen extraction from meat industry by-products. **Journal of the Science of Food and Agriculture**. 94: 585-590.

Raman, M. and Gopakumar, K. (2018). Fish collagen and its applications in food and pharmaceutical industry: a review. **ECronicon Nutrition**. 13: 752-767.

Ramachandran, G. N., Bansal, M., and Bhatnagar, R. S. (1973). A hypothesis on the role of hydroxyproline in stabilizing the collagen structure. **Biochimica et Biophysica Acta**. 322: 166-171.

Rappu, P. R., Salo, A. M., Myllyharju, J., and Heino, J. (2019). Role of prolyl hydroxylation in the molecular interactions of collagens. **Essays in Biochemistry**.

63: 325-335.

Regenstein, J. M. and Zhou, P. (2007). Collagen and gelatin from marine by-product, In: F. Shahidi (ed.), Maximising the value of marine by-products. Boca Raton, Florida: CRC Press. 279-303.

Rizk, M.A., and Mostafa, N.Y. (2016). Extraction and characterization of collagen from buffalo skin for biomedical applications. **Oriental Journal of Chemistry**. 32: 1601-1609.

Rochdi, A., Foucat, L., and Renou, J. (2000). NMR and DSC studies during thermal denaturation of collagen. **Food Chemistry**. 69: 295-299.

Rosenheck, K. and Doty, P. (1961). The far ultraviolet absorption spectra of polypeptide and protein solutions and their dependence on conformation. **Proceedings of the National Academy of Sciences**. 47: 1775-1785.

Ruotsalainen, H., Sipilä, L., Vapola, M., Sormunen, R., Salo, A. M., Uitto, L., Mercer, D. K., Robins, S. P., Risteli, M., Aszodi, A., Fässler, R., and Myllylä, R. (2006). Glycosylation catalyzed by lysyl hydroxylase 3 is essential for basement membranes. **Journal of Cell Science**. 119: 625-635.

Ryu, D. and Koh, E. (2019). Optimization of ultrasound-assisted extraction of anthocyanins and phenolic compounds from black soybeans (*Glycine max* L.). **Food Analytical Methods**. 12: 1382-1389.

Sandri, G., Rossi, S., Bonferoni, M. C., Caramella, C., and Ferrari, F. (2020). Chapter 14 Electrospinning technologies in wound dressing applications, In: J. Boateng (ed.), **Therapeutic dressings and wound healing applications**. Hoboken, NJ: John Wiley and Sons. 315-336.

Sadowska, M., and Kołdziejska, I. (2005). Optimisation of conditions for precipitation of collagen from solution using κ-carrageenan: Studies on collagen from the skin of Baltic cod (Gadus morhua). Food Chemistry. 91: 45-49.

Sadowska, M., Gutowska, J., and Malesa, M. (2005). Effect of glycosaminoglycans on reconstitution of collagen fibrils. Polish Journal of Food and Nutrition Sciences, 14/55: 303-307.

Santos, M. H., Silva, R. M., Dumont, V. C., Neves, J. S., Mansur, H. S. and Heneine, L.G.D. (2013). Extraction and characterization of highly purified collagen from bovine pericardium for potential bioengineering applications. Materials Science and Engineering part C. 33: 790-800.

São-José, J. F. B. and Vanetti, M. C. D. (2012). Effect of ultrasound and commercial sanitizers in removing natural contaminants and *Salmonella enterica* Typhimurium on cherry tomatoes. **Food Control**. 24: 95-99.

Sato, K., Yoshinaka, R., Sato, M., and Shimizu, Y. (1987). Isolation of native acid-soluble collagen from fish muscle. Nippon Suisan Gakkaishi. 53: 1431-1436.

Schmidt, M. M., Dornelles, R. C. P., Mello, R. O., Kubota, E. H., Mazutti, M. A., Kempka, A. P. and Demiate, I. M. (2016). Collagen extraction process. **International Food Research Journal**. 23: 913-922.

Schoellhammer, C. M. Polat, B. E., Mendenhall, J., Maa, R., Jones, B., Hart, D. P., Langer, R., and Blankschtein, D. (2012). Rapid skin permeabilization by the simultaneous application of dual-frequency, high-intensity ultrasound. **Journal of Controlled Release**. 163: 154-160.

Schöck, T. and Becker, T. (2010). Sensor array for the combined analysis of water-sugar-ethanol mixtures in yeast fermentations by ultrasound. **Food Control**. 21: 362-369.

Setiawati, R. and Rahardjo, P. (2018). Bone development and growth. **Intech open**. 1-20.

Seelay, R., Stephens, T., Tate, P. (2003). **Anatomy and Physiology**. Boston, MA: McGraw-Hill.

Shah, S. V. and Chakravarthy, D. (2015). Evaluation of a bovine 100% native collagen for the treatment of chronic wounds: A case series. **Journal of Wound, Ostomy & Continence Nursing**. 42: 226-234.

Shahbandeh, M. (2018). **Global number of chickens by country** [On-line]. Available: https://www.statista.com/statistics/263961/ top-countries- worldwide-by-chicken-stock-2007/.

Sharma, A., Wongkham, C., Prasongwattana, V., Boonnate, P., Thanan, R., Reungjui, S., and Cha'on, U. (2014). Proteomic analysis of kidney in rats chronically exposed to monosodium glutamate. **PLoS ONE**. 9: 1-11.

Shoulders, M. D. and Raines, R. T. (2009). Collagen Structure and Stability. **Annual Review of Biochemistry**. 78: 929-958.

Sionkowska, A., Skopinska, J., Wisniewski, M., Leznicki, A., and Fisz, J. (2006). Spectroscopic studies into the influence of UV radiation on elastin hydrolysates in water solution. **Journal of Photochemistry and Photobiology B**: **Biology**. 85: 79-84.

Silva, J. C., Barros, A. A., Aroso, I. M., Fassini, D., Silva, T. H., Reis, R. L., and Duarte, A. R. C. (2016). Extraction of collagen/gelatin from the marine

demosponge *Chondrosia reniformis* (Nardo, 1847) using water acidified with carbon dioxide-process optimization. **Industrial & Engineering Chemistry Research**. 55: 6922-6930.

Silvipriya, K. S., Kumar, K. K., Bhat, A. R., Kumar, B. D., John, A., and Lakshmanan, P. (2015). Collagen: animal sources and biomedical application. **Journal of Applied Pharmaceutical Science**. 5: 123-127.

Smith B. (2011). **Fundamentals of Fourier transform infrared spectroscopy** (pp. 87-146). Boca Raton, FL: CRC Press.

Sipilä, L., Ruotsalainen, H., Sormunen, R., Baker, N. L., Lamandé, S. R., Vapola, M., Wang, C., Sado, Y., Aszodi, A., and Myllylä, R. (2007). Secretion and assembly of type IV and VI collagens depend on glycosylation of hydroxylysines. **Journal of Biological Chemistry**. 282: 33381-33388.

Sisson, S., Grossman, J. D., and Getty, R. (1975). **The anatomy of domestic animals**. Philadelphia, PA: Saunders.

Song, W., Chen, W., Yang, Y., Li, C., and Qian, G. (2014). Extraction optimization and characterization of collagen from the lung of soft-shelled turtle *Pelodiscus sinensis*. **International Journal of Nutrition and Food Sciences**. 3: 270-278.

Song, K., Jung, S. K., Kim, Y. H., Kim, Y. E., and Lee, N. H. (2018). Development of industrial ultrasound system for mass production of collagen and biochemical characteristics of extracted collagen. **Food and Bioproducts Processing**, 110: 96-103.

Song, W., Liu, D., Sun, L., Li, B., and Hou, H. (2019). Physicochemical and biocompatibility properties of type I collagen from the skin of Nile tilapia (*Oreochromis niloticus*) for biomedical applications. **Marine Drugs**. 17: 1-14.

Soria, A. C. and Villamiel, M. (2010). Effect of ultrasound on the technological properties and bioactivity of food. **Trends in Food Science & Technology**. 21. 323-331.

Sorushanova, A., Delgado, L. M., Wu, Z., Shologu, N., Kshirsagar, A., Raghunath, R., Mullen, A. M., Bayon, Y., Pandit, A., Raghunath, M., and Zeogolis, D. I. (2019). The collagen suprafamily: From biosynthesis to advanced biomaterial development. **Advanced materials**. 1801651: 1-39.

Subramanian, A. and Rodriguez-Saona, L. (2009). Chapter 7 Fourier transform infrared (FTIR) spectroscopy, In: D. Sun (ed.), **Infrared spectroscopy for food quality analysis and control**. New York, NY: Academic Press. 145-174.

Sun, Q., Ma, Z. F., Zhang, H., Ma, S., and Kong, L. (2019). Structural characteristics and functional properties of walnut glutelin as hydrolyzed: effect of enzymatic modification. **International Journal of Food Properties**. 22: 265-279.

Sungperm, P. (2012). Physio-chemical properties and angiotensin I converting enzyme inhibitory peptides of collagen prepared from tilapia (Oreochromis niloticus) and hybrid catfish (Clarias macrocephalus × C. gariepinus) skin, M.S. thesis. Suranaree University of Technology, Nakhon Ratchasima, Thailand. 97.

Tan, C. I., Kent, G. N., Randall, A. G., Edmondston, S. J., and Singer, K. P. (2003). Age-related changes in collagen, pyridinoline, and deoxypyridinoline in normal human thoracic intervertebral discs. **Journal of Gerontology**. 58A: 387-393.

Tan, Y. and Chang, K. C. (2018). Isolation and characterization of collagen extracted from channel catfish (*Ictalurus punctatus*) skin. **Food Chemistry**. 242: 147-155.

Tanaka, T., Takahashi, K., Tsubaki, K., Hirata, M., Yamamoto, K., Biswas, A., Moriyama, T., and Kawamura, Y. (2018). Isolation and characterization of acid soluble bluefin tuna (*Thunnus orientalis*) skin collagen. **Fisheries and Aquatic Sciences**. 21: 1-8.

Tang, Y., Jin, S., Li, X., Li, X., Hu, X., Chen, Y., Huang, F., Yang, Z., Yu, F., and Ding, G. (2018). Physicochemical properties and biocompatibility evaluation of collagen from the skin of giant croaker (*Nibea japonica*). **Marine Drugs**. 16: 1-11.

Theng, C. H., Huda, N., Muhammad, N. A. N., Wariyah, C., Hashim, H. (2018). Physicochemical properties of duck feet collagen with different soaking time and its application in surimi. **Advanced Science Engineering Information Technology**. 8: 832-841.

Thompson, L. H. and Doraiswamy, L. K. (1999). Sonochemistry: science and engineering. **Industry Engineering and Chemistry Research**. 38: 1215-1249.

Thokchoma, B., Pandit, A. B., Qiu, P., Park, B., Choi, J., and Khim, J. (2015). A review on sonoelectrochemical technology as an upcoming alternative for pollutant degradation. **Ultrasonics Sonochemistry**. 27: 210-234.

Toldrá, F., Aristoy, M. C., Mora, L., and Reig, M. (2012). Innovations in value-addition of edible meat by-products. **Meat Science**. 92: 290-296.

Tranter, G. E. (2017). Protein structure analysis by CD, FTIR, and Raman spectroscopies, In: J. Lindon, G. E. Tranter, and D. Koppenaal (eds.), **Encyclopedia of spectroscopy and spectrometry** (3rd ed.). London, UK: Academic press. 740-758.

Tronci, G., Russell, S. J., and Wood, D. J. (2013). Photo-active collagen systems with controlled triple helix architecture. **Journal of Materials Chemistry B**. 1: 3705-3715.

Tronci, G. (2019). Chapter 13 the application of collagen in advanced wound dressings, In: S. Rajendran (ed.), **Advanced textiles for wound care** (2nd ed.). Kidlington, UK: Elsevier. 363-389.

Tsai, C. S. (2002). **An introduction to computational biochemistry**. New York, NY: Wiley-Liss. 73-103.

Tsai, M., Xu, Y., and Dannenberg, J. J. (2005). Completely geometrically optimized DFT/ ONIOM triple-helical collagen-like structures containing the ProProGly, ProProAla, ProPro[D]Ala, and ProPro[D]Ser triads. **Journal of the American Chemical Society**. 127: 14130-14131.

Usha, R. and Ramasami, T. (2005). Structure and conformation of intramolecularly cross-linked collagen. **Colloids and Surfaces B: Biointerfaces**. 41: 21-24.

Valverde, C. R. and Christe, K. L. (2005). Chapter 22 radiographic imaging of nonhuman primates, In: W. Sonia (ed.), **The laboratory primate: Handbook of experimental animals**. San Diego, CA: Academic Press. 371-386.

Van-Holde, K. E., Johnson, W. C., and Ho, P. S. (2006). **Principles of Physical Biochemistry**. Upper Saddle River, NJ: Pearson Prentice Hall. 72-105.

Veeruraj, A, Arumugam, M., and Balasubramanian, T. (2013). Isolation and characterization of thermostable collagen from the marine eel-fish (*Evenchelys macrura*). **Process Biochemistry**. 48: 1592-1602.

Veeruraj, A, Arumugam, M., and Balasubramanian, T. (2013). Isolation and characterization of thermostable collagen from the marine eel-fish (Evenchelys

macrura). Process Biochemistry, 48: 1592-1602.

Veenstra, T. D., Van, Q. N., Fox, S. D., and Issaq, H. J. (2020). Chapter 14 Protein and metabolite identification, In: H. J. Issaq and T. D. Veenstra (eds.), **Proteomic and Metabolomic Approaches to Biomarker Discovery** (2nd ed.). San Diego, CA: Academic Press. 247-260.

Venn, M., and Maroudas, A. (1977). Chemical composition and swelling of normal and osteoarthritic femoral head cartilage. **Annals of the Rheumatic Diseases**. 36: 121-129.

Vidal, A. R., Duarte, L. P., Schmidt, M. M., Cansian, R. L., Fernandes, I. A., Mello, R. O., Demiate, I. M., Dornelles, R. C. P. (2020). Extraction and characterization of collagen from sheep slaughter by-products. **Waste Management**. 102: 838-846.

Vittayanont, M. and Jaroenviriyapap, T. (2014). Production of crude chondroitin sulfate from duck trachea. **International Food Research Journal**. 21: 761-797.

Wade, L. G. (2013). **Organic chemistry**. Glenview, IL: Pearson Education. 1155-1198.

Wahab, N., Roman, M., Chakravarthy, D., and Luttrell, T. (2015). The use of a pure native collagen dressing for wound bed preparation prior to use of a living bi-layered skin substitute. **The American College of Clinical Wound Specialists**. 6: 2-8.

Wang, T., Lew, J., Premkumar, J., Poh, C. L., and naing, M. W. (2017). Production of recombinant collagen: state of the art and challenges. **Journal of Biological Engineering**. 1: 18-23.

Wei, P., Zheng, H., Shi, Z., Li, D., and Xiang, Y. (2019). Isolation and characterization of acid-soluble collagen and pepsin-soluble collagen from the skin of hybrid sturgeon. **Journal of Wuhan University of Technology**. 34: 950-959.

Wiegand, C., Buhren, B. A., Bünemann, E., Schrumpf, H., Homey, B., Frykberg, R. G., Lurie, F., and Gerber, P. A. (2016). A novel native collagen dressing with advantageous properties to promote physiological wound healing. **Journal of Wound Care**. 25: 713-720.

Weiss, J. B. (1976). Enzymic degradation of collagen, In: D. A. Hall and D. S. Jackson (eds.), **International review of connective tissue research**. New York, NY: Academic Press. 102-149.

Wood, A., Ogawa, M., Portier, R. J., Schexnayder, M., Shirley, M., and Losso, J. N. (2008). Biochemical properties of alligator (*Alligator mississippiensis*) bone collagen. **Comparative Biochemistry and Physiology B**. 151: 246-249.

Wu, J., Guo, X., Liu, H., and Chen, L. (2019). Isolation and comparative study on the characterization of guanidine hydrochloride soluble collagen and pepsin soluble collagen from the body of surf clam shell (*Coelomactra antiquata*). **Foods**. 8: 1-13.

Wu, J., Kong, L., Zhang, J. and Chen, W. (2019). Extraction and properties of acid-soluble collagen and pepsin-soluble collagen from silver carp (*Hypophthalmichthys molitrix*) scales: prerequisite information for fishery processing waste reuse. **Polish Journal of Environmental Studies**. 28: 2923-2930.

Yang, S., Leong, K. F., Du, Z., Chua, C. K. (2001). The design of scaffolds for use in tissue engineering. Part I. Traditional factors. **Tissue Engineering**. 7: 679-689.

Yang, X., Li, Y., Li, S., Oladejo, A. O., Wang, Y., Huang, S., Zhou, C., Ye, X., Ma, H., and Duan, Y. (2018). Effects of ultrasound-assisted α-amylase degradation treatment with multiple modes on the extraction of rice protein. **Ultrasonics Sonochemistry**. 40: 890-899.

Yamamoto, T., Uemura, K., Sawashi, Y., Mitamura, K., and Taga, A. (2016). Optimization of method to extract collagen from "emperor" tissue of soft-shelled turtles. **Journal of Oleo Science**. 65: 169-175.

Yamauchi, M. and Sricholpech, M. (2012). Lysine post-translational modifications of collagen. **Essays in Biochemistry**. 52: 113-133.

Yamauchi, M., Barker, T. H., Gibbons, D. L., and Kurie, J. M. (2018). The fibrotic tumor stroma. **The Journal of Clinical Investigation**. 128: 16-25.

Yamauchi, M., Sricholpech, M., Terajima, M., Tomer, K. B., and Perdivara, I. (2019). Glycosylation of type I collagen, In: C. Kannicht (ed.), **Post-translational modification of proteins tools for functional proteomics** (3rd ed.). New York, NY: Humana Press. 127-144.

Yiin, T. A., Huda, N., Ariffin, F., and Easa, A. M. (2014). Effect of fat extraction treatment on the physicochemical properties of duck feet collagen and its application in surimi. Asia Pacific Journal of Sustainable Agriculture Food and Energy, 2: 9-16.

Zaelani, B. F. D., Safithri, M., Tarman, K., Setyaningsih, I., and Meydia (2019). Collagen isolation with acid soluble method from the skin of Red Snapper (*lutjanus* sp.). **Earth and Environmental Science**. 241: 012033.

Zeek, P. M. (1951). Double trachea in penguins and sea lions. **The anatomical Record**. 111: 327-343.

Zeng, S., Yin, J., Yang, S., Zhang, C., Yang, P., Wu, W. (2012). Structure and characteristics of acid and pepsin-solubilized collagens from the skin of cobia (*Rachycentron canadum*). **Food Chemistry**. 135: 1975-1984.

Zhao, S., Zhang, M., Li, G., and Liu, W. (2009). Preparation and characterization of alkali-soluble collagen from pig skin shavings. **Journal of the American Leather Chemists Association**. 104: 344-351.

Zhao, Y., Wang, Z., Zhang, J. and Su, T. (2018). Extraction and characterization of collagen hydrolysates from the skin of *Rana chensinensis*. **3 Biotech**. 181: 1-8.

Zhang, J., and Duan, R. (2017). Characterisation of acid-soluble and pepsin-solubilised collagen from frog (*Rana nigromaculata*) skin. **International Journal of Biological Macromolecules**. 101: 638-642.

Zhi, X., Wang, Y., Li, P., Yuan, J., and Shen, J. (2015). Preparation of keratin/chlorhexidine complex nanoparticles for long-term and dual stimuli-responsive release. **RSC advances**. 5: 82334-82341.

Zhou, P. and Regenstein, J. M. (2005). Effects of alkaline and acid pretreatments on Alaska pollock skin gelatin extraction. **Journal of Food Science**. 70: C392-C396.

Zhou, Y. (2014). **Structural analysis of proteins by covalent labeling and mass spectrometric detection**, Ph.D. dissertations, 171 pp. University of Massachusetts. Amherst, MA.

Zhou, C., Li, Y., Yu, X., Yang, H., Ma, H., Yagoub, A. E. A., Cheng, Y., Hu, J., and Otu, P. N. Y. (2016). Extraction and characterization of chicken feet soluble collagen. **LWT- Food Science and Technology**. 74: 145-153.

Zhu, R., Zacharias, L., Wooding, K. M., Peng, W., and Mechref, Y. (2017). Chapter 21-glycoprotein enrichment analytical techniques: advantages and disadvantages, In: A. K. Shukla (ed.), **Proteomics in biology, Part A**. London, UK: Academic Press. 397-429.

Zhu, L., Xie, Y., Wen, B., Ye, M., Liu, Y., Imam, K.S.U., Cai, H., Zhang, C., Wang, F., and Xin, F. (2020). Porcine bone collagen peptides promote osteoblast proliferation and differentiation by activating the PI3K/Akt signaling pathway. **Journal of Functional Foods**. 64: 103697.

Zou, Y., Wang, L., Li, P., Cai, P., Zhang, M., Sun, Z., Sun, C., Geng, Z., Xu, W., Xu, X., and Wang, D. (2017). Effects of ultrasound assisted extraction on the physiochemical, structural and functional characteristics of duck liver protein isolate. **Process Biochemistry**. 52: 174-182.

Zou, Y., Xu, P., Li, P., Cai, P., Zhang, M., Sun, Z., Sun, C., Xu, W., and Wang, D. (2017). Effect of ultrasound pre-treatment on the characterization and properties of collagen extracted from soft-shelled turtle (*Pelodiscus sinensis*). **LWT- Food Science and Technology**. 82: 72-81.

Zou, Y., Yang, H., Zhang, X., Xu, P., Jiang, D., Zhang, M., Xu, W., and Wang, D. (2020). Effect of ultrasound power on extraction kinetic model, and physicochemical and structural characteristics of collagen from chicken lung. **Journal of Food Production, Processing and Nutrition**. 2: 1-12.

Żelechowska, E., Sadowska, M., and Turk, M. (2010). Isolation and some properties of collagen from the backbone of Baltic cod (Gadus morhua). **Food Hydrocolloids**. 24: 325-329.

BIOGRAPHY

Kitsanapong Kaewbangkerd was born in July 16th, 1993, at Nakhon Sawan, Thailand. He studied for high school diploma at Nawamindarajudis Mutchim School, Nakhon Sawan, Thailand (2009-2012).

In 2016, he received Bachelor's degree of Science (Food Technology) from Suranaree University of Technology. He continually started to work as research assistance at food protein research laboratory.

In 2017, he decided to study his Master's program for Food Technology under supporting by Suranaree University of Technology with One Research One Graduate (OROG) fund. During his graduate study, he presented poster proceeding part of his research work at the 5th international conference 2020 on Food and Applied Bioscience (FAB) (Chiangmai, Thailand, February 6-7th, 2020) in the title of Extraction and characterization of collagen from broiler chicken trachea.